

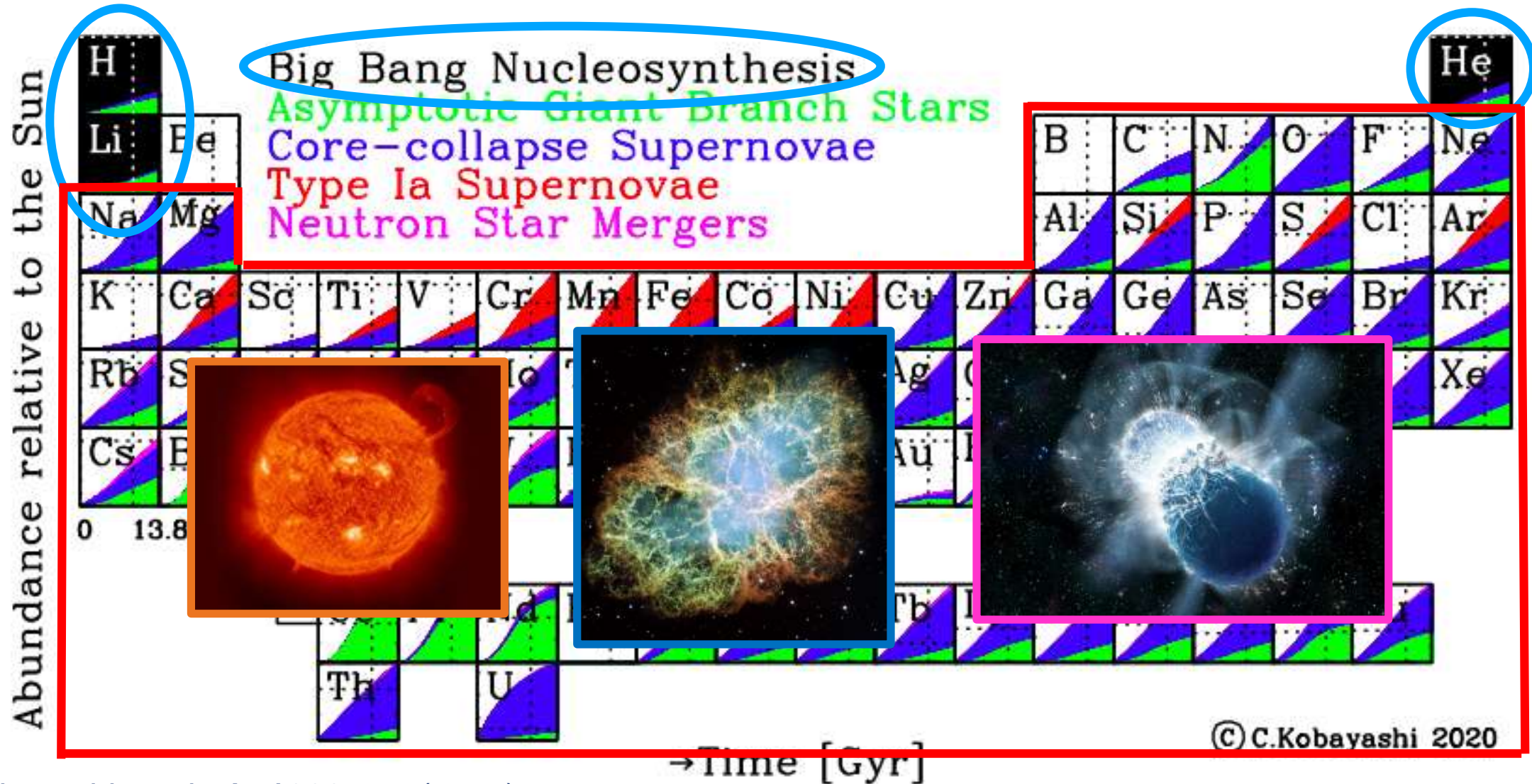
Nuclear Astrophysics at TRIUMF

ECT* Workshop Nuclear Astrochemistry

Dr. Matthew Williams
STFC Ernest Rutherford Fellow

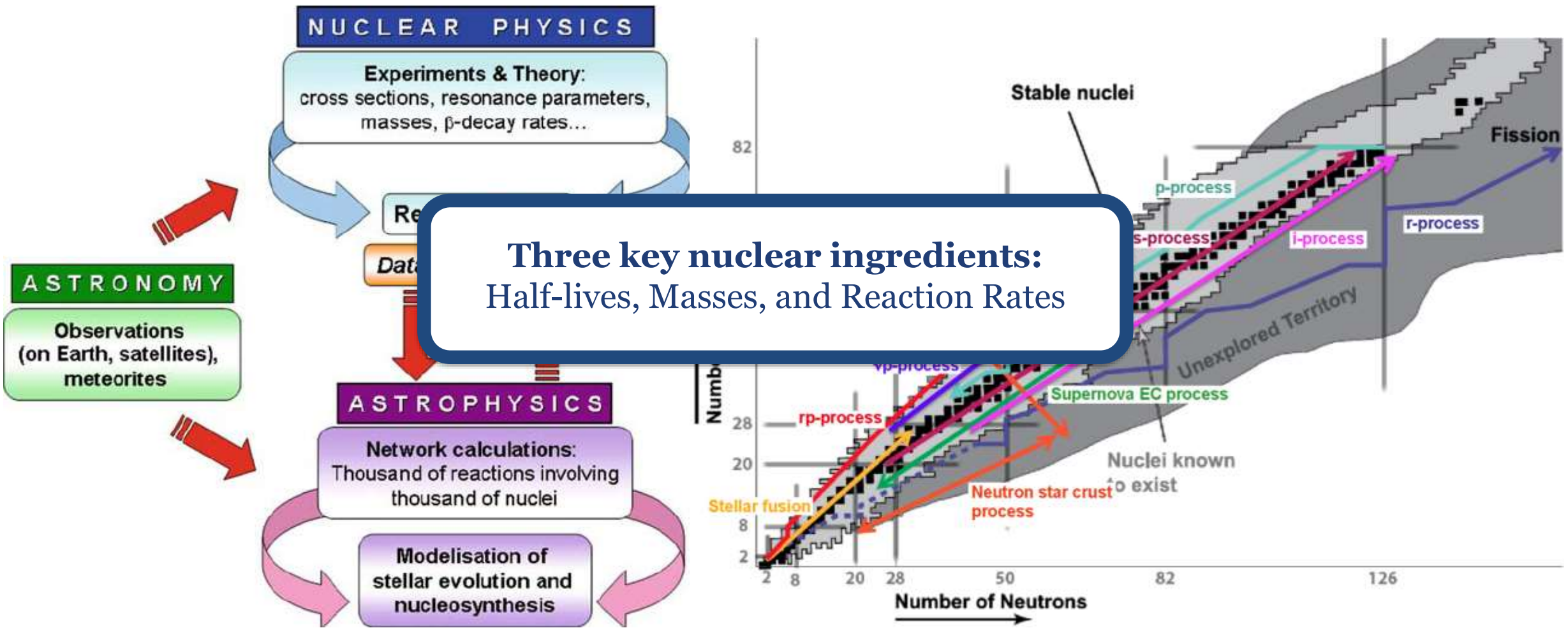
University of Surrey

Origin of the Elements

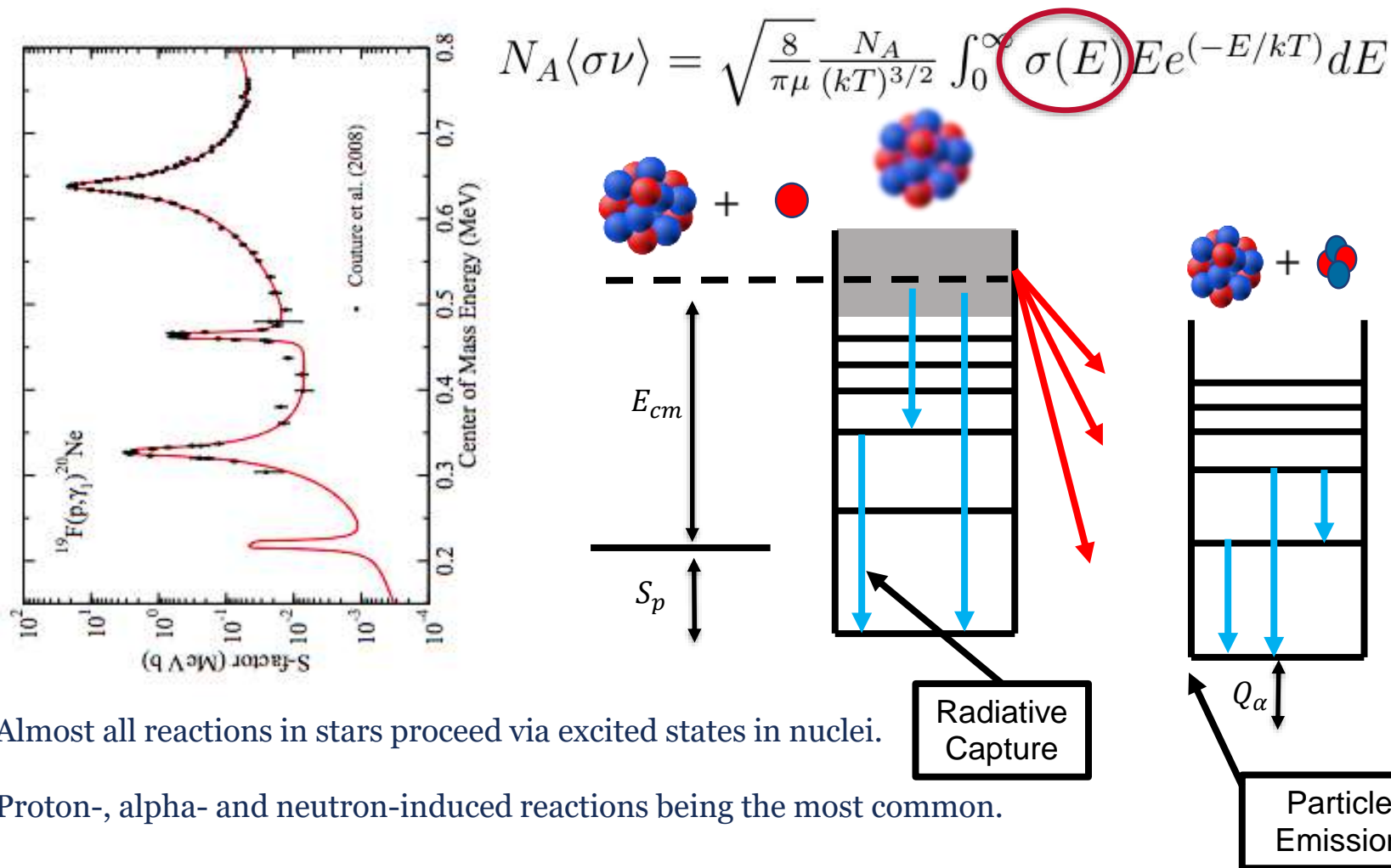


C. Kobayashi *et al.*, *ApJ* **900** 179 (2020)

Nuclear Astrophysics: a multidisciplinary field



Nuclear Reactions in Stars



- Cross-section determined by:**
- Number of states.
 - Energies of states.
 - Spin & parity of states.
 - Total and partial decay widths.

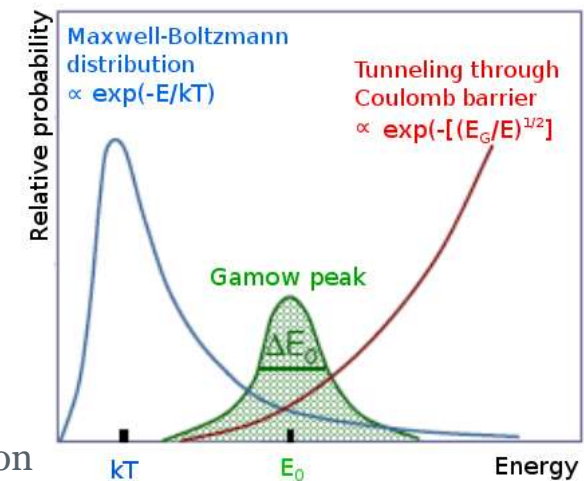
$$\omega\gamma = \frac{(2J + 1)}{(2j_p + 1)(2j_t + 1)} \frac{\Gamma_i \Gamma_f}{\Gamma}$$

Almost all reactions in stars proceed via excited states in nuclei.

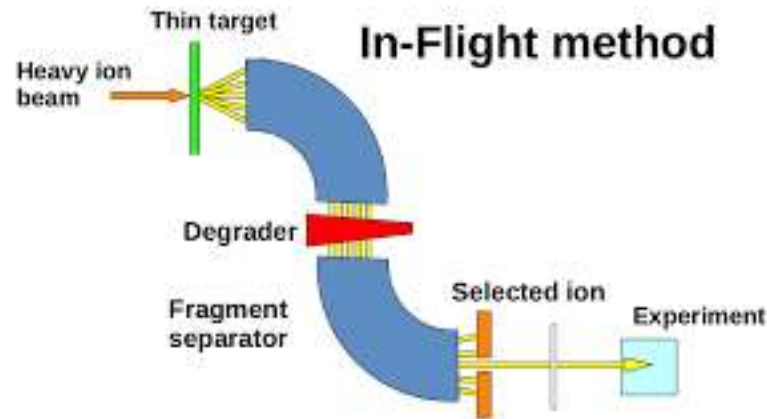
Proton-, alpha- and neutron-induced reactions being the most common.

Direct Methods: Measure a nuclear reaction cross-section at the relevant energies for astrophysics

Indirect Methods: Measure properties of the nucleus & individual nuclear states that influence the cross-section



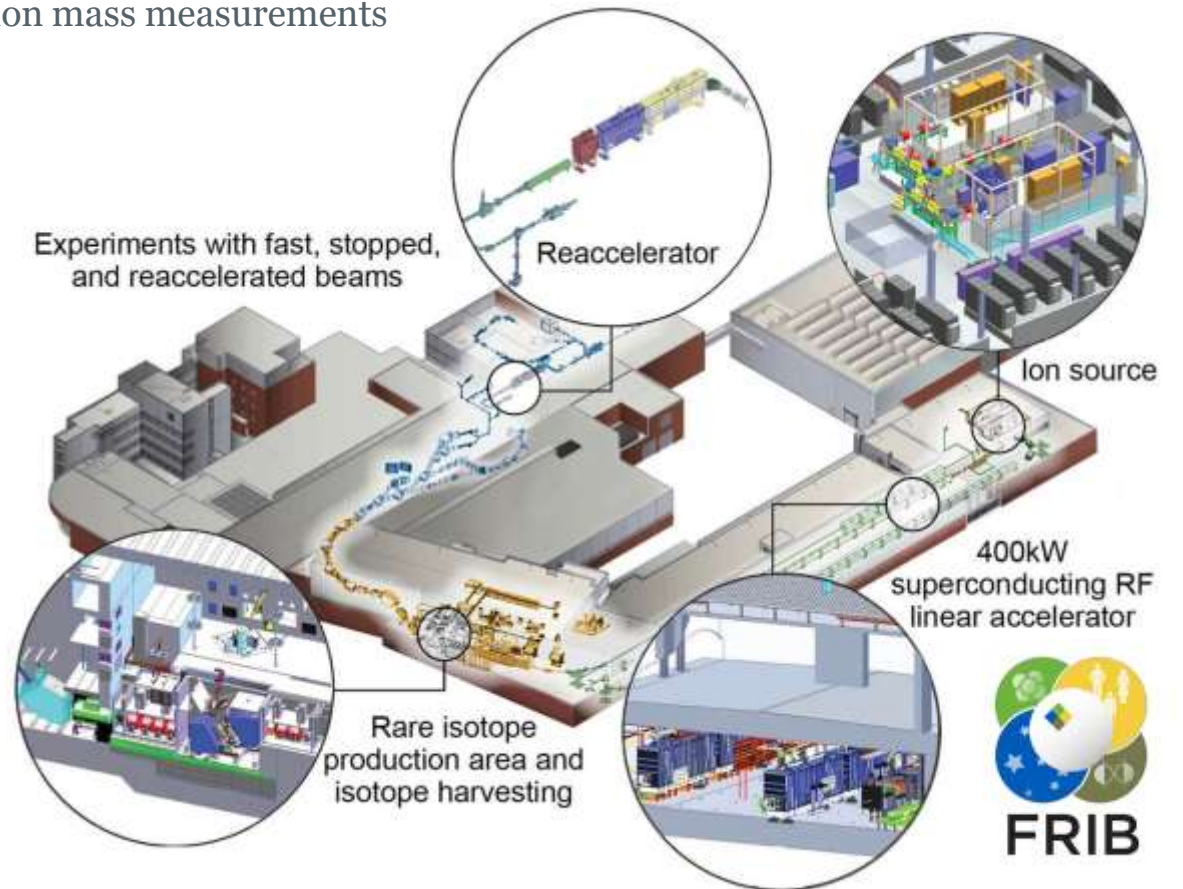
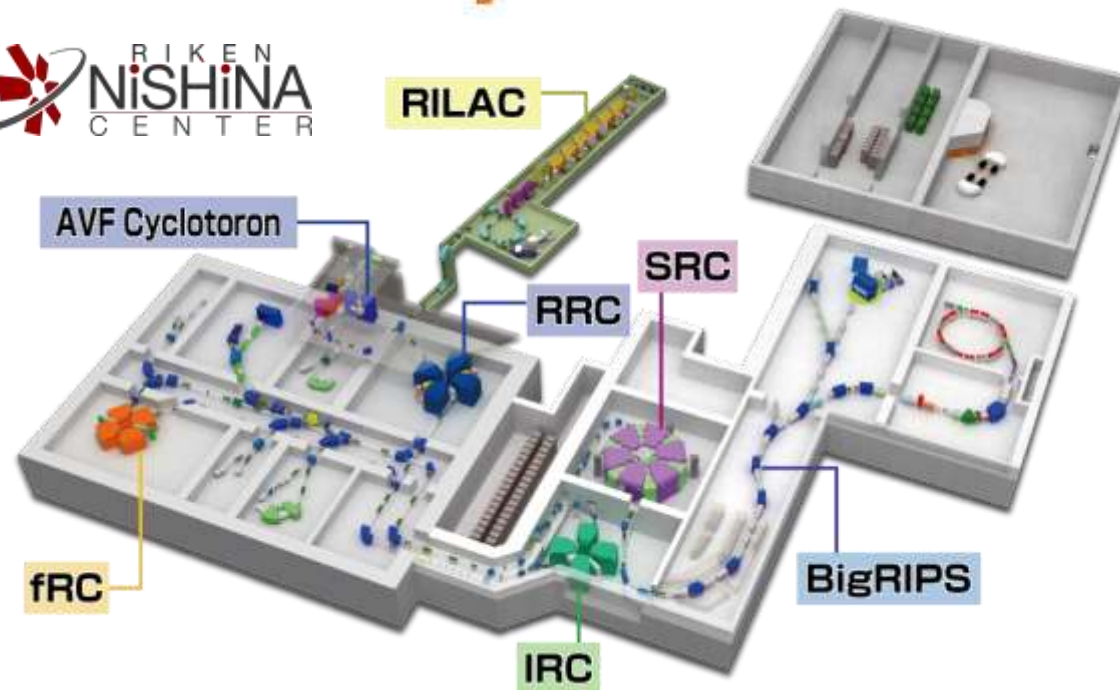
Producing Radioactive Nuclei in the Laboratory



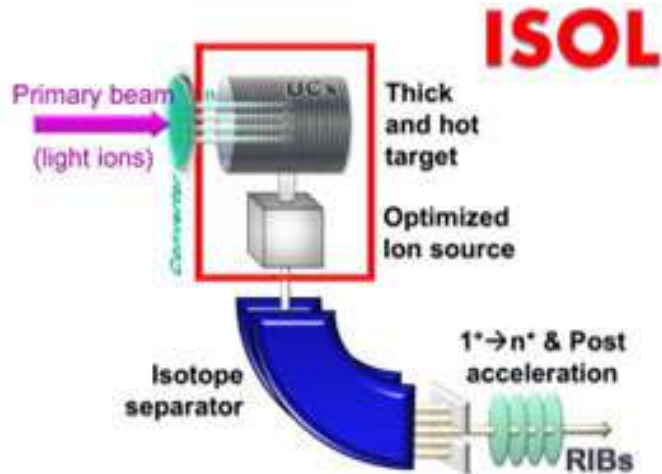
- Fast beam of heavy-ions (e.g. Uranium) fragments on a thin low-Z target (e.g. Beryllium).
- Forward-moving fragments are mass-separated and sent to experimental areas.

Advantage: Can produce very exotic nuclei far from stability.

Disadvantage: Far-beyond relevant energy ranges to study stellar reaction rates and too fast-moving for precision mass measurements



Producing Radioactive Nuclei in the Laboratory

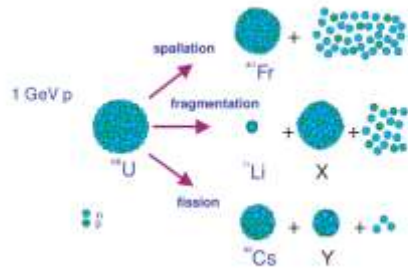


Isotope Separation On-Line

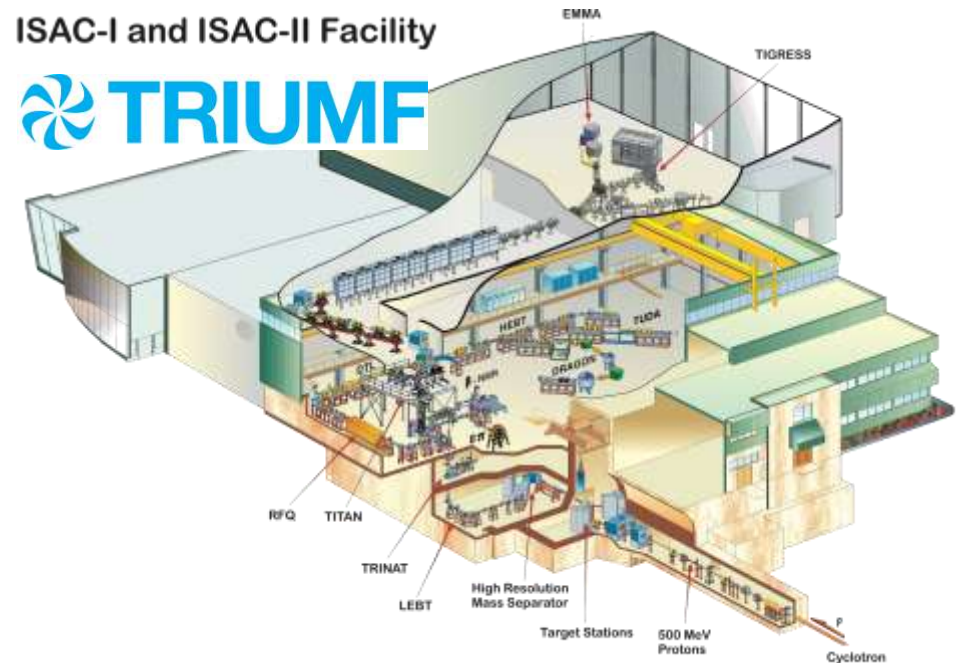
- Light-ion primary beam (e.g. protons) impinged on a thick higher-Z target.
- Radioactive nuclei diffuse out of the source and are ionized by an optimised ion-source.
- Ions are extracted, mass-separated, formed into beams, and (optionally) accelerated.

Advantage: Can produce very intense radioactive beams with high purity, low-emittance, and easily variable acceleration. Good for reaction rate studies and mass-measurements.

Disadvantage: Limited by chemical properties of beams as some elements don't make it out of the target easily.



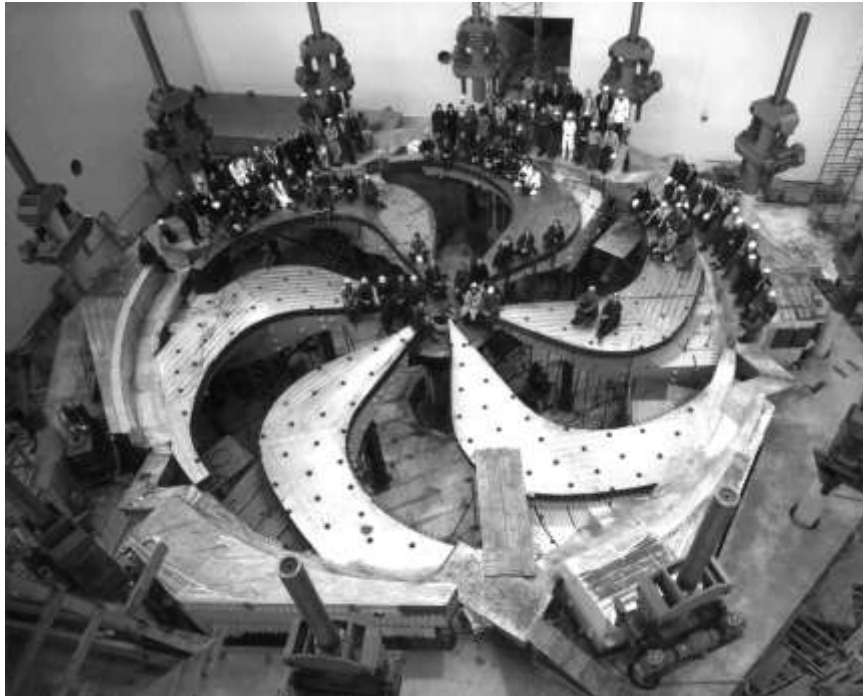
ISAC-I and ISAC-II Facility



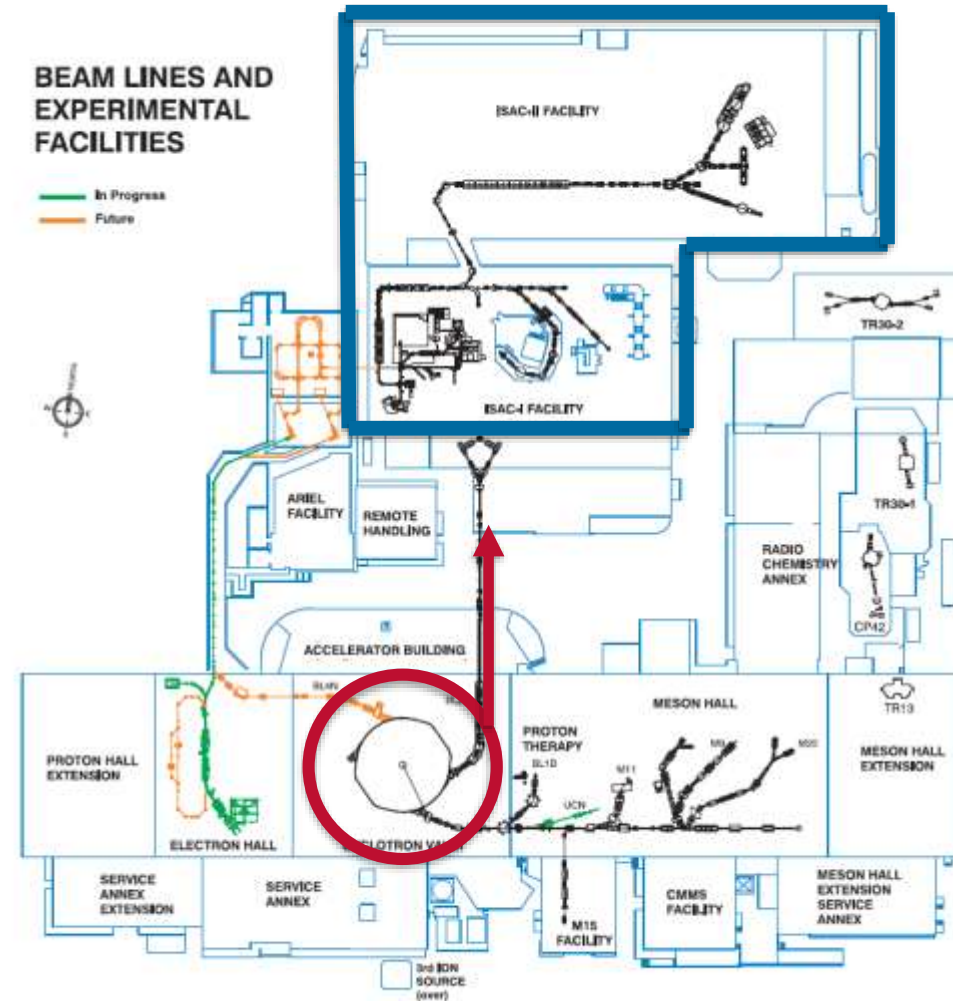
TRIUMF: Canada's national particle accelerator centre



Largest cyclotron in the world

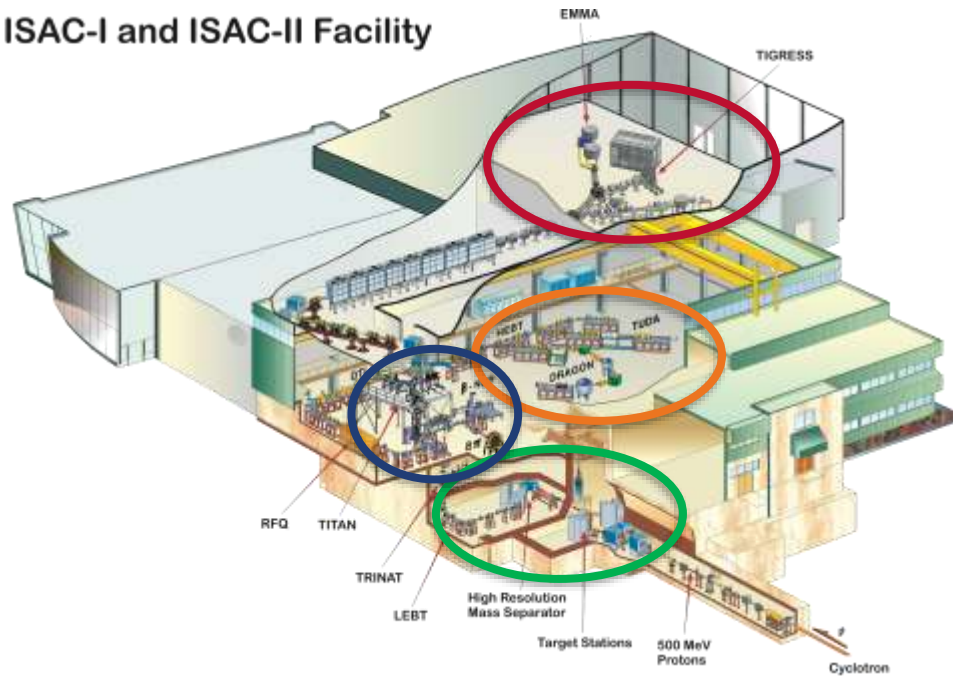


Main cyclotron accelerates H⁻ ions to 500 MeV and ejected by stripping.



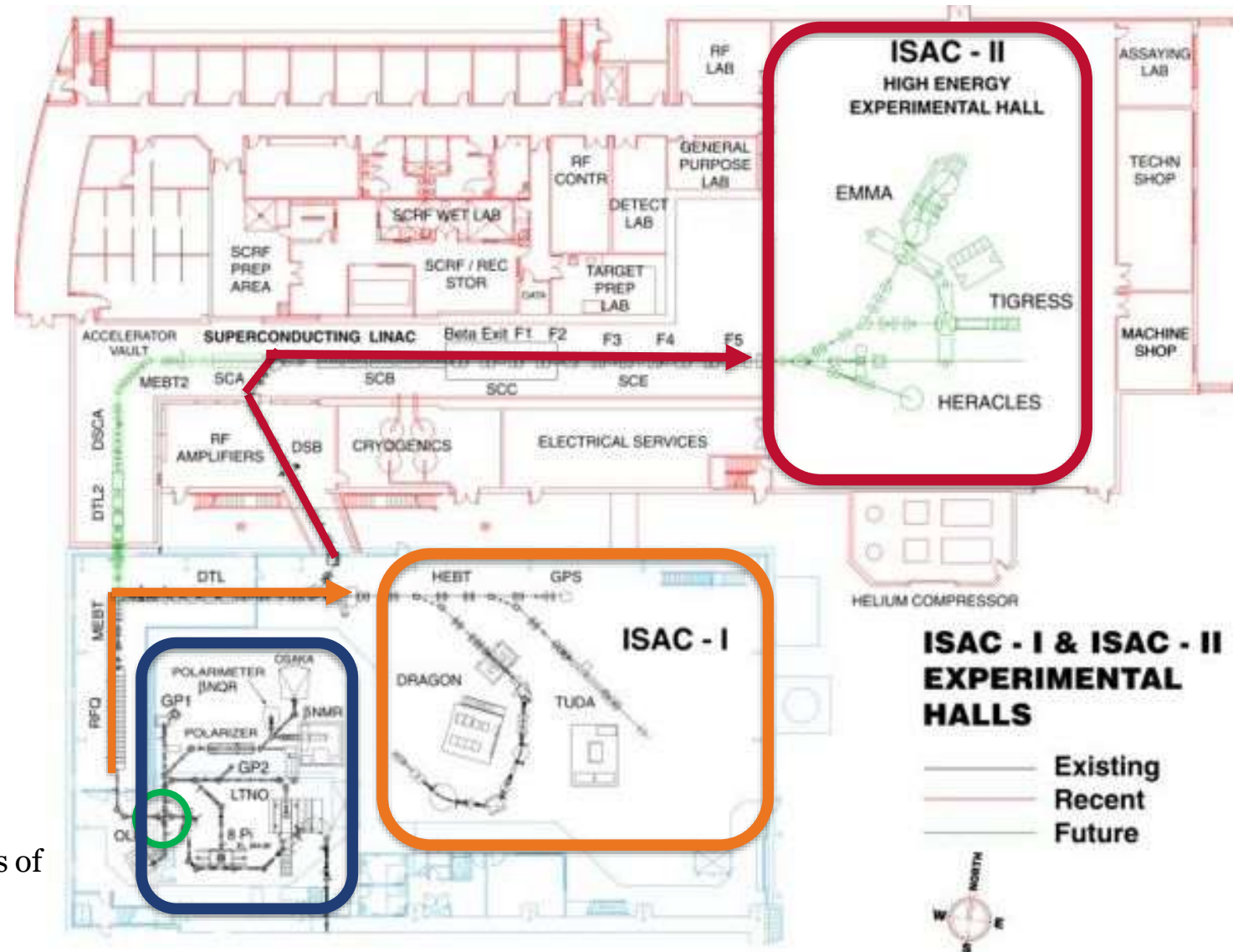
The Isotope Separator and Accelerator (ISAC) Facility

ISAC-I and ISAC-II Facility

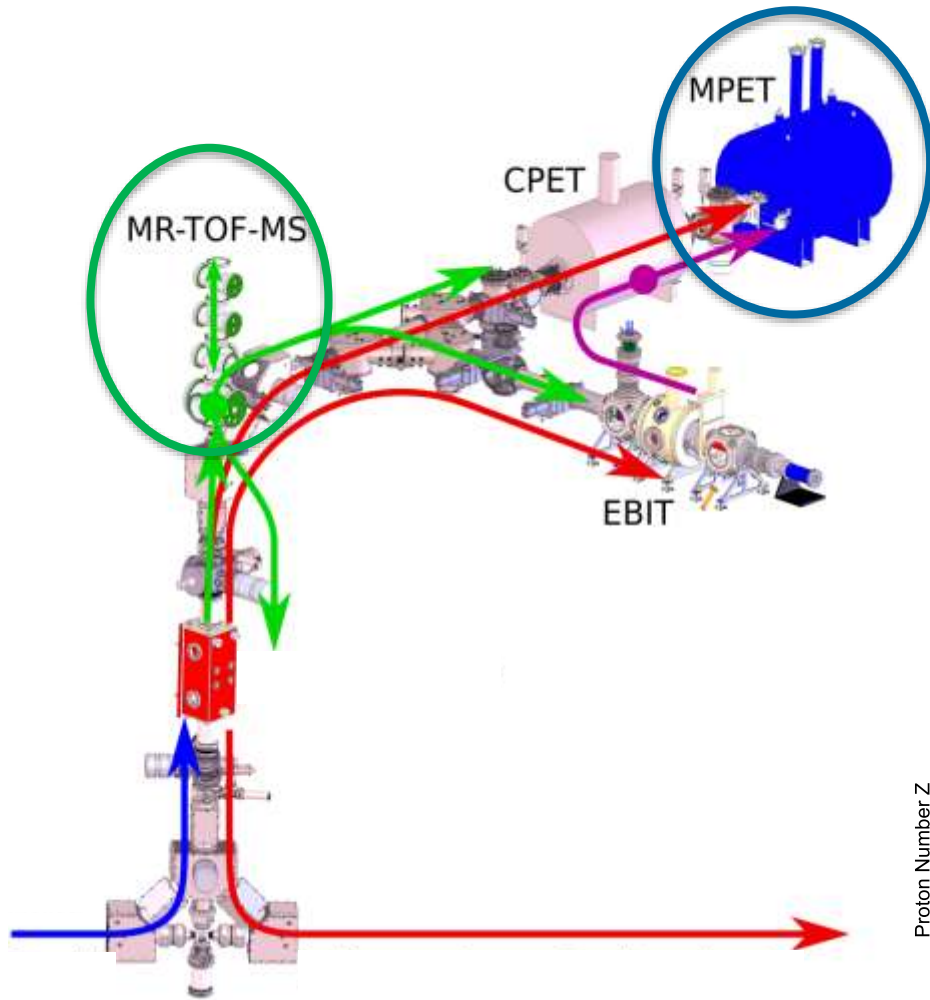


ISAC Facility:

- ISOL targets and mass separator room in basement.
- Low energy area for mass-measurements and decay studies.
- Medium energy area (150 keV/u to 1.8 MeV/u) for reaction studies at astrophysical energies
- High energy hall (up-to 16 MeV/u) for indirect studies of excited nuclear states.

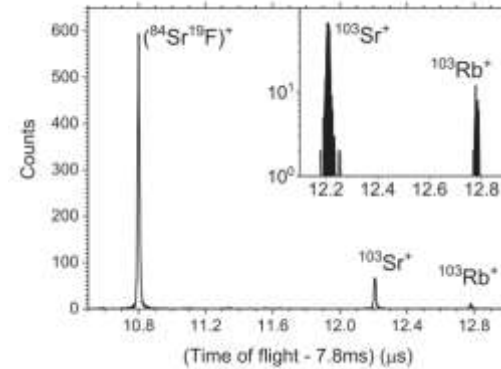
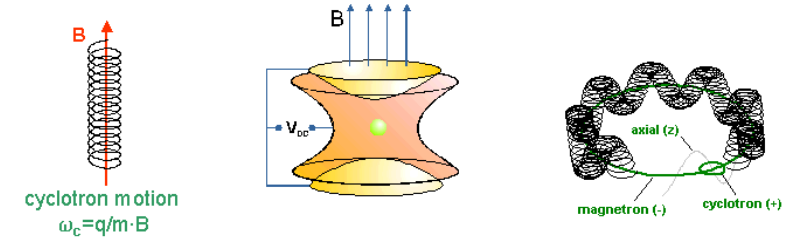


Mass Measurements with the TITAN Facility



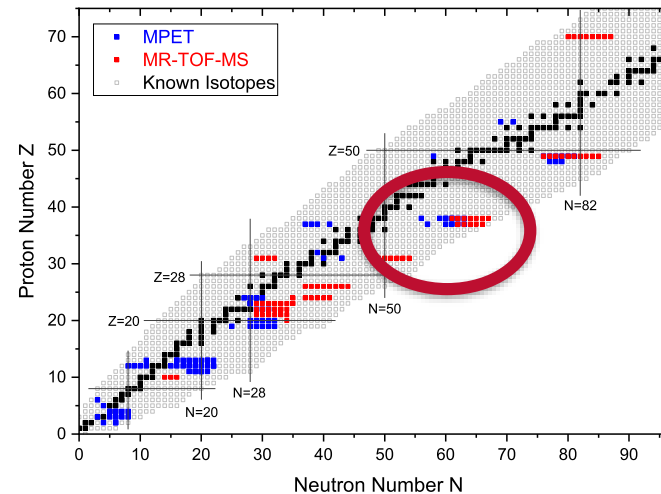
Measurement Penning Trap:

Precision mass measurements through determining the cyclotron frequency.



Multi-reflection TOF spectrometer:

Cleans beam contaminants and can get a less-precise mass measurement through time-of-flight for very short-lived nuclei.



TITAN has performed >160 mass measurements motivated by both nuclear structure and astrophysics.

Mass Measurements for the r-process:

Uncertainties in masses far from stability impact the predicted shape of the r-process peaks.

I. Mukul, et al., Phys Rev C 103, 044320 (2021)



High Efficiency array of 16 HPGe clovers with a suite of ancillary detectors:

- SCEPTAR: Plastic scintillators for β -particle tagging
- PACES: Si(Li) detectors for conversion electron spectroscopy.
- DESCANT: Array of liquid scintillators for beta-delayed neutron emission.
- LaBr₃ Detectors: Fast timing detectors for lifetime measurements.

Measured β -decay half-lives and β -delayed neutron emission of nuclei in the vicinity of $N=82$ which is a key waiting-point region for the r-process.

β and β -delayed neutron decay of the $N = 82$ nucleus $^{131}_{49}\text{In}_{82}$

R. Dunlop,^{1,*} C. E. Svensson,¹ C. Andreoiu,² G. C. Ball,³ N. Bernier,^{3,4} H. Bidaman,¹ V. Bildstein,¹ M. Bowry,³ D. S. Cross,² I. Dillmann,^{3,5} M. R. Dunlop,¹ F. H. Garcia,² A. B. Garnsworthy,³ P. E. Garrett,¹ G. Hackman,³ J. Henderson,^{3,†} J. Measures,^{3,6} D. Mücher,¹ B. Olaizola,^{1,3} K. Ortner,² J. Park,^{3,4,‡} C. M. Petrache,⁷ J. L. Pore,^{2,§} J. K. Smith,^{3,¶} D. Southall,^{3,**} M. Ticu,² J. Turko,¹ K. Whitmore,² and T. Zidar¹

¹Department of Physics, University of Guelph, Guelph, Ontario N1G 2W1, Canada

²Department of Chemistry, Simon Fraser University, Burnaby, British Columbia V5A 1S6, Canada

³TRIUMF, 4004 Wesbrook Mall, Vancouver, British Columbia V6T 2A3, Canada

⁴Department of Physics and Astronomy, University of British Columbia, Vancouver, British Columbia V6T 1Z4, Canada

⁵Department of Physics and Astronomy, University of Victoria, Victoria, British Columbia V8P 5C2, Canada

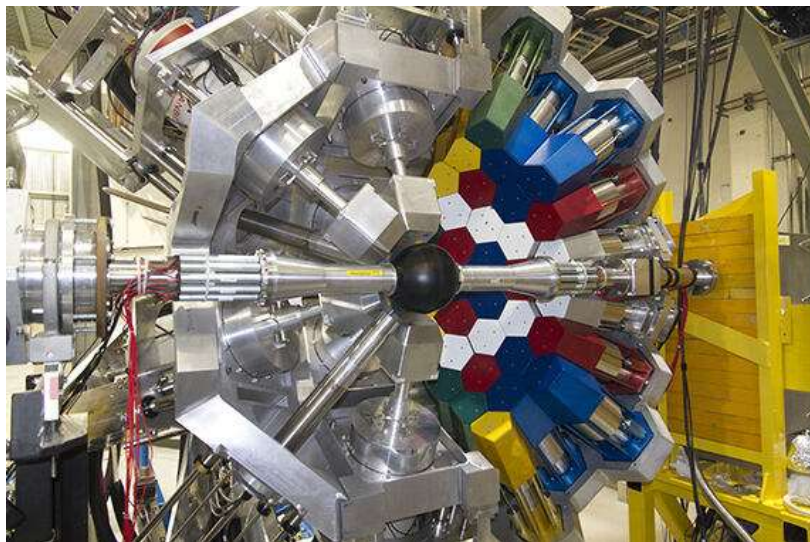
⁶Department of Physics, University of Surrey, Guildford GU2 7XH, United Kingdom

⁷Centre de Sciences Nucléaires et Sciences de la Matière,
CNRS/IN2P3, Université Paris-Saclay, 91405 Orsay, France

(Dated: September 12, 2021)

A. Garnsworthy, et al., Nucl. Inst. Meth. A **918**, 9-29 (2019)

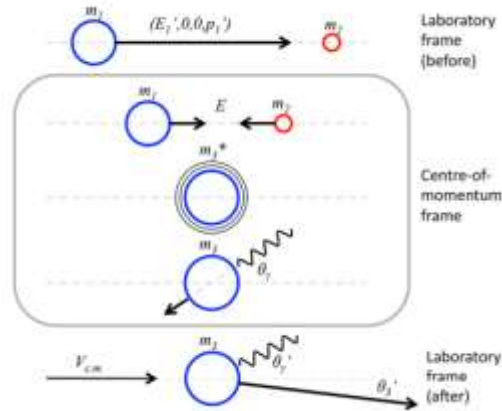
R. Dunlop, et al., Phys. Rev. C **99**, 045805 (2019)



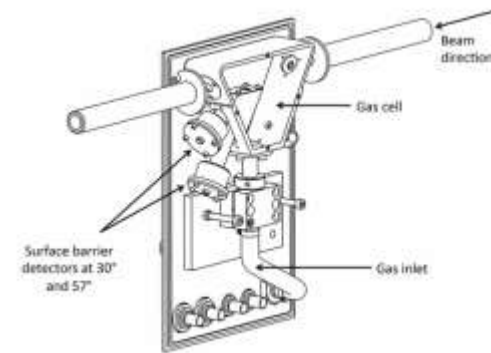
The DRAGON facility

DRAGON specializes in **radiative capture** measurements of protons (**p, γ**) and alphas (**α , γ**) on heavy-ions, which are important in almost every nucleosynthesis scenario.

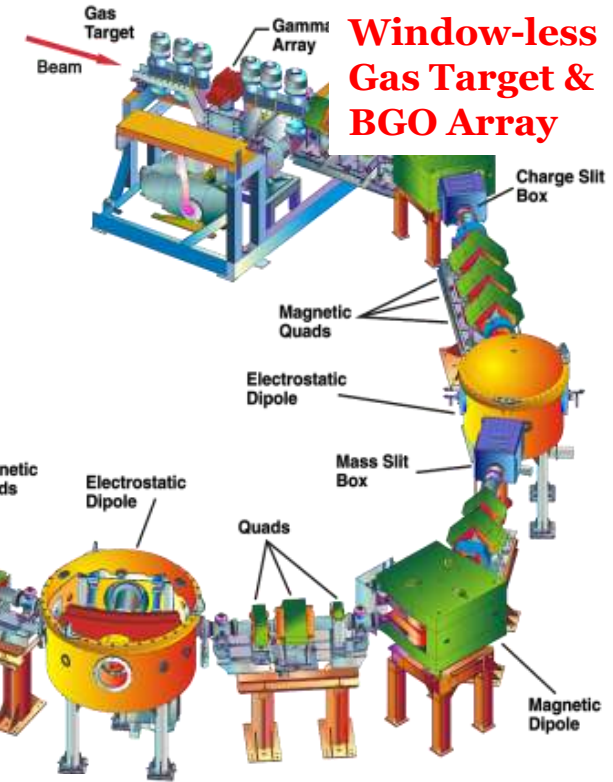
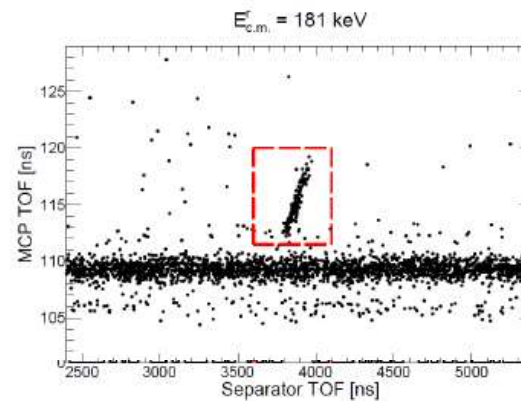
Reactions are carried out in **inverse kinematics** to allow studies using **radioactive beams**



Gas Cell:
Window-less H_2 or He gas cell pressure of up-to 8 Torr



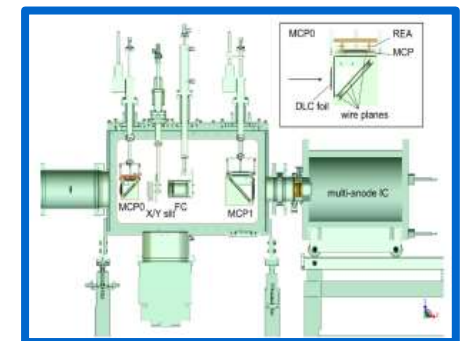
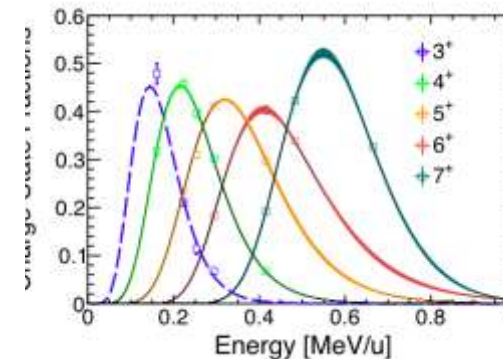
Particle ID:
MCP-TOF vs Separator TOF.
Beam suppression of $>10^{17}$



Suite of Focal Plane Detectors

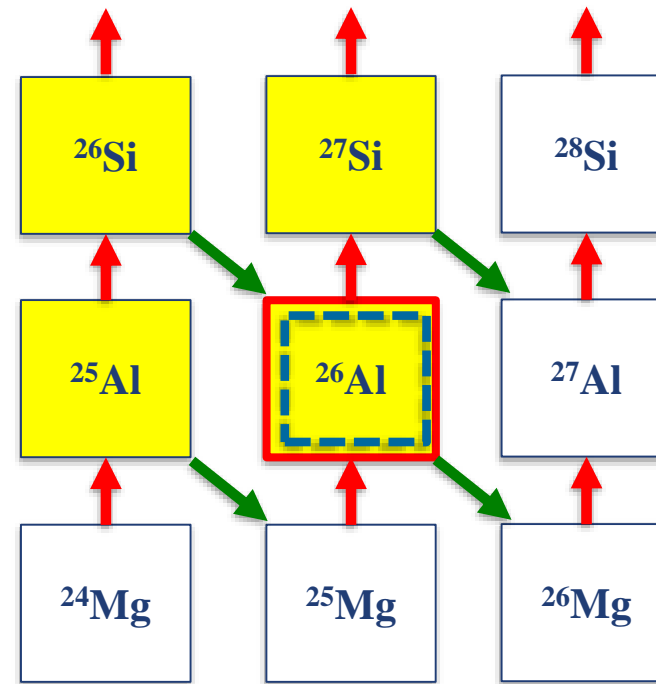
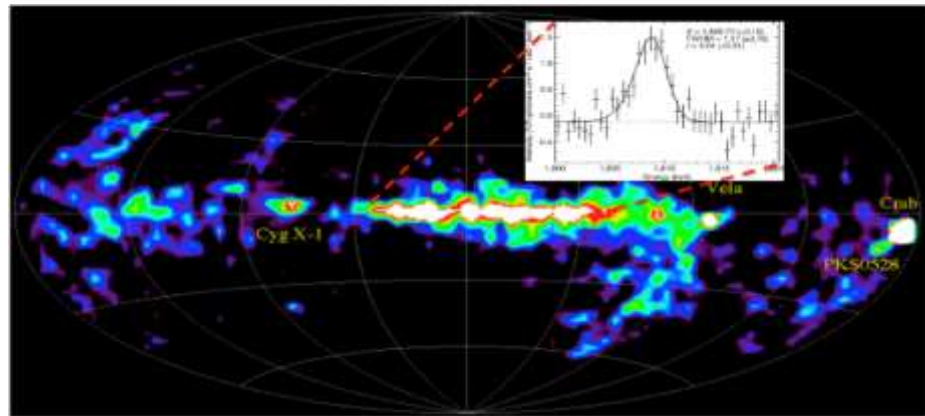
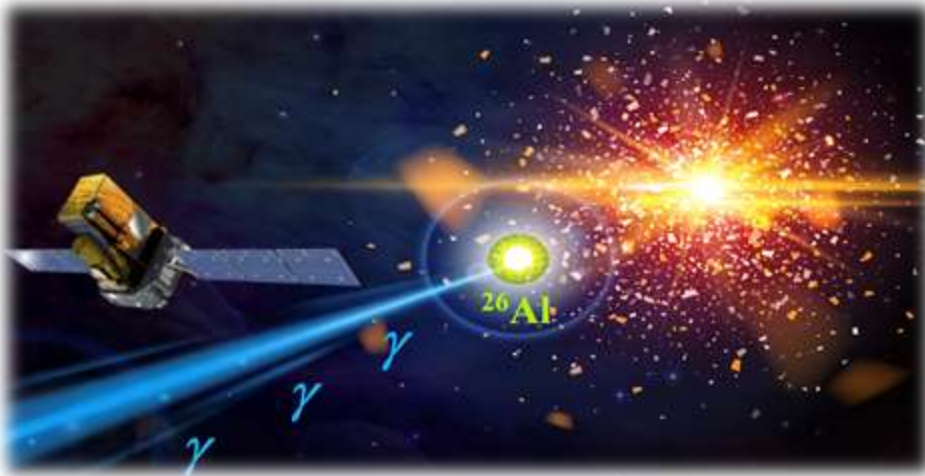
- | | | |
|--|--|--|
| $^3\text{He}(\alpha, \gamma)^7\text{Be}$ | $^{17}\text{O}(\alpha, \gamma)^{21}\text{Ne}$ | $^{23}\text{Mg}(p, \gamma)^{24}\text{Al}$ |
| $^6\text{Li}(\alpha, \gamma)^{10}\text{B}$ | $^{18}\text{O}(\alpha, \gamma)^{22}\text{Ne}$ | $^{26g}\text{Al}(p, \gamma)^{27}\text{Si}$ |
| $^7\text{Be}(\alpha, \gamma)^{11}\text{C}$ | $^{18}\text{F}(p, \gamma)^{19}\text{Ne}$ | $^{26m}\text{Al}(p, \gamma)^{27}\text{Si}$ |
| $^{12}\text{C}(\alpha, \gamma)^{16}\text{O}$ | $^{19}\text{F}(p, \gamma)^{20}\text{Ne}$ | $^{33}\text{S}(p, \gamma)^{34}\text{Cl}$ |
| $^{12}\text{C}(^{12}\text{C}, \gamma)^{24}\text{Mg}$ | $^{19}\text{Ne}(p, \gamma)^{20}\text{Na}$ | $^{34}\text{S}(p, \gamma)^{35}\text{Cl}$ |
| $^{12}\text{C}(^{16}\text{O}, \gamma)^{28}\text{Si}$ | $^{20}\text{Ne}(p, \gamma)^{21}\text{Na}$ | $^{38}\text{K}(p, \gamma)^{39}\text{Ca}$ |
| $^{14}\text{N}(p, \gamma)^{15}\text{O}$ | $^{21}\text{Ne}(p, \gamma)^{22}\text{Na}$ | $^{33}\text{S}(\alpha, \gamma)^{38}\text{Ar}$ |
| $^{15}\text{N}(\alpha, \gamma)^{19}\text{F}$ | $^{22}\text{Ne}(p, \gamma)^{23}\text{Na}$ | $^{40}\text{Ca}(\alpha, \gamma)^{44}\text{Ti}$ |
| $^{16}\text{O}(\alpha, \gamma)^{20}\text{Ne}$ | $^{22}\text{Ne}(\alpha, \gamma)^{26}\text{Mg}$ | $^{58}\text{Ni}(p, \gamma)^{59}\text{Cu}$ |
| $^{17}\text{O}(p, \gamma)^{18}\text{F}$ | $^{21}\text{Na}(p, \gamma)^{22}\text{Mg}$ | $^{76}\text{Se}(\alpha, \gamma)^{80}\text{Kr}$ |

Of the 11 (p, γ) or (α , γ) reactions ever to be measured with radioactive beams, DRAGON is responsible for 8.

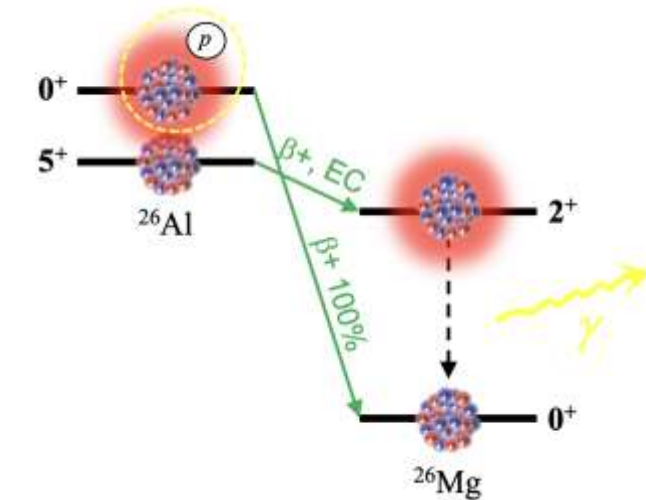


Investigating the Origin of ^{26}Al

The decay of ^{26g}Al ($T_{1/2} = 0.72$ Myr) provides direct evidence of ongoing nucleosynthesis in galaxy and provided an important heat source in the early solar system.



Formation of ^{26}Al is complicated by the existence of an isomeric state ($T_{1/2} = 6.34$ s) that will bypass ^{26g}Al entirely and not emit a 1809 keV γ -ray

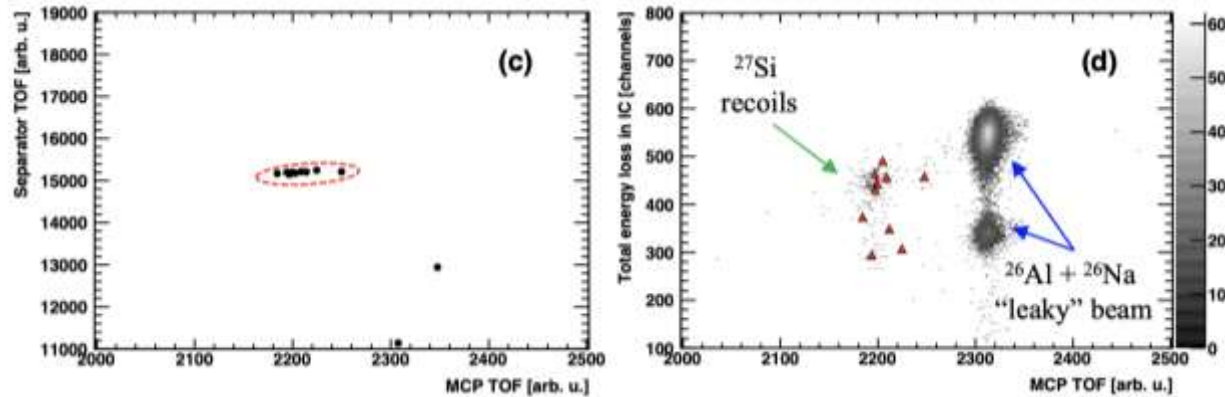


Need to measure all production and destruction channels to determine ^{26g}Al yields in stars

...including proton capture on $^{26m}\text{Al} \rightarrow$ **challenging!**

First Proton Capture on an Isomeric Beam

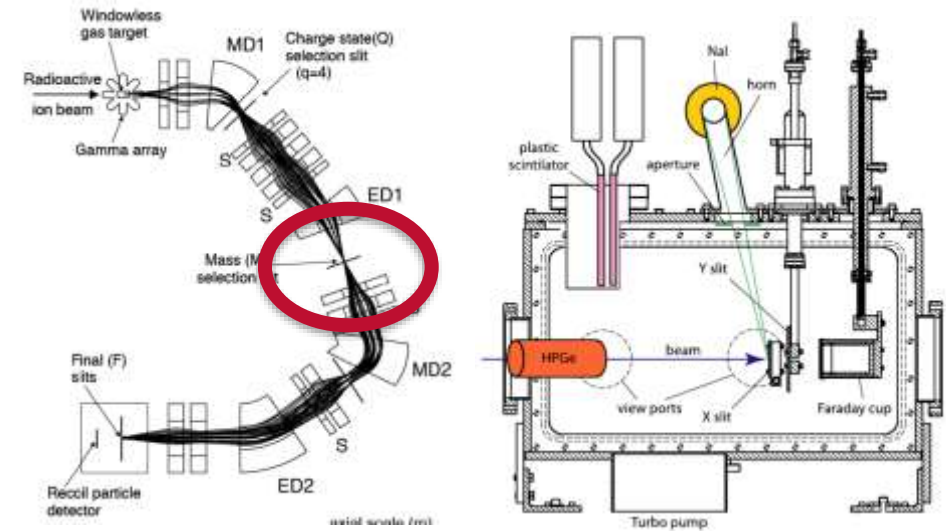
Objective to measure the 447 keV resonance, which is thought to dominate the reaction rate at temperatures above 300 MK



The ratio of ^{26g}Al to ^{26m}Al was measured by the decay of beam built-up on the mass slits

Recoils were identified through characteristic separator-TOF vs MCP-TOF in addition to energy loss in an ion chamber .

Beam contained ^{26g}Al , ^{26m}Al and ^{26}Na . Careful off-resonance data-points were taken to ensure the signal was not from beam contaminants.

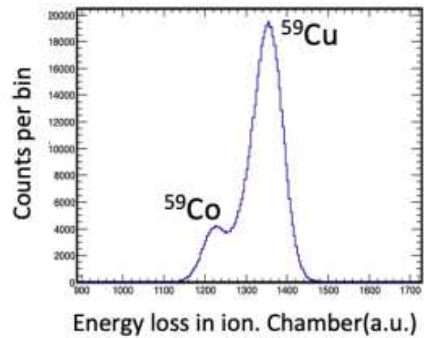


Measured the resonance strength to be very strong at $\omega\gamma = 432 \pm 137_{\text{stat}} \pm 51_{\text{sys}} \text{ meV}$

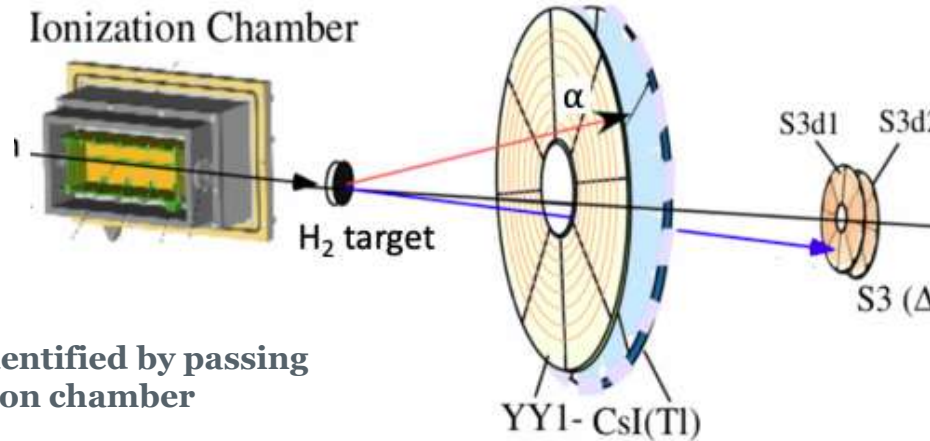
First Measurement of proton capture reaction on an isomeric beam

Constraining X-Ray Burst Light Curves with IRIS

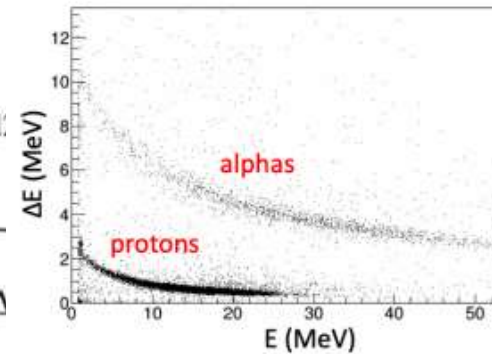
Set-up for inelastic scattering of exotic nuclei



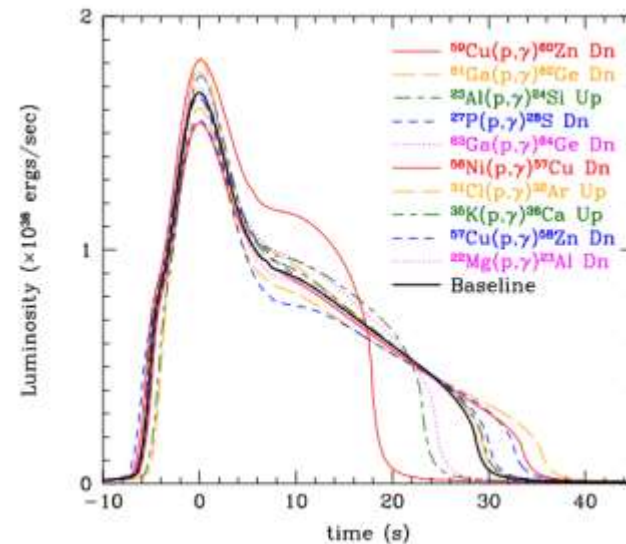
Beam contaminants identified by passing through an upstream ion chamber



Light charged-particles identified by silicon detectors backed by CsI



The IRIS target is solid hydrogen formed by freezing H_2 or D_2 on a helium cooled Ag foil



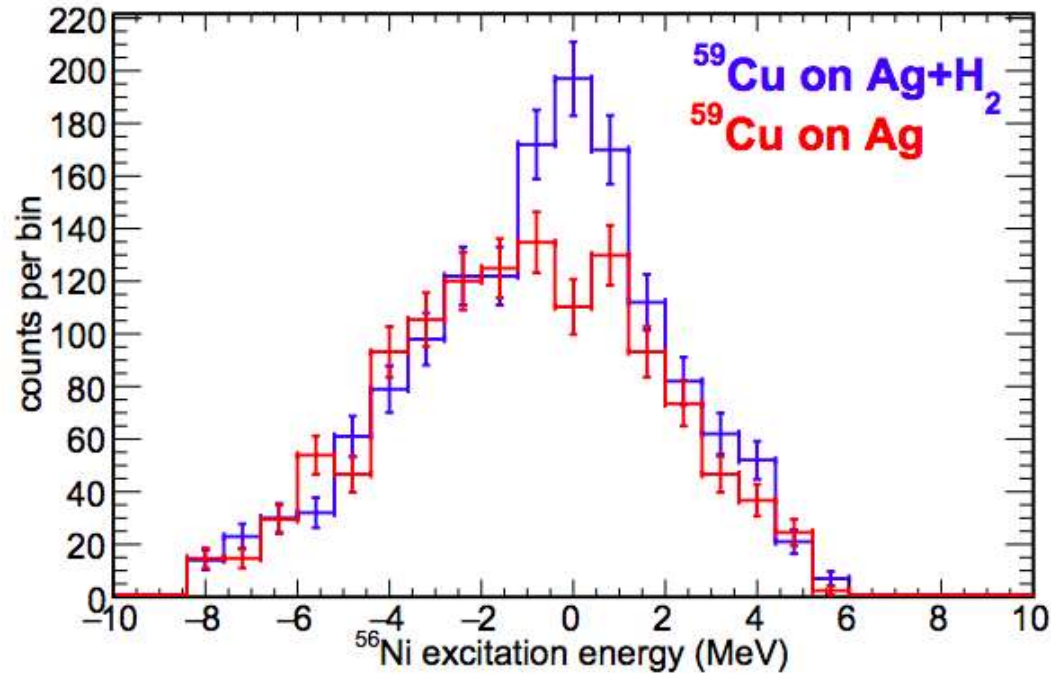
Measurement using the IRIS facility of $^{59}\text{Cu}(p,\alpha)$, which competes with influential $^{59}\text{Cu}(p,\gamma)$ reaction.

X-Ray Bursts (XRBs)

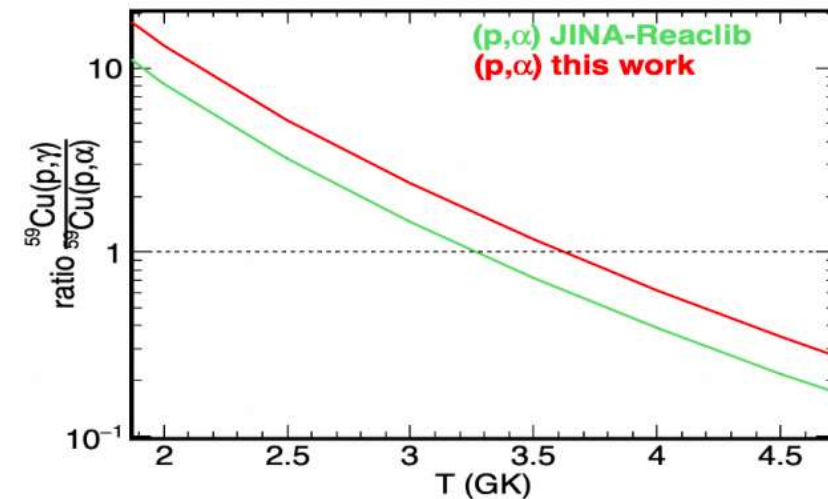
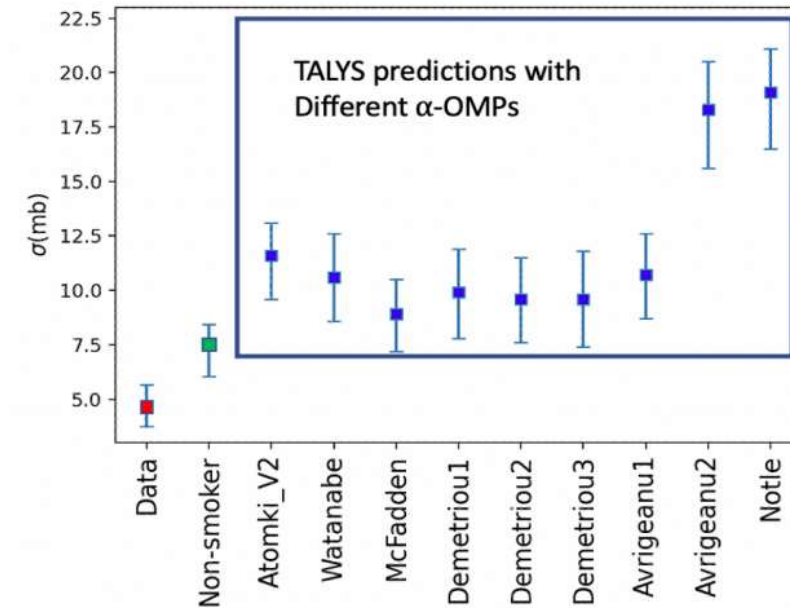
- Recurrent explosive events caused by material accreted onto a neutron star from a binary partner.
- Energy is generated by nuclear reactions on the surface, which impact the observed light curve.

J. S. Randhawa, *Phys. Rev. C*, **104**(4), L042801 (2021).

First Direct Measurement of $^{59}\text{Cu}(p,\alpha)$ Reaction



- Identify genuine reaction events through the missing-mass technique.
- Cross-section is lower than predicted by statistical model calculations.
- Result is a greater (p,γ) to (p,α) ratio than predicted.



First Scientific Campaign with the EMMA-TIGRESS set-up

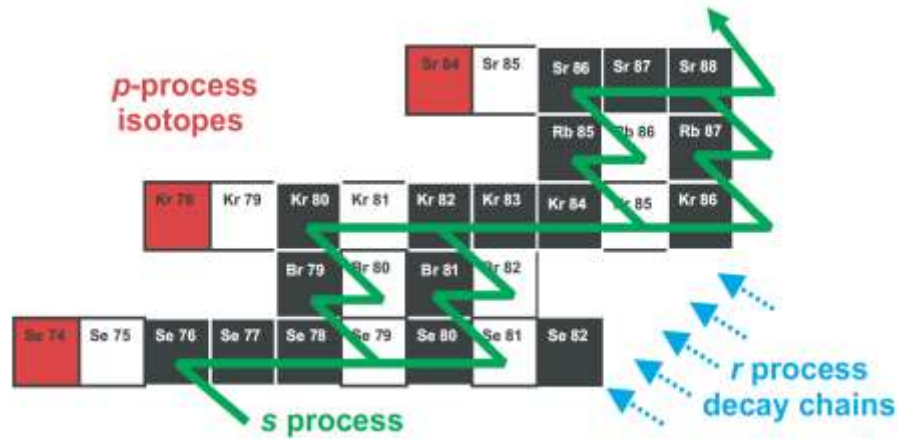


B. Davids, M. Williams et al., Nucl. Instr. Meth. A 930, 191-195 (2019)

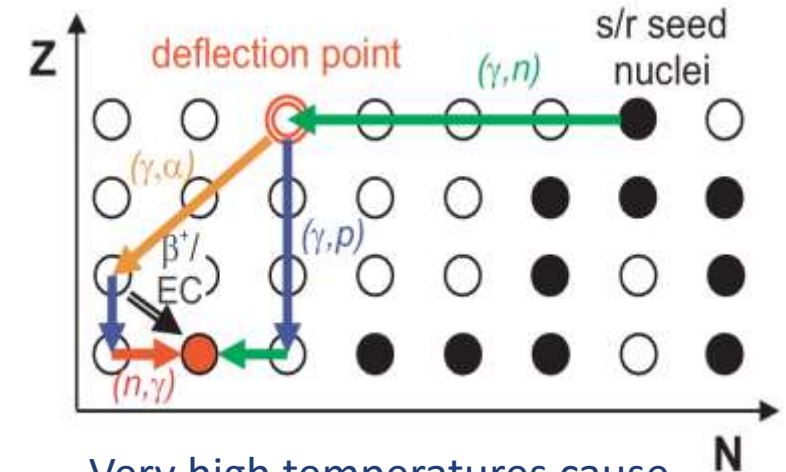
C.E. Svensson, et al., J. Phys. G: Nucl. Part. Phys. 31 (2005) S1663–S1668

First measurement with EMMA: Solving the puzzle of the p-nuclei

~30 stable isotopes cannot be produced via neutron capture processes.



Best candidate: Core-collapse Supernovae of massive stars



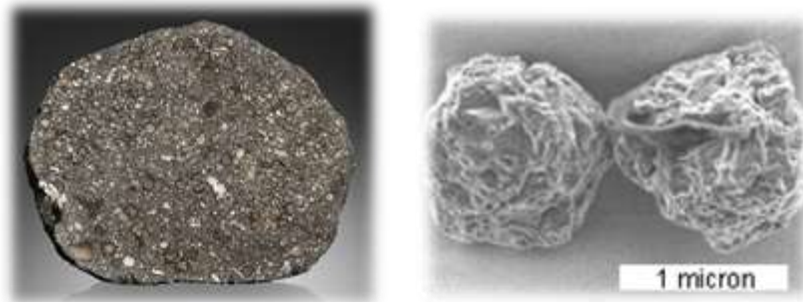
Very high temperatures cause stable nuclei to shed neutrons.

Observed abundances vary from prediction by orders of magnitude.

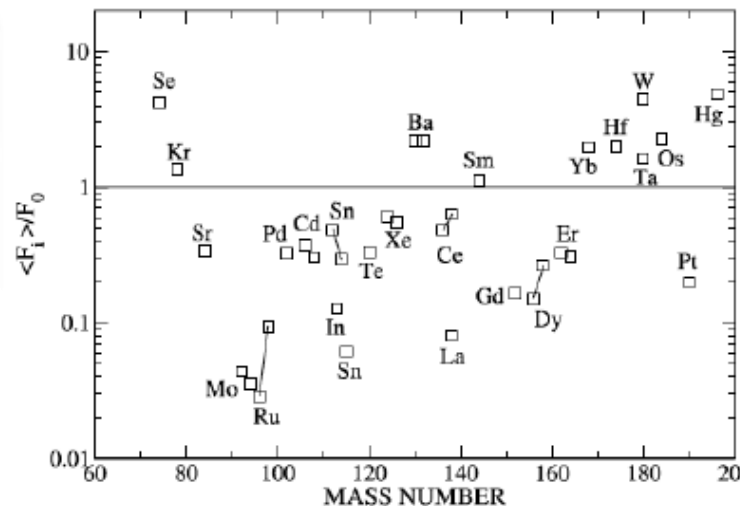
Questions:

Is there just one astrophysical source for all p-nuclei?

Could other scenarios contribute to p-nuclei?

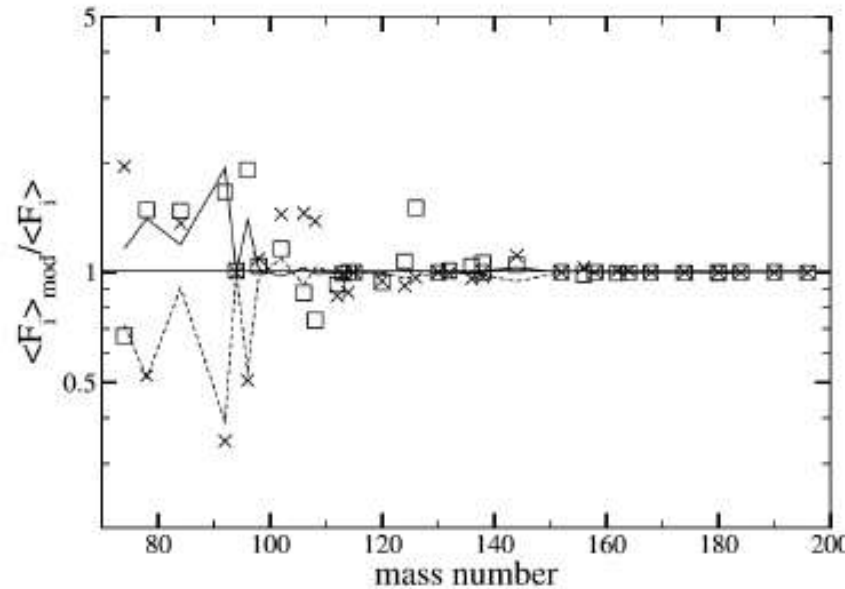
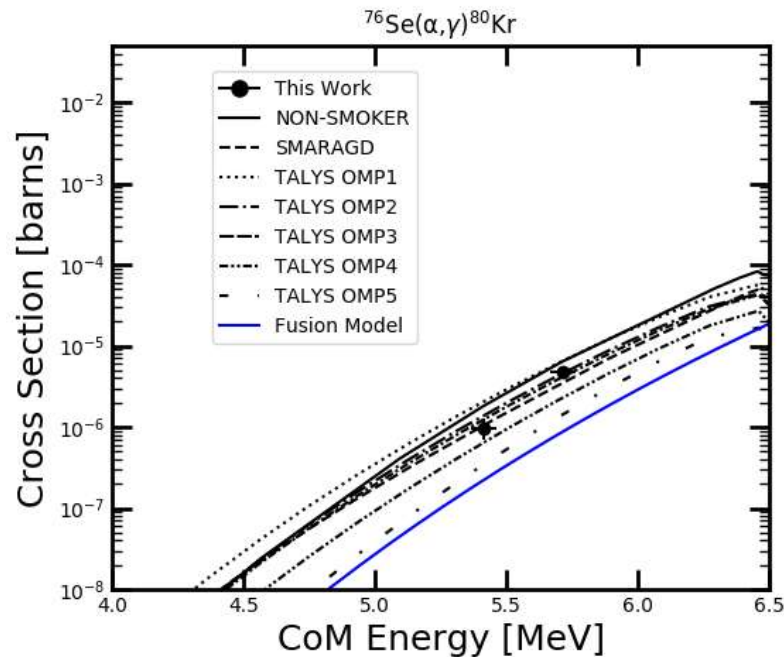


Small abundance, so can only be observed via isotopic analysis of meteorite grains.
Origin of the p-nuclei not well understood.



Nuclear uncertainties in the p-process

- Production of p-nuclei involves many reactions on radioactive nuclei, none of which have been measured directly.
- Models rely on cross-sections predicted by statistical models that can vary depending on the calculation inputs (e.g. Optical model parameters, γ SF, NLD) largely based on studies of stable nuclei.
- For light p-nuclei, production rates are most sensitive to variations in $(\gamma, p) / (p, \gamma)$ cross sections.



Challenge:

- Cross-sections are very weak.
- Difficult to separate recoils from beam in inverse kinematics

Fallis, J. et al. Physics Letters B 807 (2020) 135575.

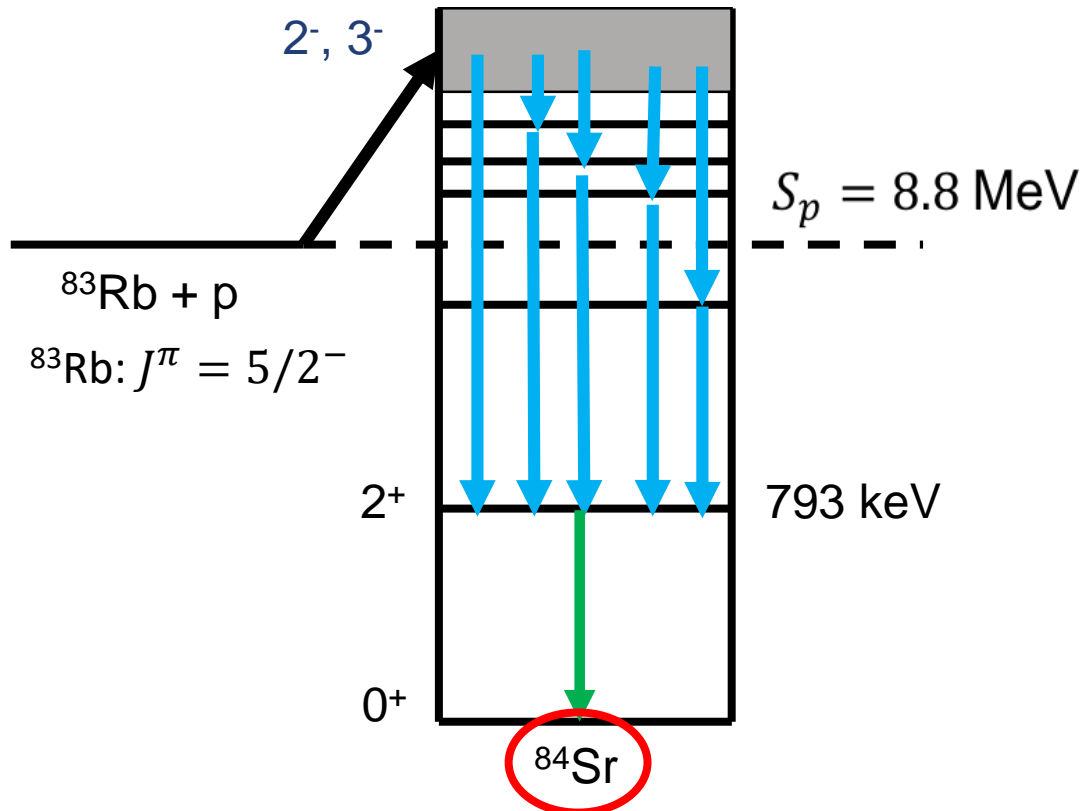
Rapp, W., et al. The Astrophysical Journal 653.1 (2006): 474.

Rayet, M., et al. Astronomy and Astrophysics 298 (1995): 517.

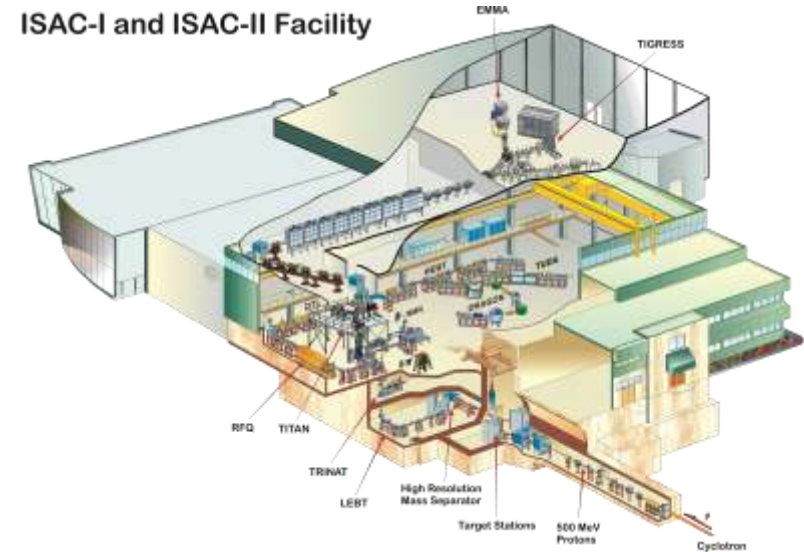
Measurement of $^{83}\text{Rb}(p, \gamma)^{84}\text{Sr}$ at TRIUMF

Can a mass spectrometer and HPGe array be used to measure p-process reactions?

- Targeted $^{83}\text{Rb}(p, \gamma)^{84}\text{Sr}$ reaction (important for ^{84}Sr p-nucleus abundance) using a ^{83}Rb beam intensity of 5×10^7 pps
- Impinged on CH_2 foil targets to populate ^{84}Sr . (thicknesses between 300 and $900 \mu\text{g}/\text{cm}^2$) at bombarding energies of 2.7 and 2.4 A MeV .



ISAC-I and ISAC-II Facility



Use the EMMA mass spectrometer to transmit $A=84$ recoil products to the focal plane detectors.

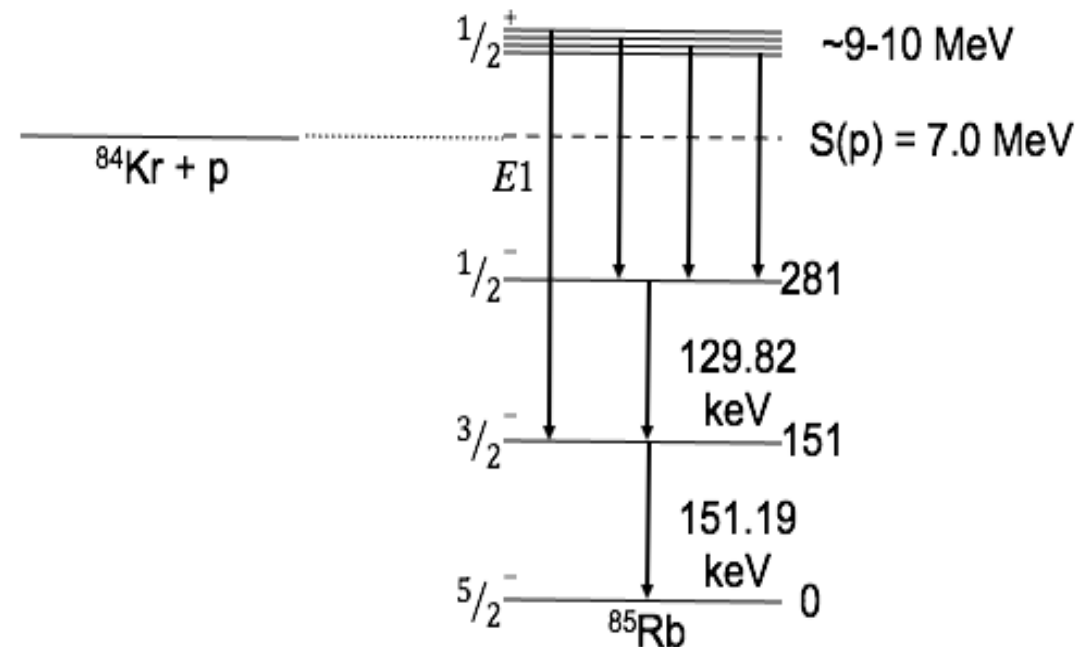
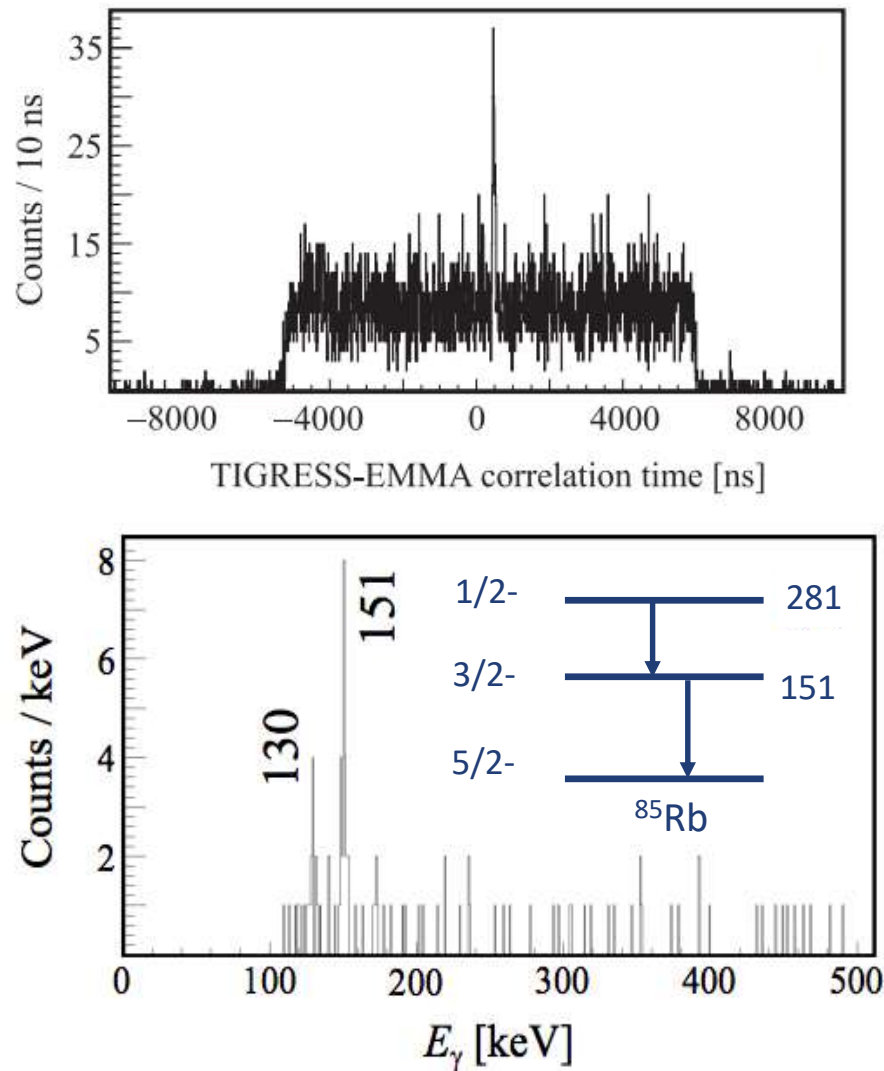
Search for characteristic secondary γ -rays in coincidence with TIGRESS Compton suppressed HPGe array.

12 clovers in use:
x8 at 90° , x4 at 135°

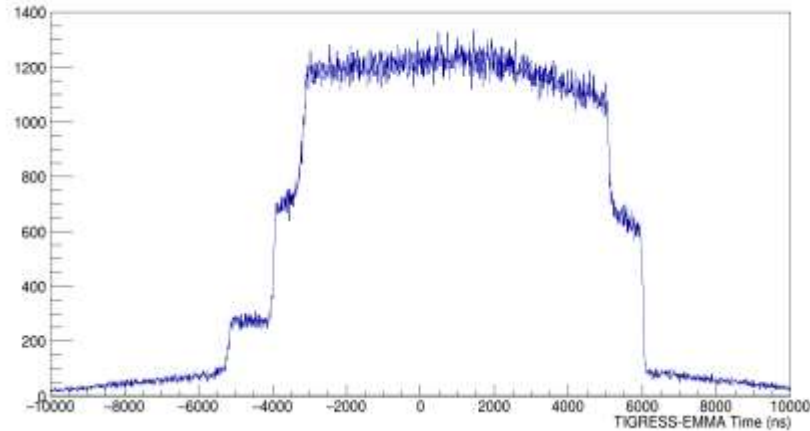
Measurement of $^{84}\text{Kr}(p, \gamma)^{85}\text{Rb}$

Raw beam suppression was enough to see a clear timing correlation peak between TIGRESS and EMMA events.

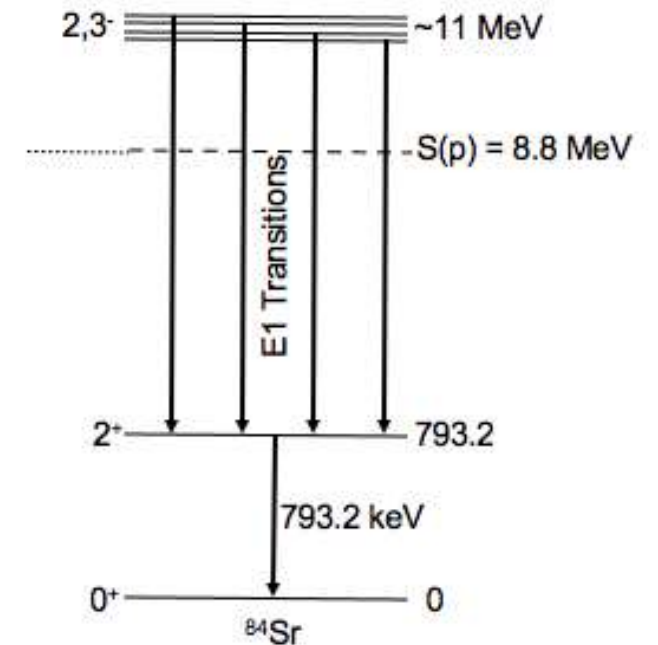
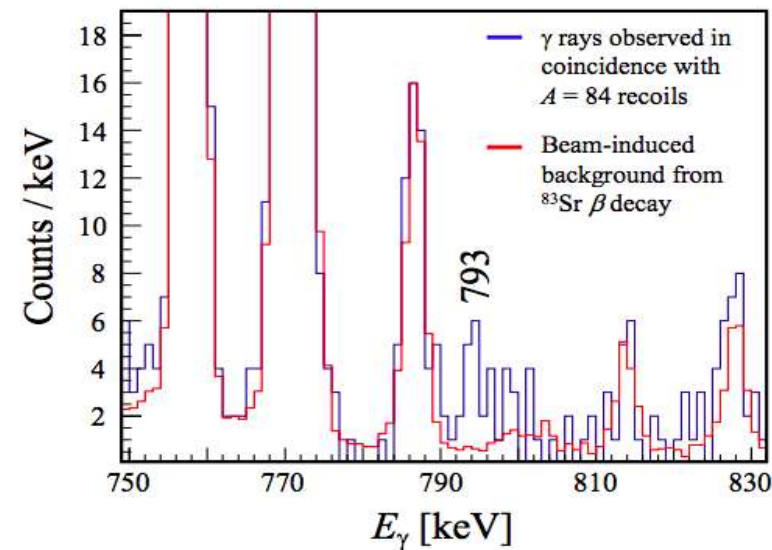
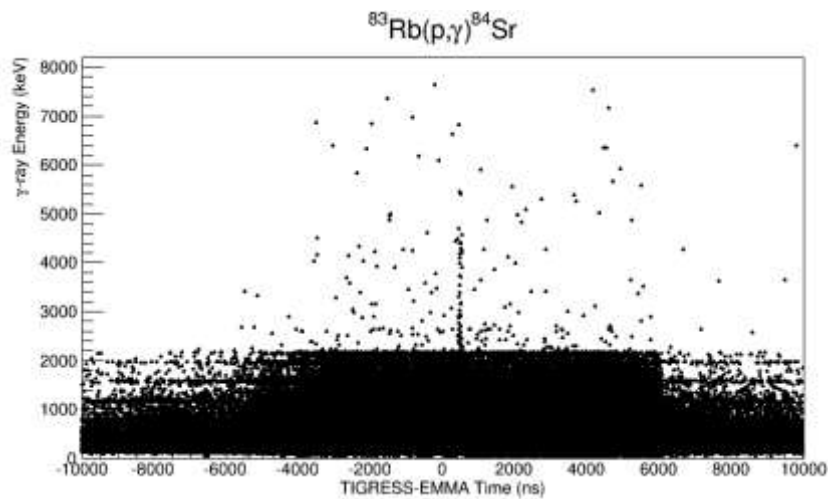
Gating on the timing peak reveals characteristic low-lying γ -rays in the ^{85}Rb final nucleus.



Measurement of $^{83}\text{Rb}(p, \gamma)^{84}\text{Sr}$



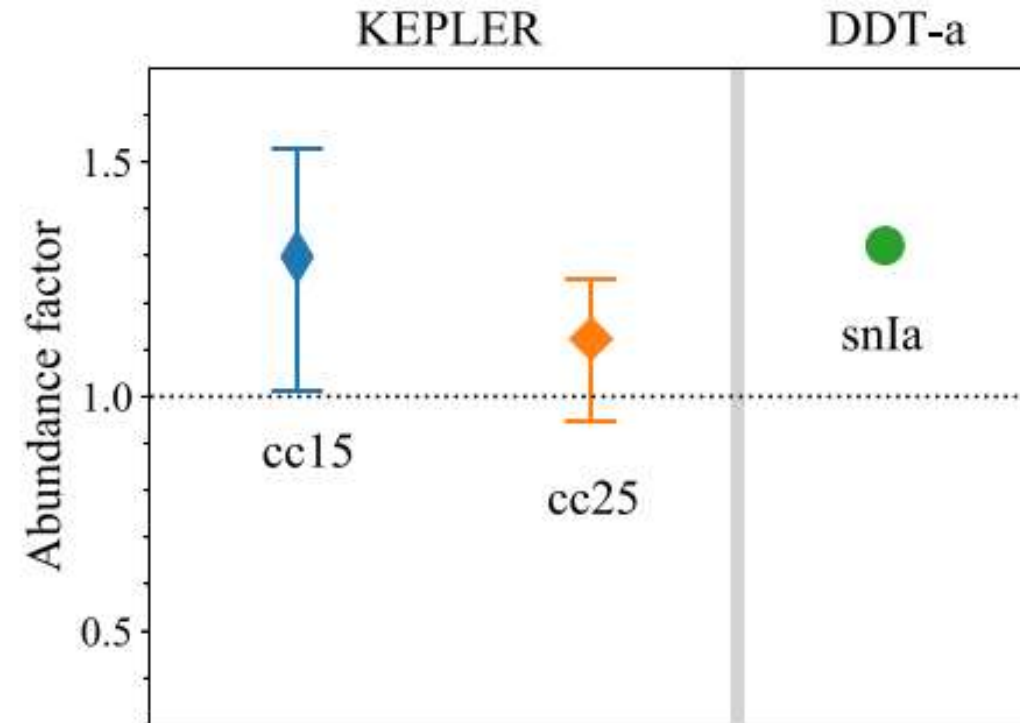
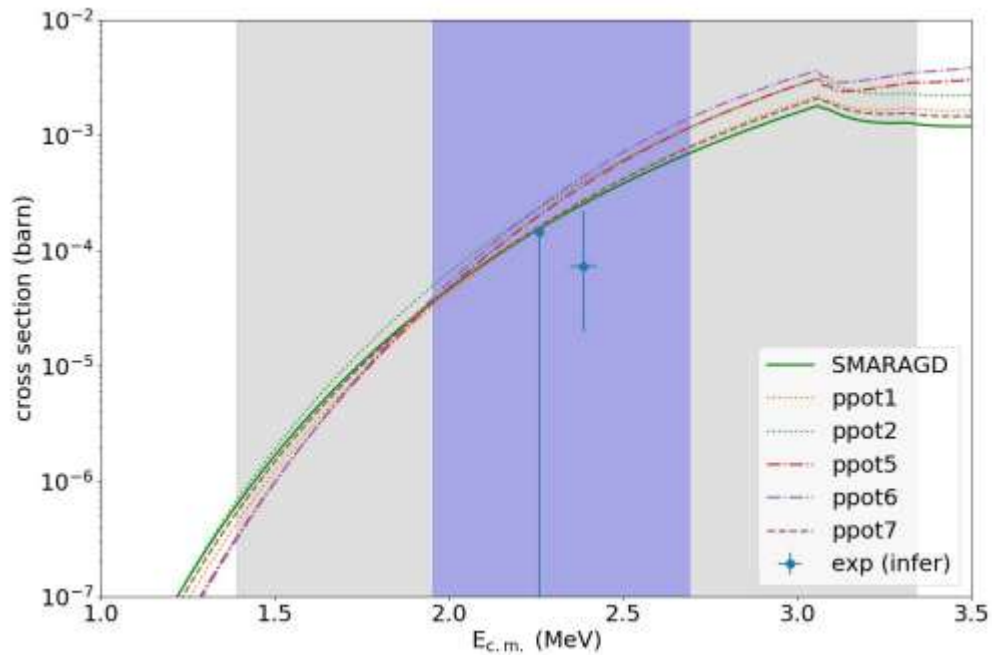
- Large background from ^{83}Sr contamination in the beam, which scatters onto EMMA's entrance aperture \rightarrow obscures the timing peak!
- Plotting γ -ray energy vs the correlation time reveals signal of high energy γ -rays at the expected correlation time.
- Gating around the correlation peak reveals the transition from the first 2^+ to ground state transition in ^{84}Sr . (16 events above background)



First measurement of a p-process reaction with a radioactive beam

Total cross sections are approximately 4x smaller than predicted by statistical models

Result is an increase in the ^{84}Sr abundance produced by supernovae models

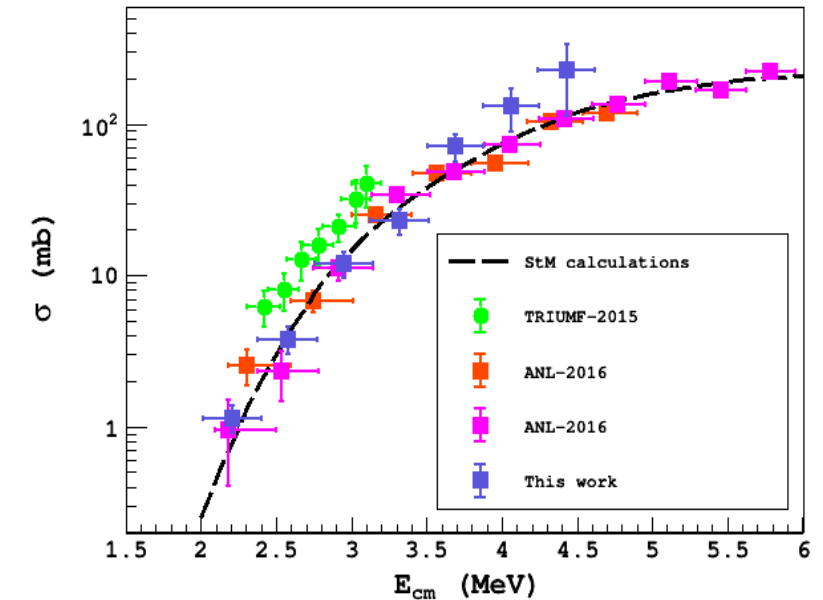
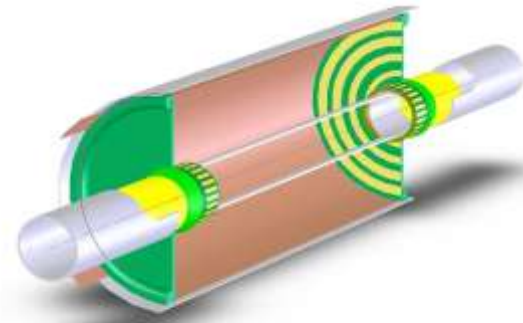
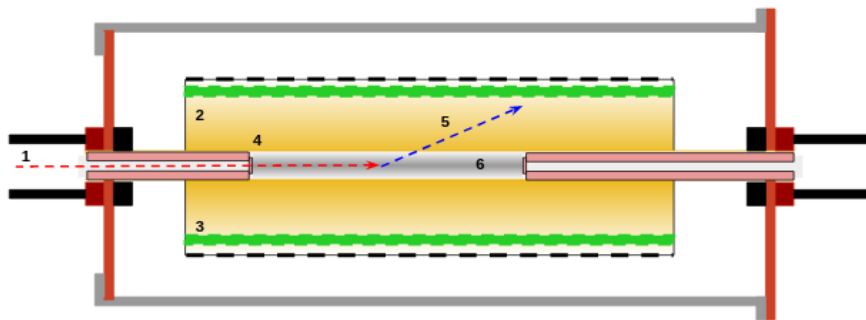


M. Williams, *et al.*, *Phys. Rev. C* **107**, 035803 (2023).

G. Lotay, S. Gillespie, M. Williams, *et al.*, *Phys. Rev. Lett.* **127**, 112701 (2021).

Statistical modeling by T. Rauscher
Astrophysical modeling by N. Nishimura

Newly Commissioned Detector: TACTIC



Active target where the detection medium also acts as the target for (a,p), (p,a) and (a,n) reactions.

Time-projection technique allows vertex reconstruction to find point of interaction.
Can cover multiple energies simultaneously.

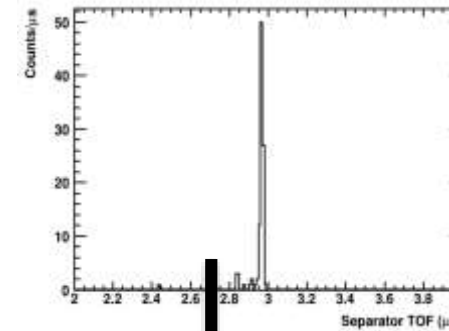
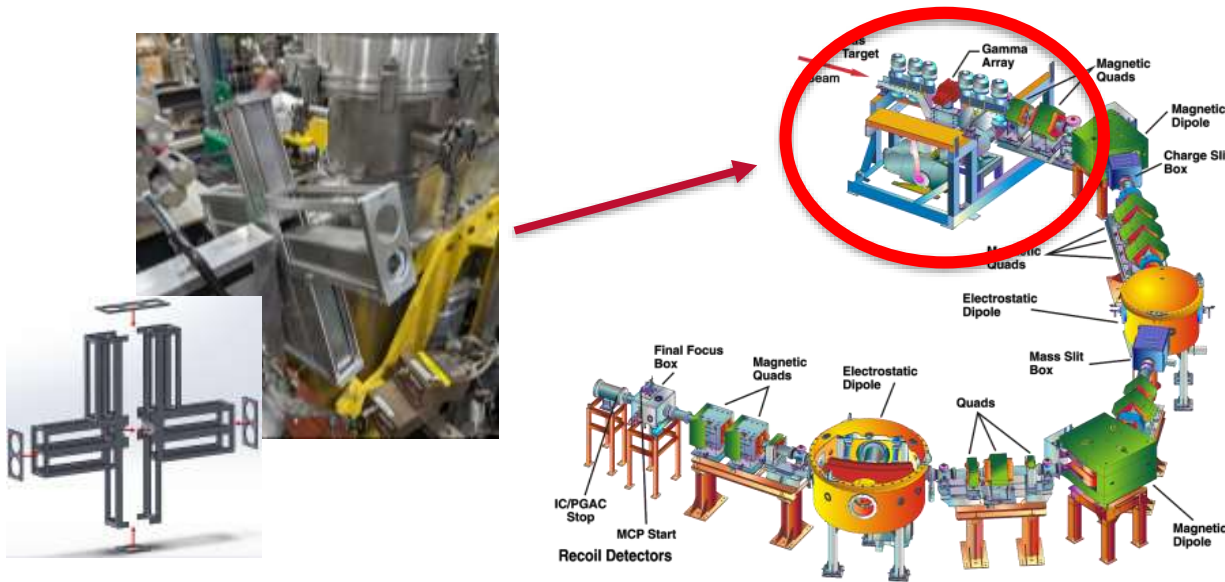
Blind to the central cylinder where the beam passes through, enabling high beam intensities.

Recently commissioned using the $^{23}\text{Na}(a,p)$ reaction with $\frac{1}{4}$ of the detector instrumented.

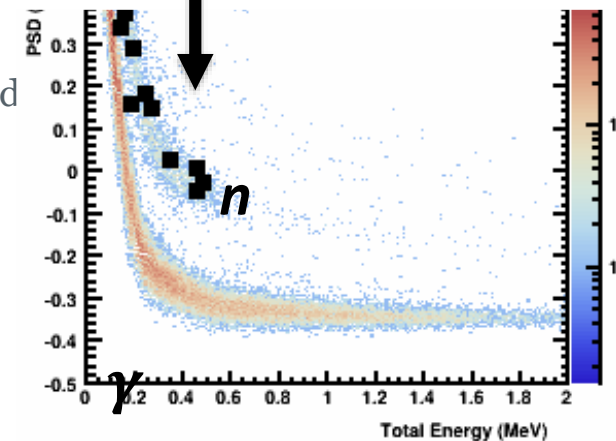
Organic Glass Scintillator Array: DEMAND

Demonstrator array of 8 detectors fixed downstream of the DRAGON gas target

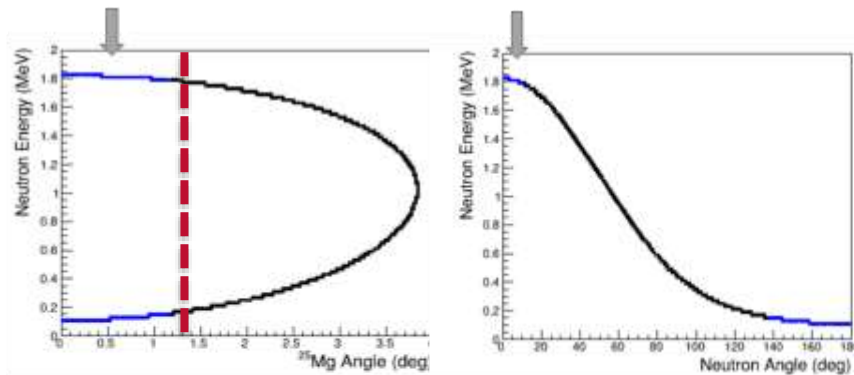
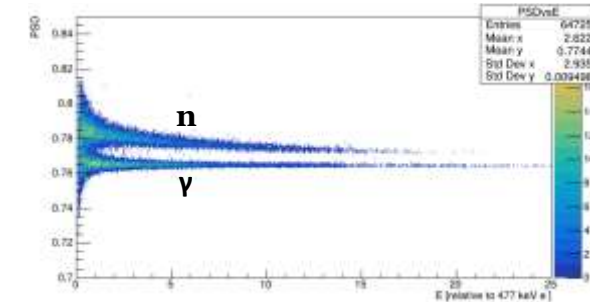
Goal to measure $^{22}\text{Ne}(\alpha, n)^{25}\text{Mg}$ important for the s-process in massive stars



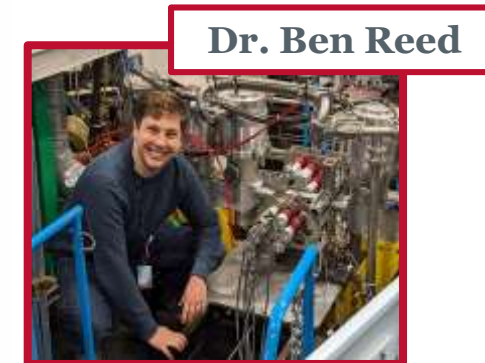
Neutrons in Coincidence with Separator-TOF peak



Neutron-gamma discrimination



The recoil cone goes beyond DRAGON's acceptance so tune to one part of the momentum cone

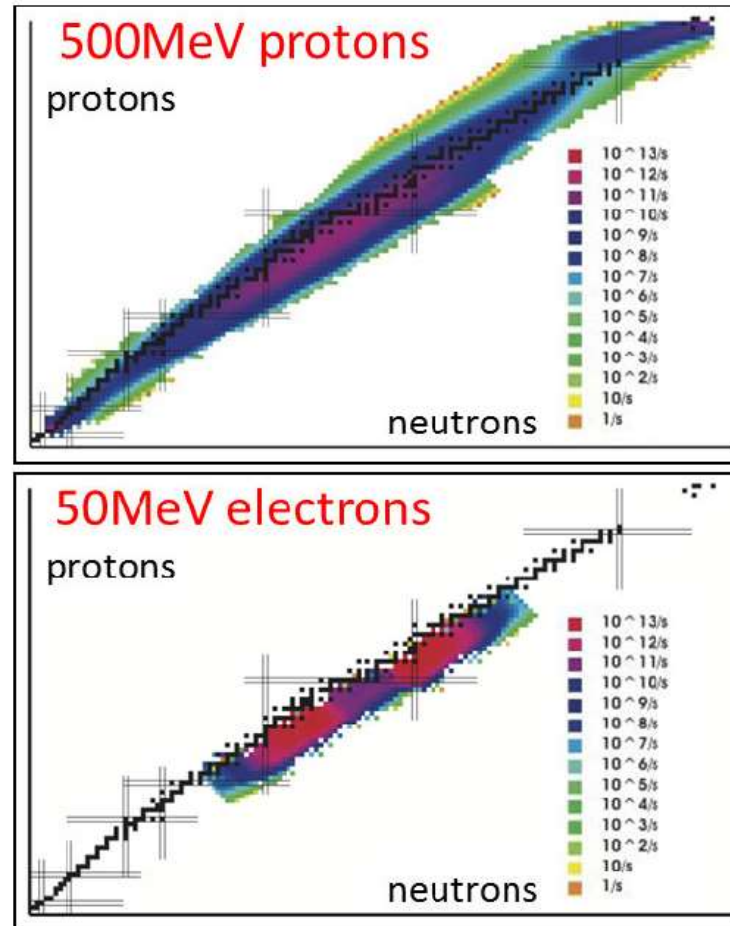


Dr. Ben Reed

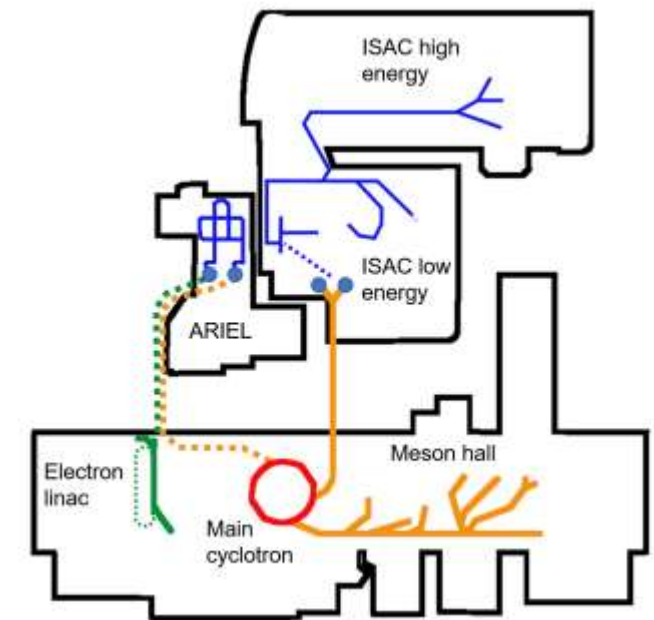
ARIEL: Advanced Rare Isotope Laboratory



The Advanced Rare Isotope Laboratory will use photofission of Uranium induced by an electron beam on a solid stopper



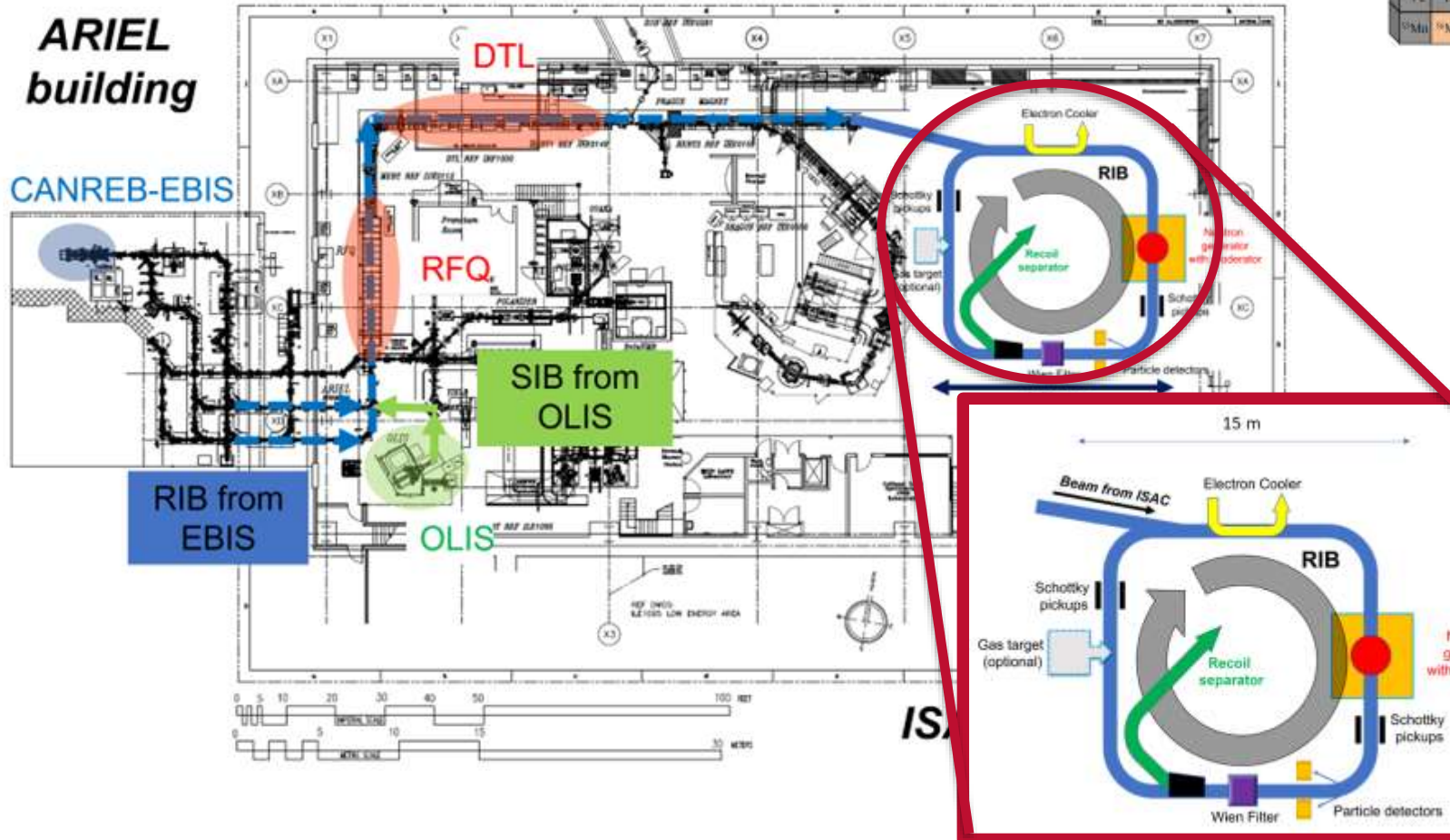
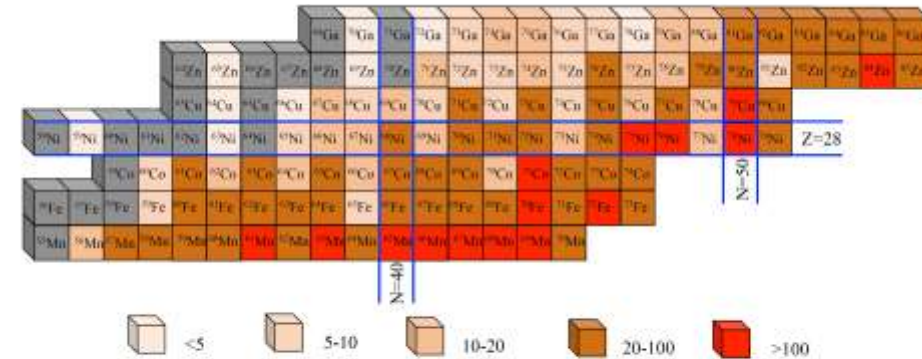
In-target yields concentrated in neutron-rich region of interest for neutron capture driven nucleosynthesis



Future Prospects: TRIUMF Storage Ring

The r-process involves many neutron capture reactions on unstable nuclei for which predicted reaction rates are highly uncertain

Presently no way to directly measure (n,γ) cross-sections on short-lived radioactive nuclei



Storage rings all the beam to circulate through a target continuously, amplifying intensity by orders of magnitude.

Can combine with (d,t) neutron generators to form an effective neutron target (requires R&D feasibility study)

Recoils must be extracted using a Wien Filter and recoil separator (a world-unique concept)

I. Dillmann, et al., Eur. Phys. J. A (2023) 59 :105

- Nuclear Astrophysics continues to be a strong research theme at TRIUMF, with facilities that are well-suited to addressing many outstanding questions on the origin of the elements.
- Several world-firsts have been achieved for direct reaction measurements: First measurement of a p-process reaction with a RIB and first measurement of proton capture using an isomeric beam.
- The ARIEL facility will expand available beams towards neutron rich nuclei important for astrophysics.
- New detector systems and concepts are being developed to target even more reaction rate studies.



UNIVERSITY OF SURREY



UNIVERSITY of York

UNIVERSITY of GUELPH



COLORADO SCHOOL OF MINES

SFU

SIMON FRASER UNIVERSITY



Universität Basel

Bucknell UNIVERSITY

McMaster University 

THE UNIVERSITY OF BRITISH COLUMBIA



SAINT MARY'S UNIVERSITY

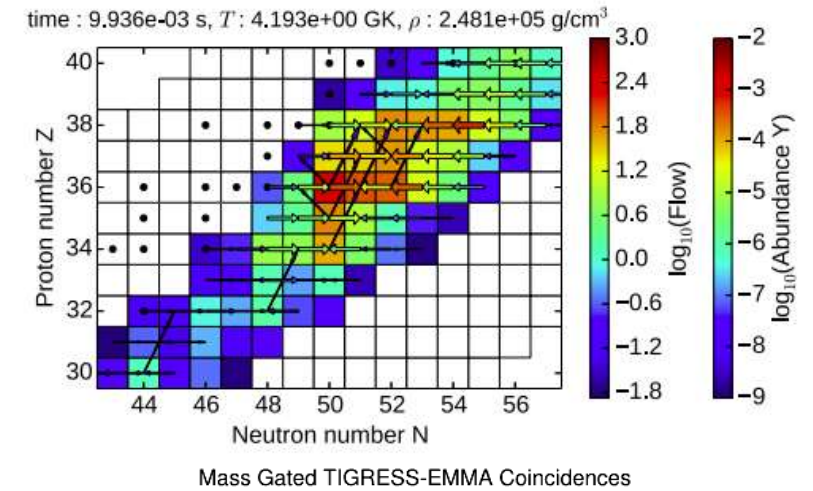
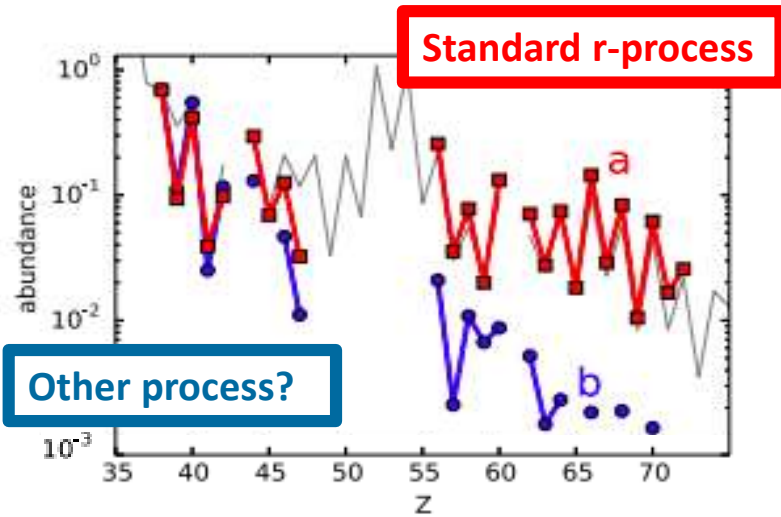
 RIKEN

P. Adsley, A. M. Amthor, D. Baal, G. C. Ball, S. Bhattacharjee, H. Behnamian, V. Bildstein, C. Burbadge, W. N. Catford, B. Davids, P. Dennisenkov, C. Aa. Diget, D. T. Doherty, N. Esker, J.E. Escher, F. H. Garcia, A. B. Garnsworthy, S. A. Gillespie, U. Griefe, G. Hackman, S. Hallam, F. Herwig, K. Hudson, D. Hutcheon, S. Jazrawi, J. Karpesky, E. Kasanda, A. R. L. Kennington, Y. H. Kim, A. M. Laird, A. Lennarz, G. Lotay, M. Lovely, R. S. Lubna, C. Natzke, N. Nishimura, B. Olaizola, S.D. Pain, C. Paxman, G. Potel, A. Psaltis, T. Rauscher, A. Ratkiewicz, C. Ruiz, C. E. Svensson, B. Wallis, J. Williams, M. Williams and D. Yates.

Heavy elements synthesis in the early universe

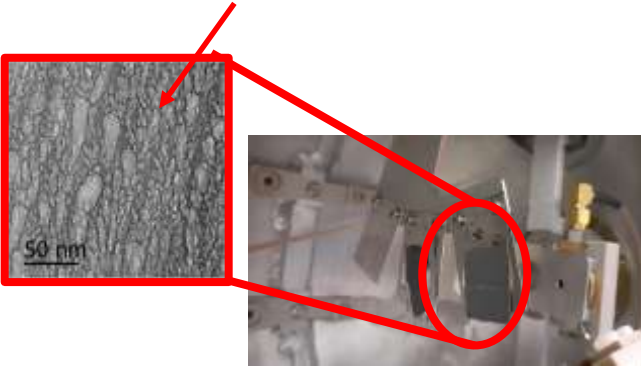
Many of the oldest stars show an over-abundance in mid-mass elements ($Z \sim 50$) relative to the typical r-process pattern.

Were other processes active in the early universe?

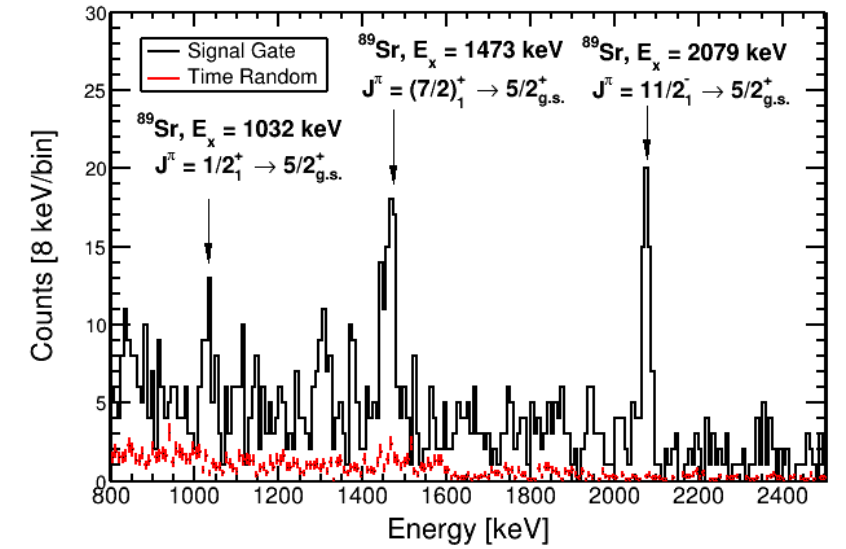
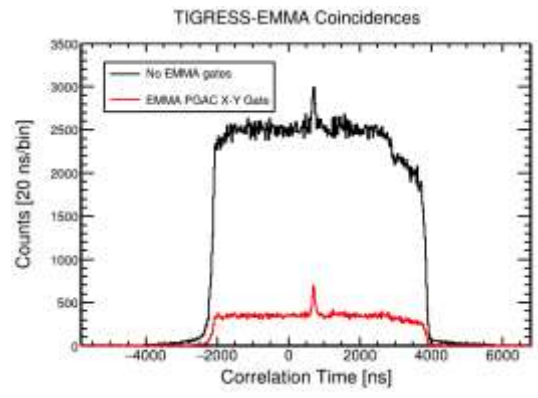


A weak r-process in SNe winds?

Helium Nano-pockets

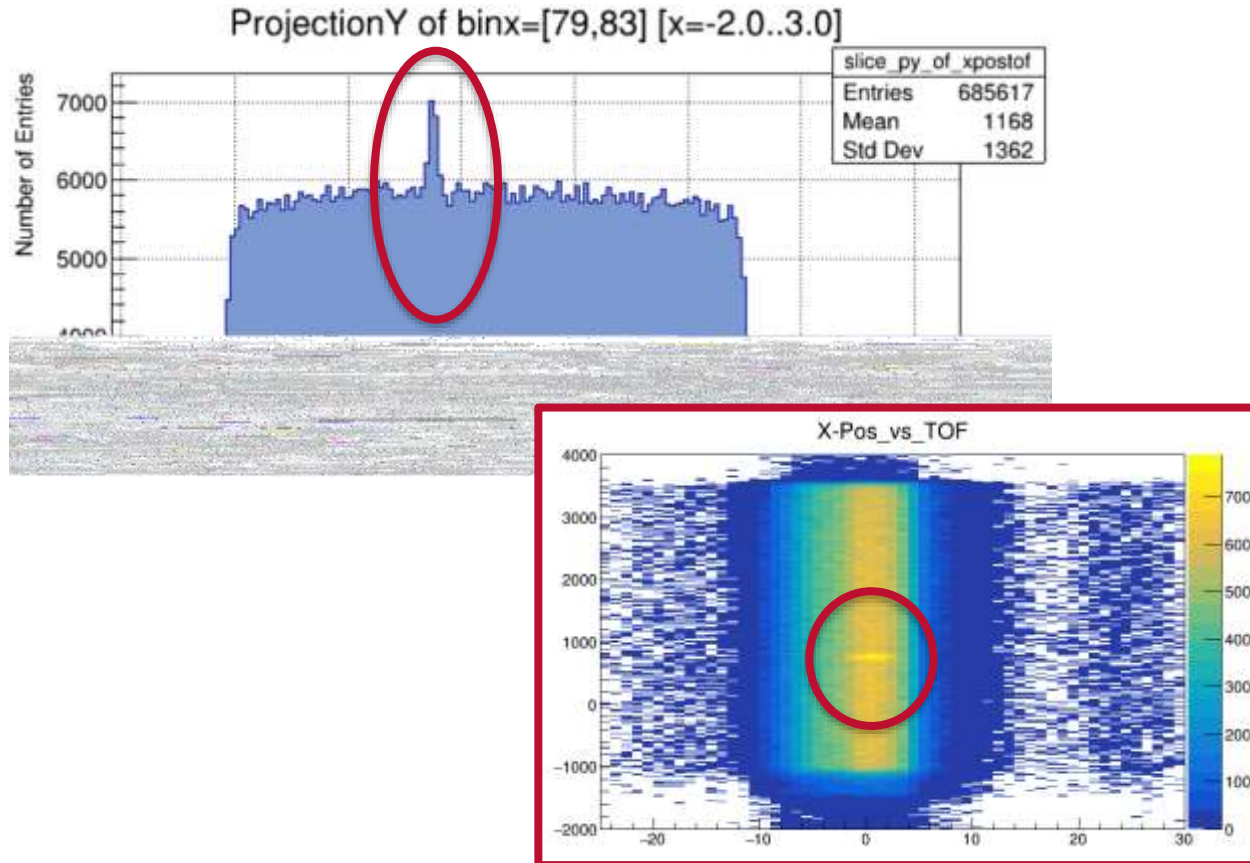


Test measurement on $^{86}\text{Kr}(\alpha, n)^{89}\text{Sr}$

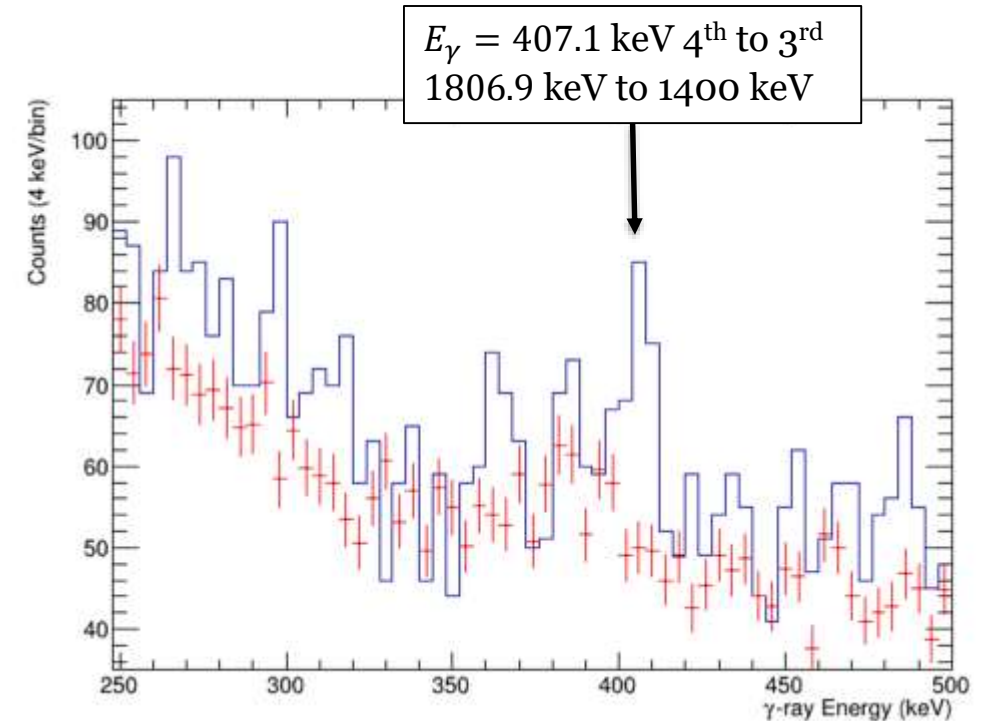


Measurement of $^{94}\text{Sr}(\alpha,n)^{97}\text{Zr}$ December 2023

See clear timing peak when gated on PGAC X-position from -2 to 3 mm



Still identifying γ -rays from ^{97}Zr . The dominant transition from the 4th to 3rd excited state appears clear

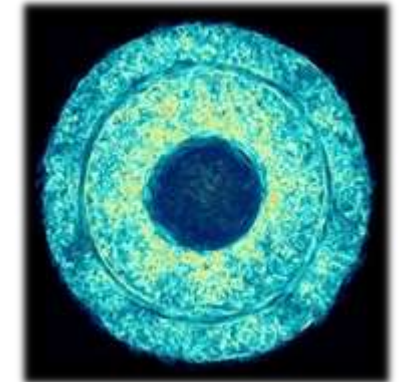
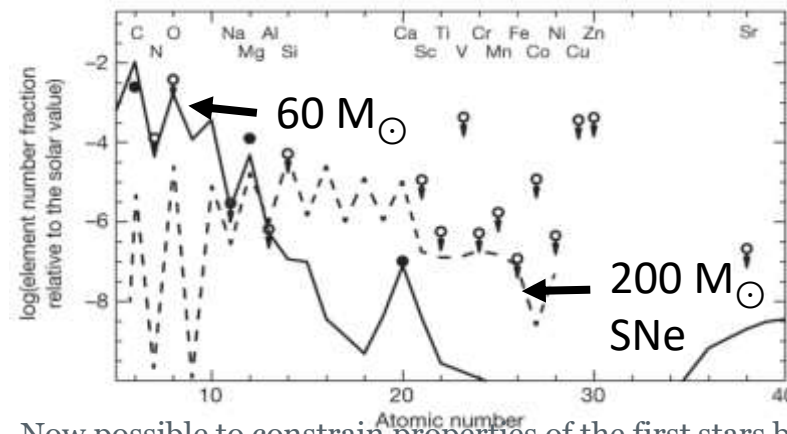


Stellar Archaeology

The first stars (Pop-III) were formed from pristine material left over from the Big Bang

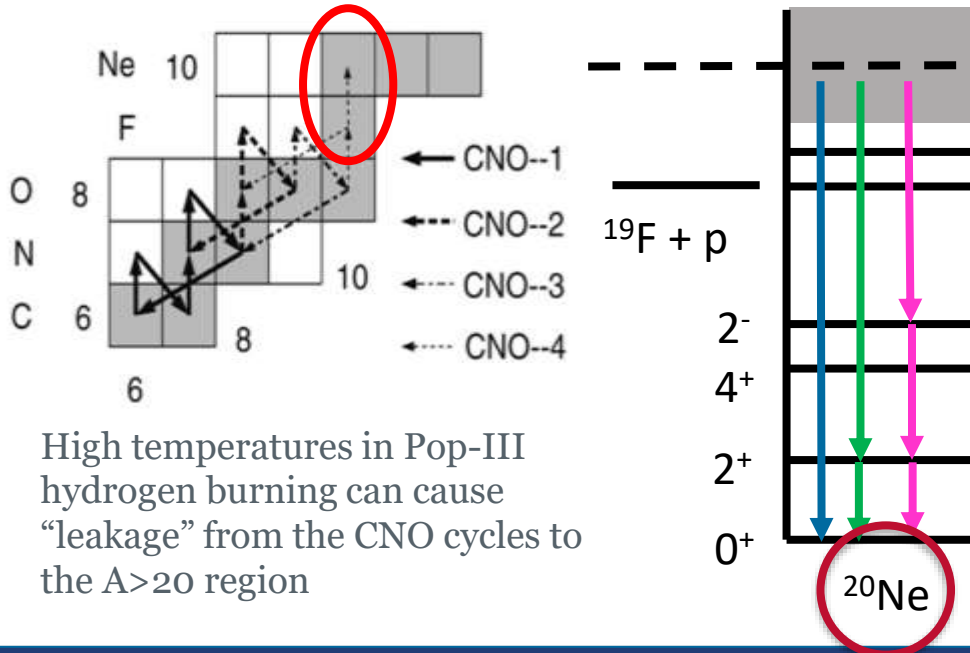
Big Questions:

- What elements were produced by the first stars?
- How did the first stars evolve?
- What was their fate?

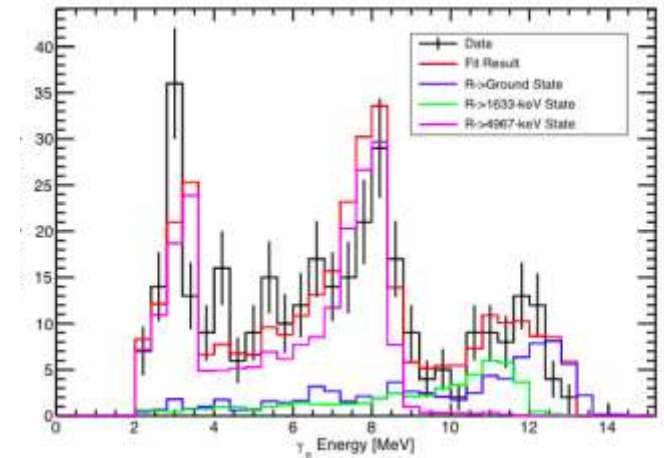
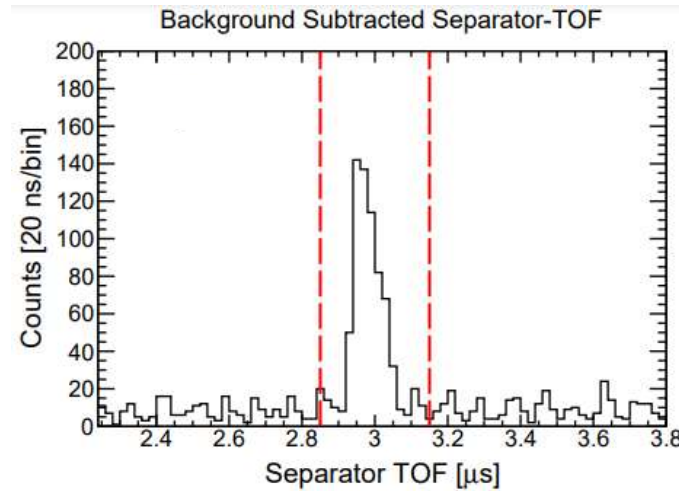


Believed to be very massive, Pop-III stars died away quickly making direct observation very challenging even for JWST.

Now possible to constrain properties of the first stars by combining sophisticated 3D models with observations of very old Pop-II stars that preserve elemental signatures from Pop-III



High temperatures in Pop-III hydrogen burning can cause “leakage” from the CNO cycles to the $A > 20$ region

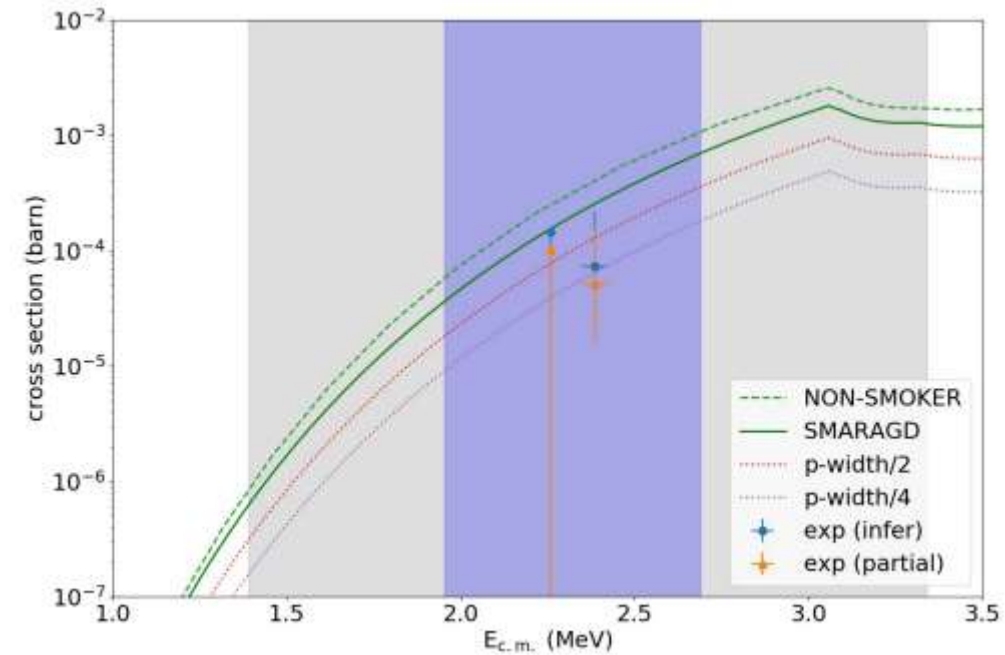
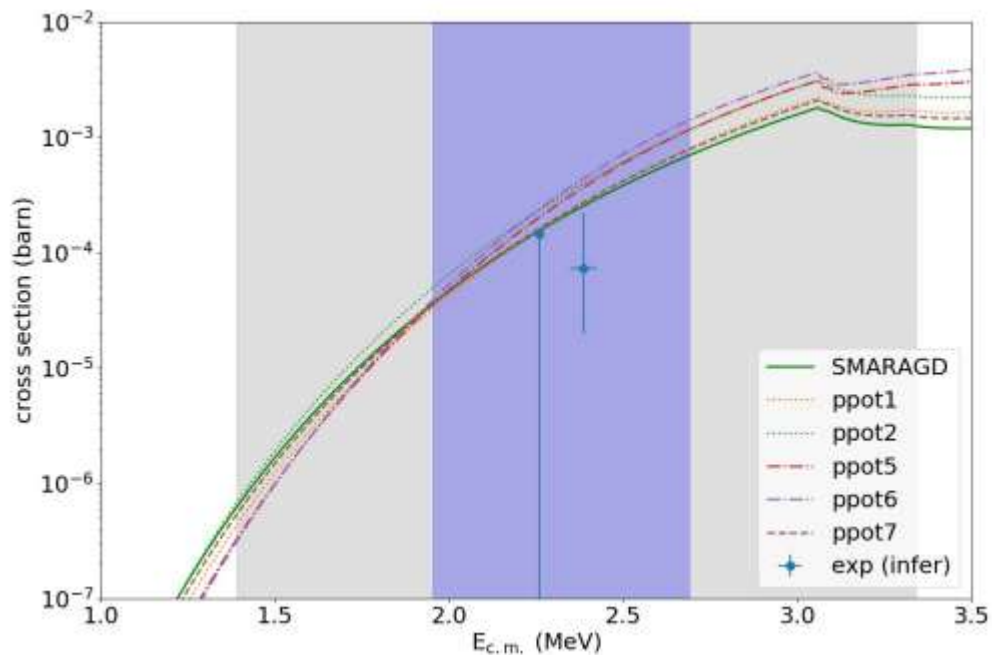


M. Williams, *et al.*, Phys. Rev. C **103**, 055805 (2021)

First measurement of a p-process reaction with a radioactive beam

Partial cross-section is converted to the full reaction cross section using γ -cascade models (included in the SMARAGD code), which predict $71 \pm 10\%$ of (p, γ) reactions result in a $2^+ \rightarrow 0^+(\text{g.s.})$ decay.

Total cross sections are approximately 4x smaller than predicted by Hauser-Feshbach models



M. Williams, *et al.*, *Phys. Rev. C* **107**, 035803 (2023).

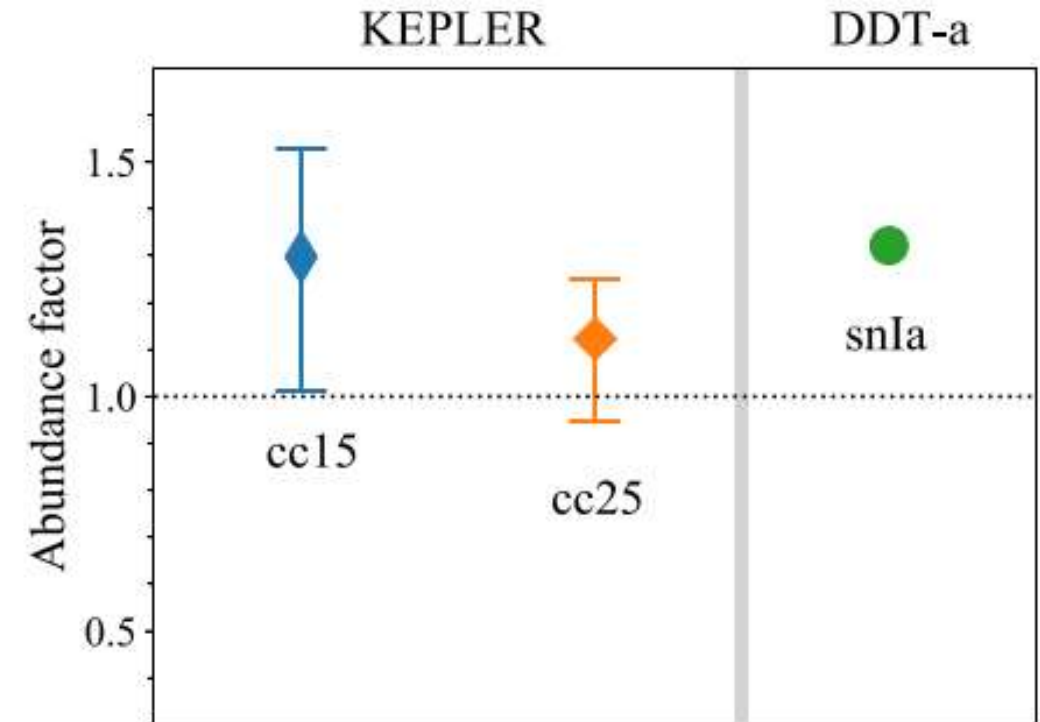
G. Lotay, S. Gillespie, M. Williams, *et al.*, *Phys. Rev. Lett.* **127**, 112701 (2021).

Statistical modeling by T. Rauscher

Astrophysical impact of $^{83}\text{Rb}(p, \gamma)^{84}\text{Sr}$ measurement

Impact investigated for both Type II and Type Ia supernovae explosions

- Lower $^{83}\text{Rb}(p, \gamma)^{84}\text{Sr}$ cross-section leads to less efficient destruction of the ^{84}Sr p-nucleus in supernovae, raising its production factor.
- The total uncertainty in ^{84}Sr production is reduced by a factor of 2 from previous sensitivity study.
- Uncertainties represent the combined effect of all reaction rates variations – not just $^{83}\text{Rb}(p, \gamma)^{84}\text{Sr}$.
- Abundance enhancement not sufficient to explain enhanced ^{84}Sr seen in Allende Meteorite, but could relieve tension – full GCE simulations required!

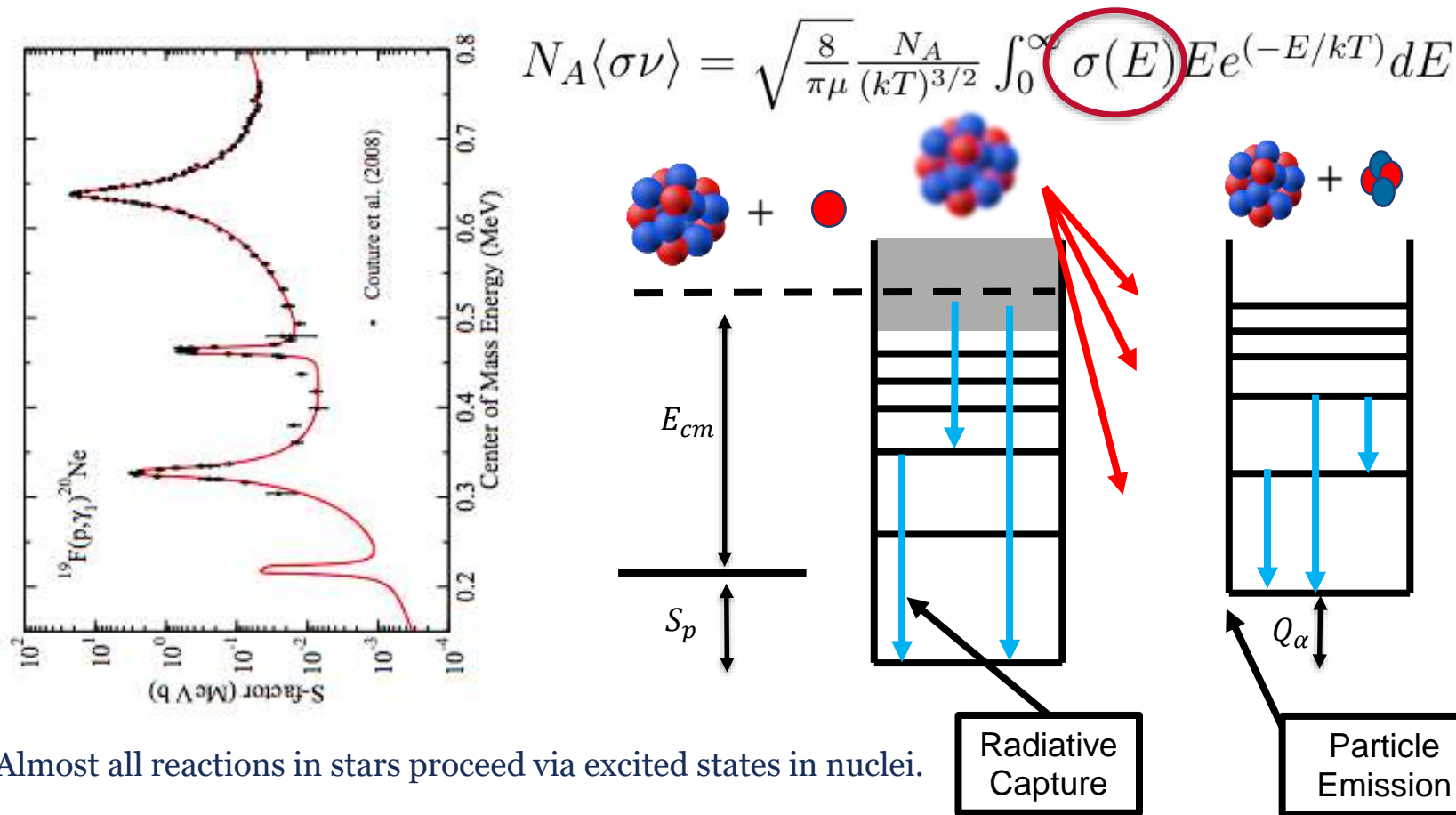


$15 M_{\odot}$ CCSNe = +30 %
 $25 M_{\odot}$ CCSNe = +12 %
 Type 1a SNe = +32 %

M. Williams, *et al.*, *Phys. Rev. C* **107**, 035803 (2023).

Astrophysical modeling by N. Nishimura

Nuclear Reactions in Stars



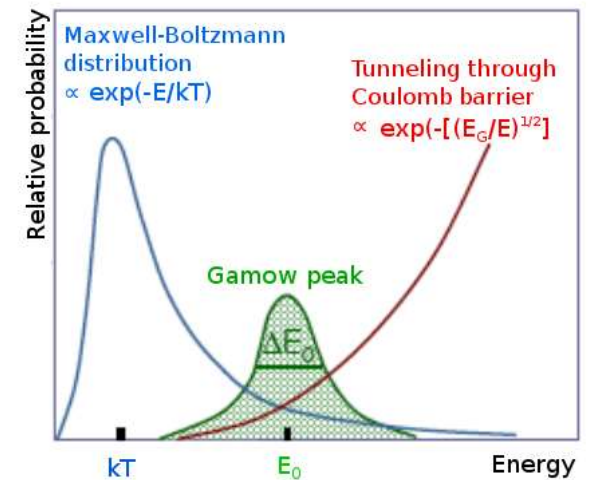
- Cross-section determined by:**
- Number of states.
 - Energies of states.
 - Spin & parity of states.
 - Total and partial decay widths.

Almost all reactions in stars proceed via excited states in nuclei.

Proton-, alpha- and neutron-induced reactions being the most common.

Direct Methods: Measure a nuclear reaction cross-section at the relevant energies for astrophysics

Indirect Methods: Measure properties of the nucleus & nuclear states that influence the cross-section



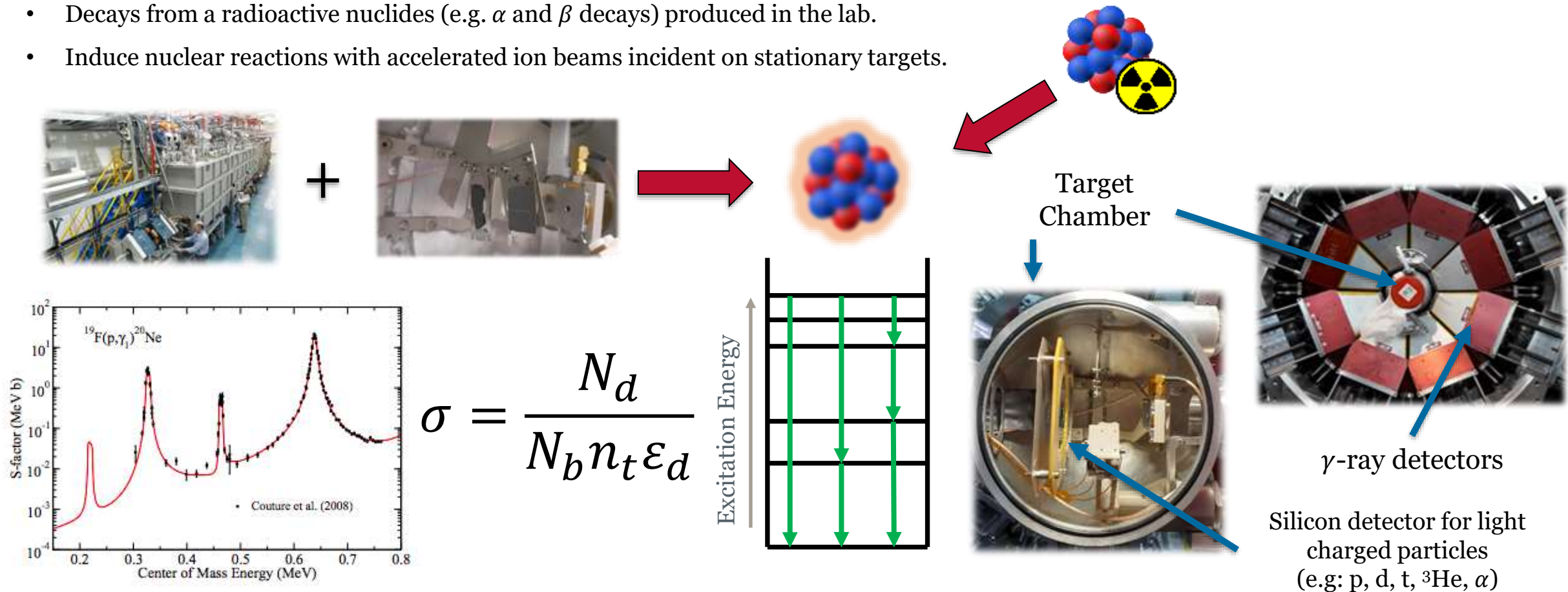
Nuclear Reactions in the Lab

Direct Methods: Measure a nuclear reaction cross-section at the relevant energies for astrophysics

Indirect Methods: Measure properties of the nucleus & nuclear states that influence the cross-section

How do we access excited nuclear states?

- Decays from a radioactive nuclides (e.g. α and β decays) produced in the lab.
- Induce nuclear reactions with accelerated ion beams incident on stationary targets.



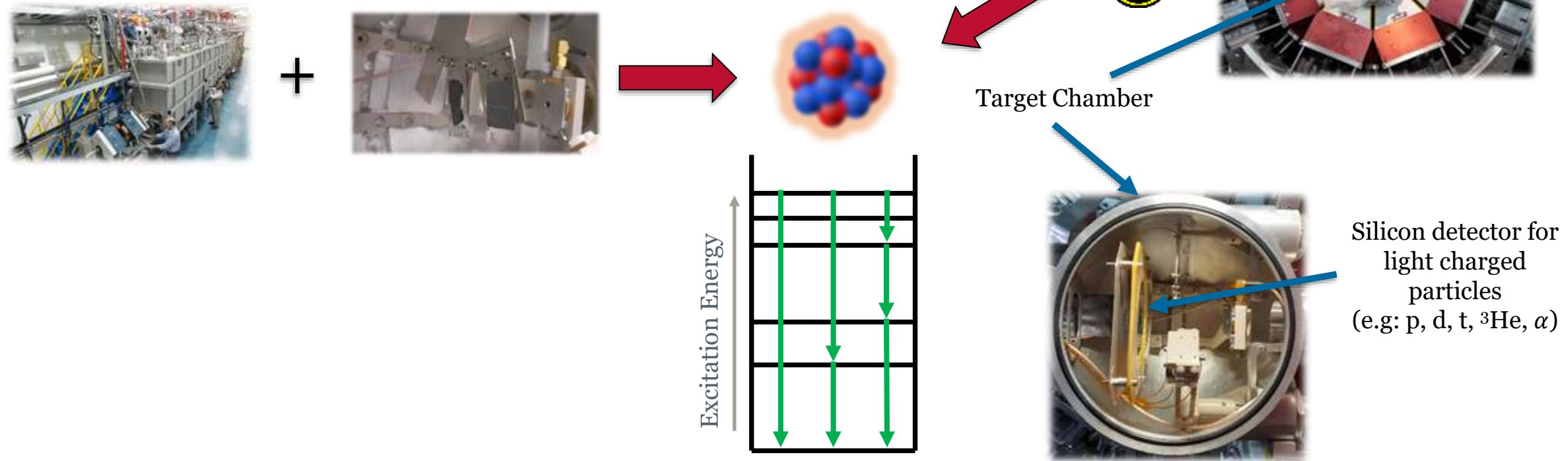
Nuclear Reactions in the Lab

Direct Methods: Measure a nuclear reaction cross-section at the relevant energies for astrophysics

Indirect Methods: Measure properties of the nucleus & nuclear states that influence the cross-section

How do we access excited nuclear states?

- Decays from a radioactive nuclides (e.g. α and β decays) produced in the lab.
- Induce nuclear reactions with accelerated ion beams incident on stationary targets.



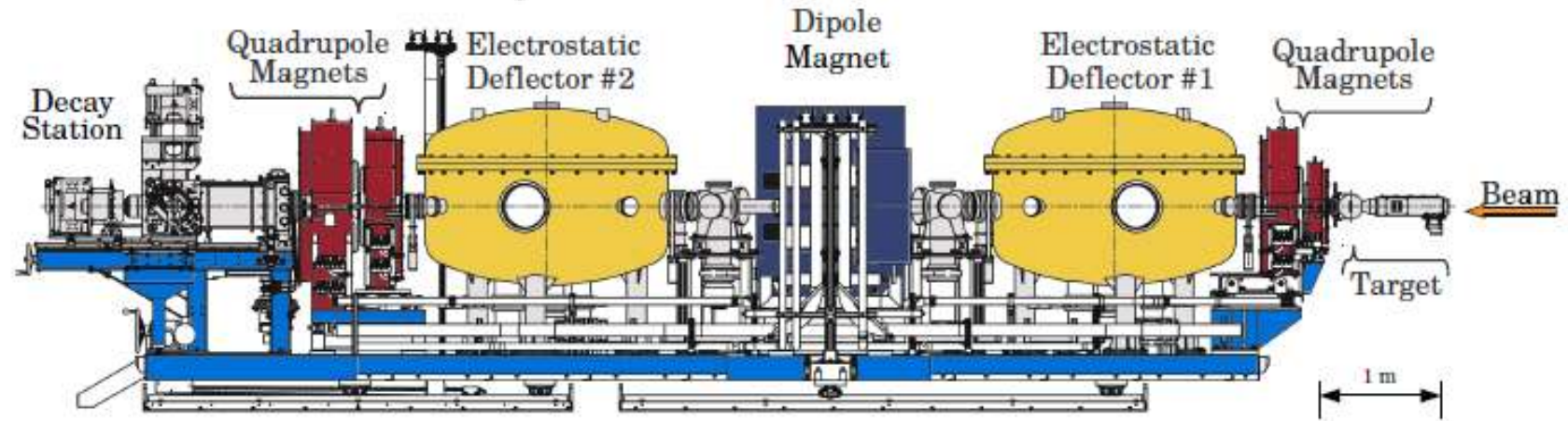
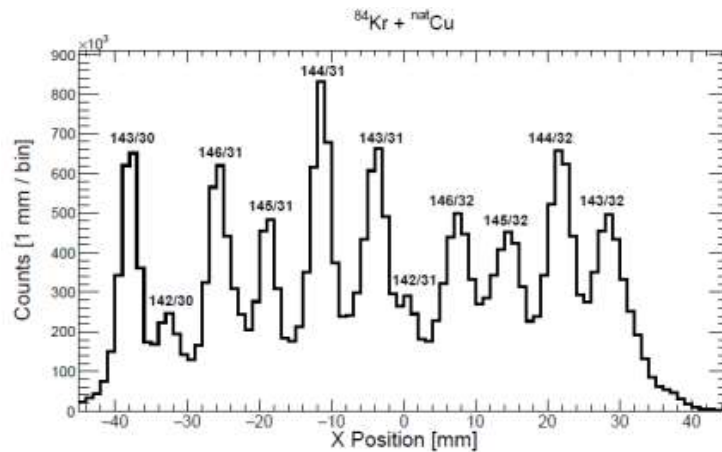
My Research at TRIUMF: the EMMA spectrometer

Challenges: Many different reactions are possible or even (more likely) no reaction at all.

$$\mathbf{F} = q(\mathbf{E} + \mathbf{v} \times \mathbf{B})$$

$$\rho_B = \frac{|\mathbf{p}|}{q} \approx \frac{\sqrt{2mT}}{q|\mathbf{B}|}, \quad \rho_E = \frac{2T}{q|\mathbf{E}|}$$

Electrostatic Deflector



My Research at TRIUMF: Commissioning the EMMA Spectrometer

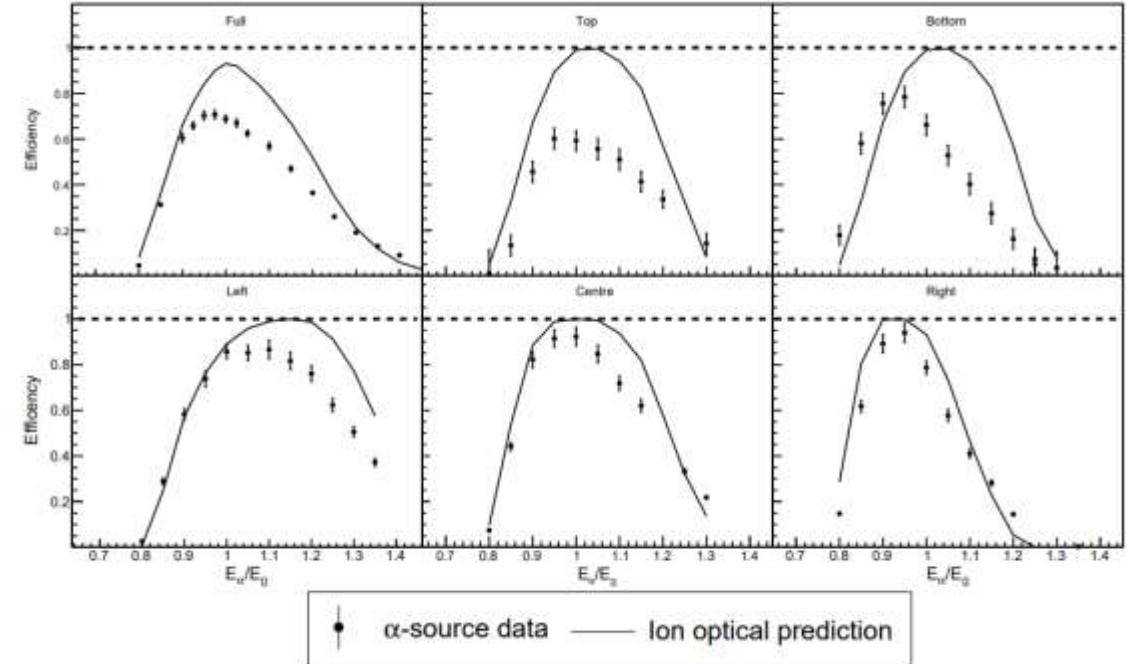
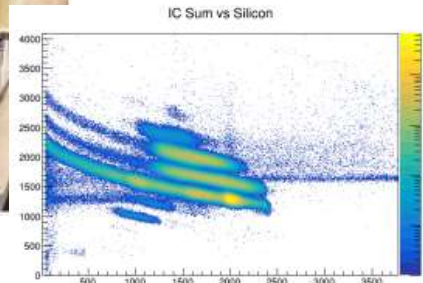


Assembled and installed the electrostatic dipoles



Mapping transport efficiency of EMMA as a function of energy and angle using a monoenergetic alpha source and apertures with different angular coverages.

Field mapping and calibration of quadrupole magnet lenses



Installed, tested and commissioned the focal plane detectors including the data acquisition system.

PGAC, Ion-chamber, Silicon Detector

M. Williams, PhD Thesis (2018)

B. Davids, M. Williams, N.E. Esker *et al.*, *Nucl. Instr. Meth. A* **930**, 191-195 (2019).

M. Williams, K. Hudson, B. Davids, *et al.*, in preparation.

First experiment with EMMA: Measurement of $^{83}\text{Rb}(p,\gamma)^{84}\text{Sr}$

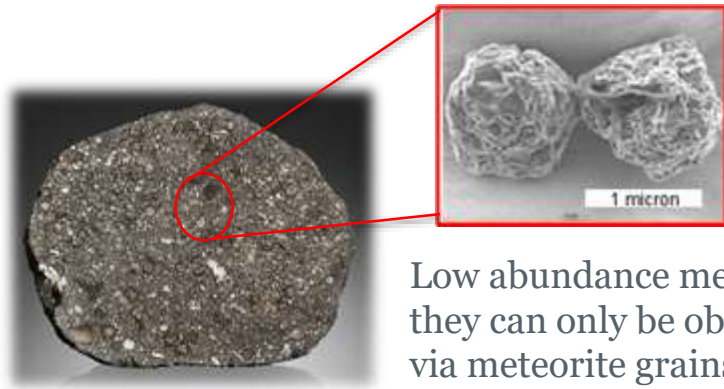
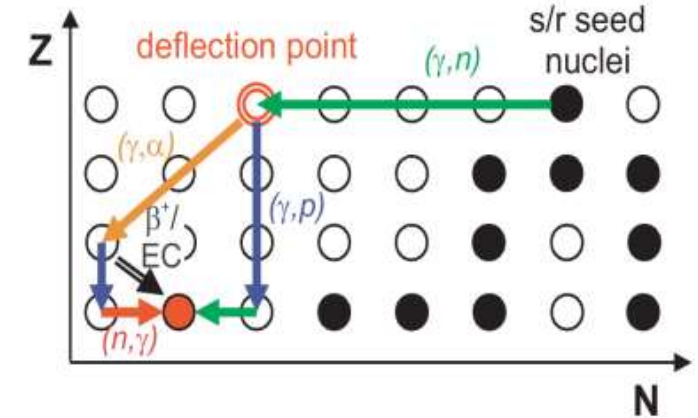
~30 stable isotopes cannot be produced by neutron capture processes.



Best Candidate: Core-collapse supernovae of massive stars.



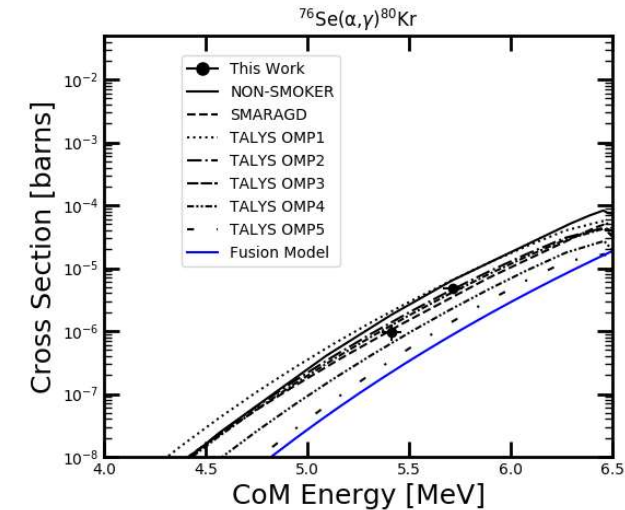
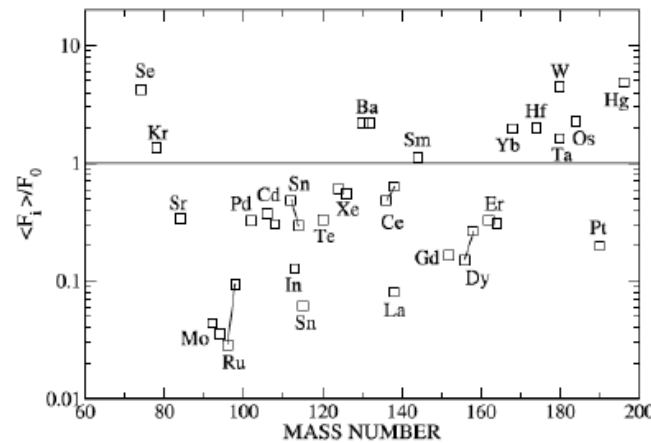
High temperatures cause stable seed nuclei to shed neutrons



Low abundance means they can only be observed via meteorite grains...

...but their origin is a mystery

There are (were) no measurements of a p-process reaction cross-section with a radioactive ion beam!

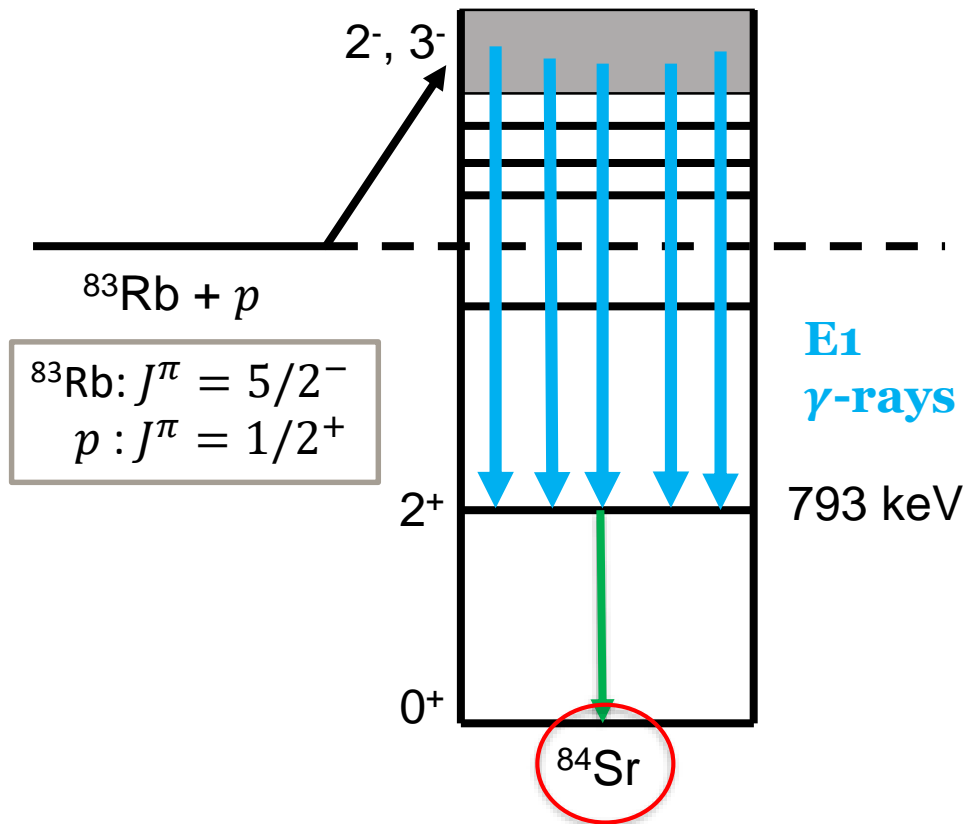


Observed abundances vary from model predictions by orders of magnitude in some cases.

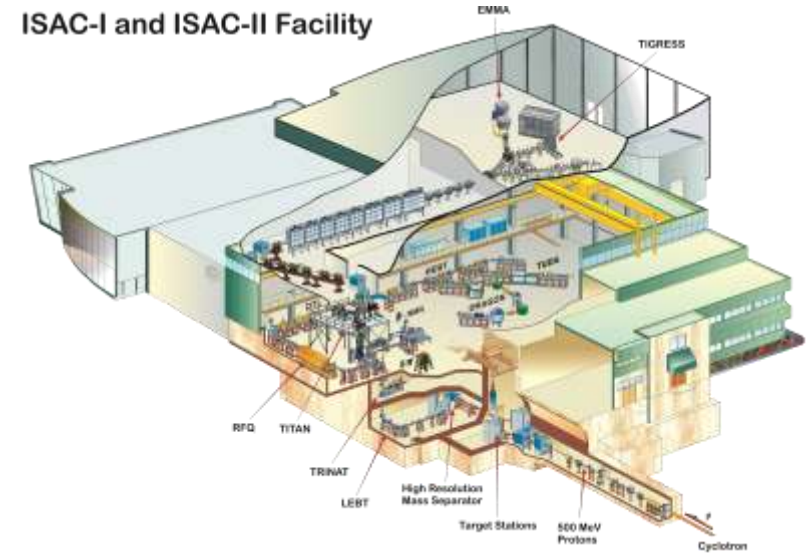
First Science Measurement with EMMA

Measured $^{83}\text{Rb}(p,\gamma)^{84}\text{Sr}$ reaction, which is the reverse of $^{84}\text{Sr}(\gamma,p)^{83}\text{Rb}$ which governs destruction of the p-nucleus ^{84}Sr .

- Produced a radioactive ^{83}Rb beam at TRIUMF by impinging 500 MeV protons on a ZrC_x target.
- ^{83}Rb beam was incident on CH_2 foils to populate ^{84}Sr at bombarding energies of 2.7 and 2.4 A MeV.



ISAC-I and ISAC-II Facility

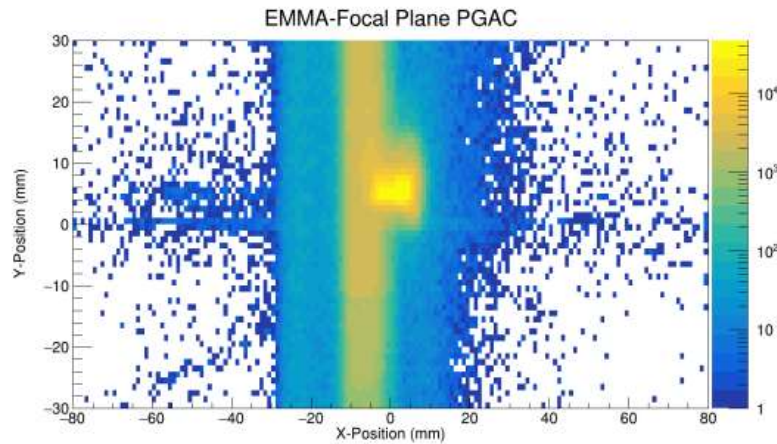


Use EMMA to select $A=84$ recoil products

Search for characteristic secondary γ -rays using TIGRESS HPGe Array in coincidence with recoil events.

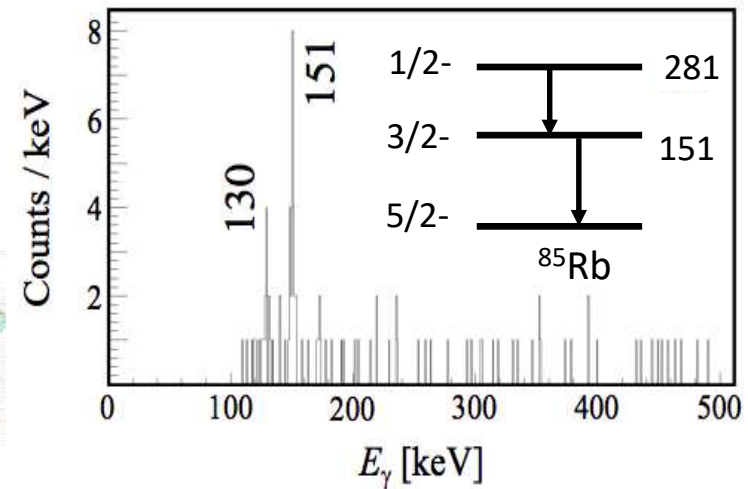
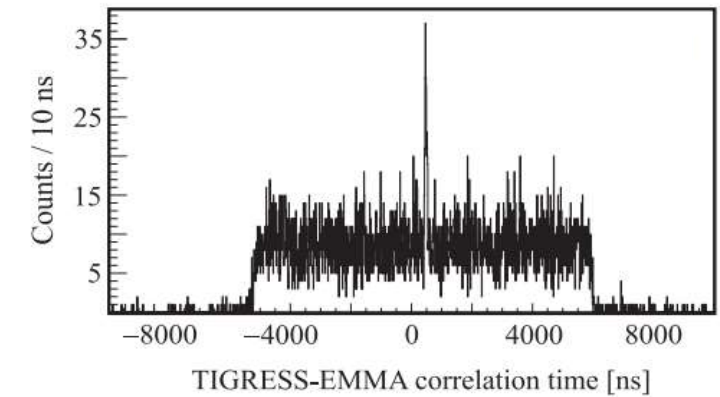
First Science measurement with EMMA

First tested method using a stable ^{84}Kr beam

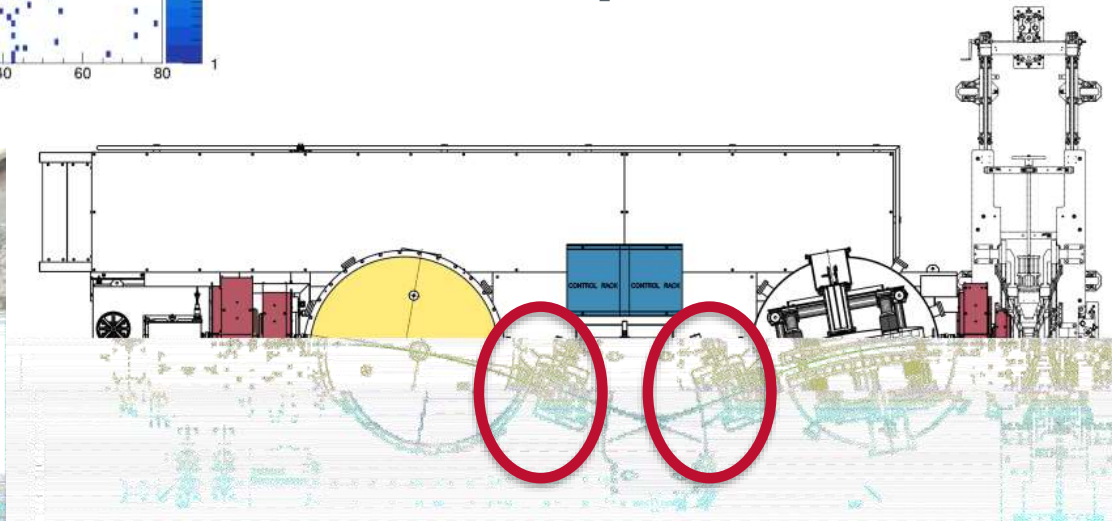


EMMA designed to maximise acceptance at the expense of beam suppression... opposite of what p-process reactions demand.

Needed to close-down focal plane slits and beam suppression slits to obtain workable beam-rate at focal plane.

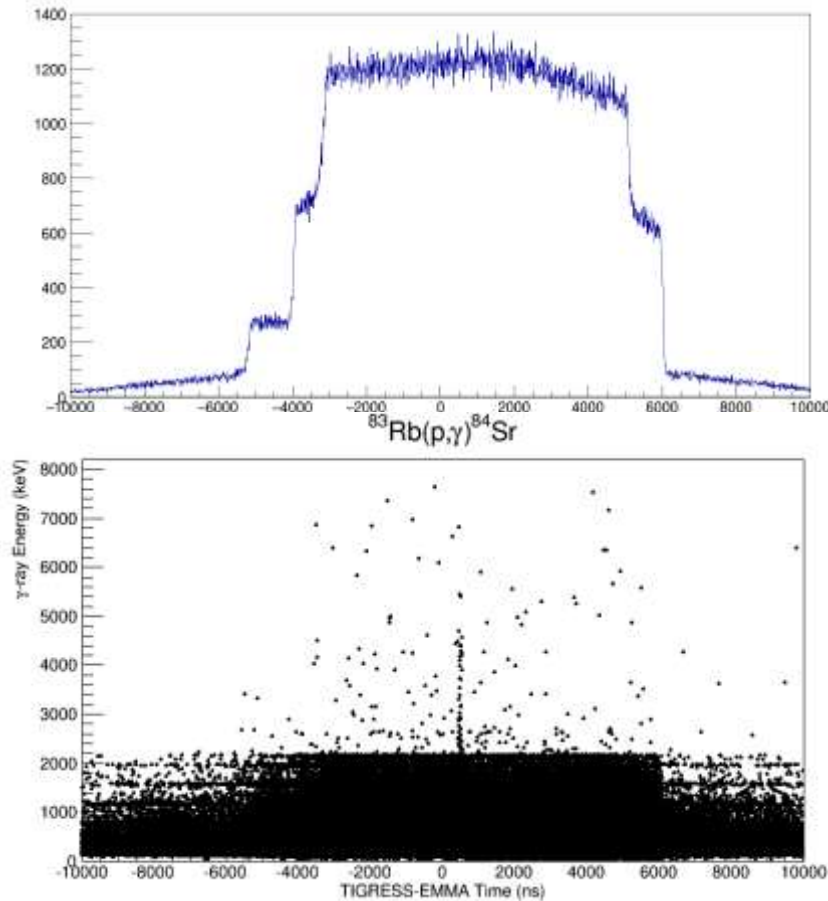


Focal Plane Slits

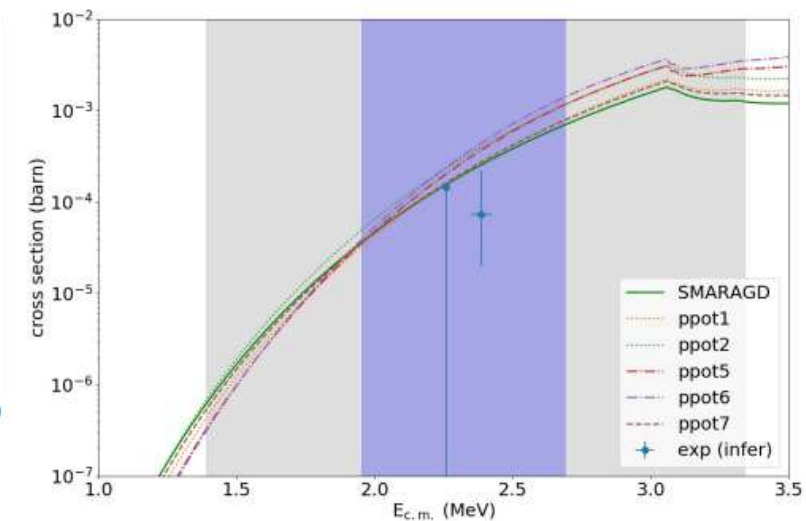
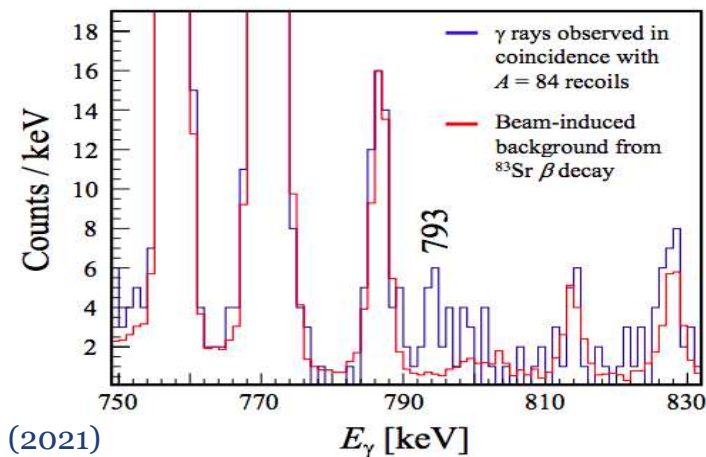


Beam suppression slits

First Science Measurement with EMMA



- Large background from ^{83}Sr contamination in the beam, which scatters onto EMMA's entrance aperture \rightarrow obscures the timing peak!
- Plotting γ -ray energy vs the correlation time reveals signal of high energy γ -rays at the expected correlation time.
- Gating around the correlation peak reveals the transition from the first 2^+ to ground state transition in ^{84}Sr . (16 events above background)
- Allowing the first-ever cross-section measurement of a p-process reaction with a radioactive beam.

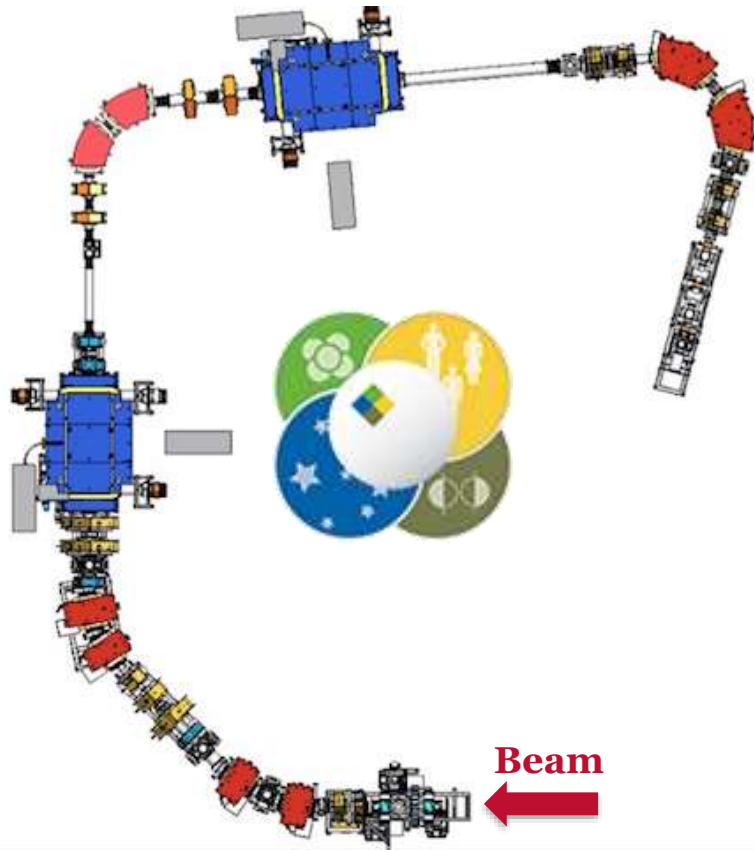


G. Lotay, S. Gillespie, M. Williams *et al.*, Phys Rev. Lett. **127**, 112701 (2021)

M. Williams, *et al.*, Phys. Rev. C **107**, 035803 (2023)

ERF research theme 1: Solving the Puzzle of the p-nuclei at FRIB

First radiative capture experiment with SECAR and radioactive beams at FRIB

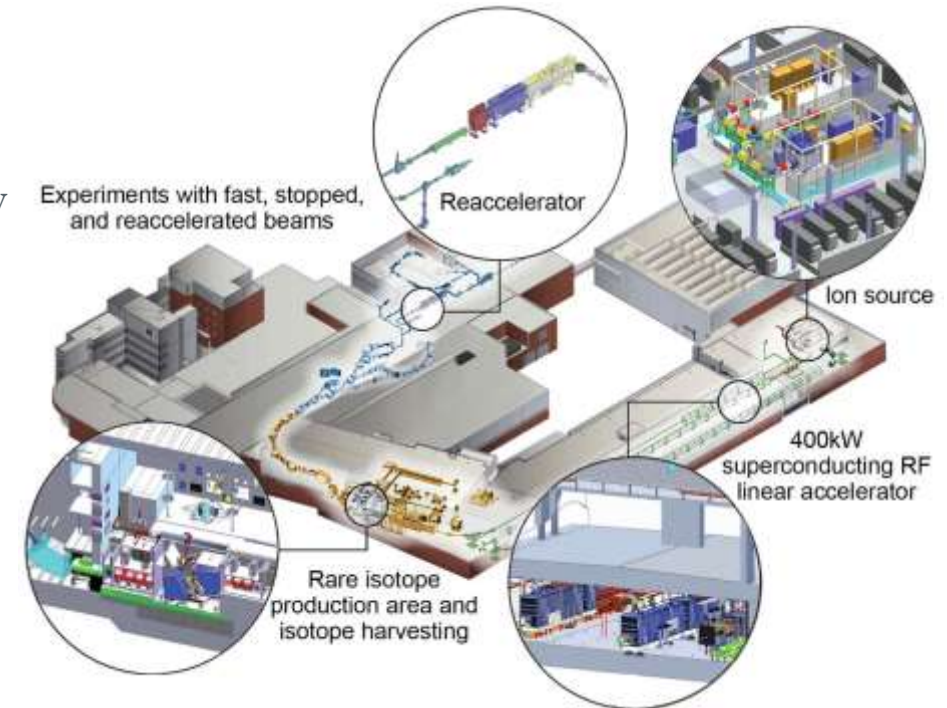


The **SE**parator for **CA**apture **R**eactions at FRIB is optimised for beam rejection, while the Wien Filter design gives flexibility on the high rigidity requirements for p-process reactions.

Awarded ~100 hours from PAC-2 to carry out a study of $^{77}\text{Br}(p, \gamma)$

First radioactive beam experiment to use the full SECAR device.

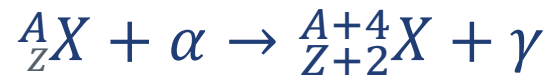
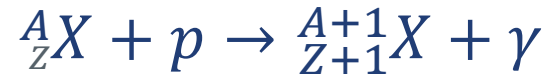
First radiative capture experiment using SECAR.



Experiment must occur within the next 3 years, likely next year or 2025

Studies of Radiative Capture for Astrophysics with DRAGON

Radiative capture of protons and alphas are ubiquitous in nuclear astrophysics

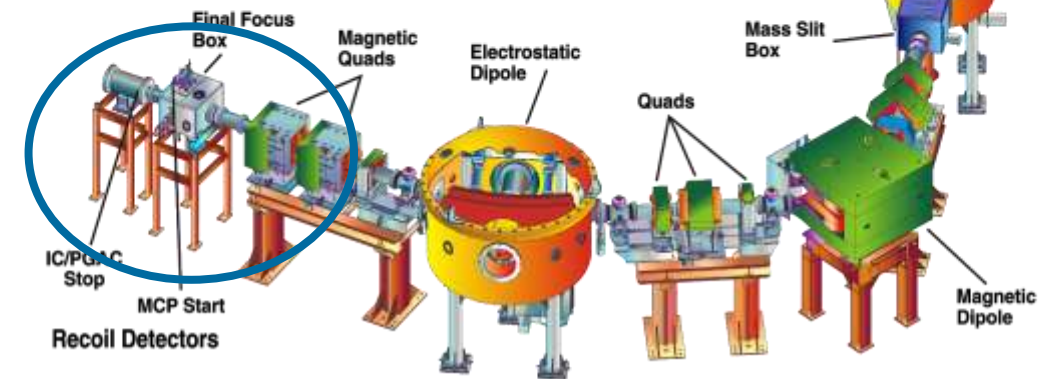
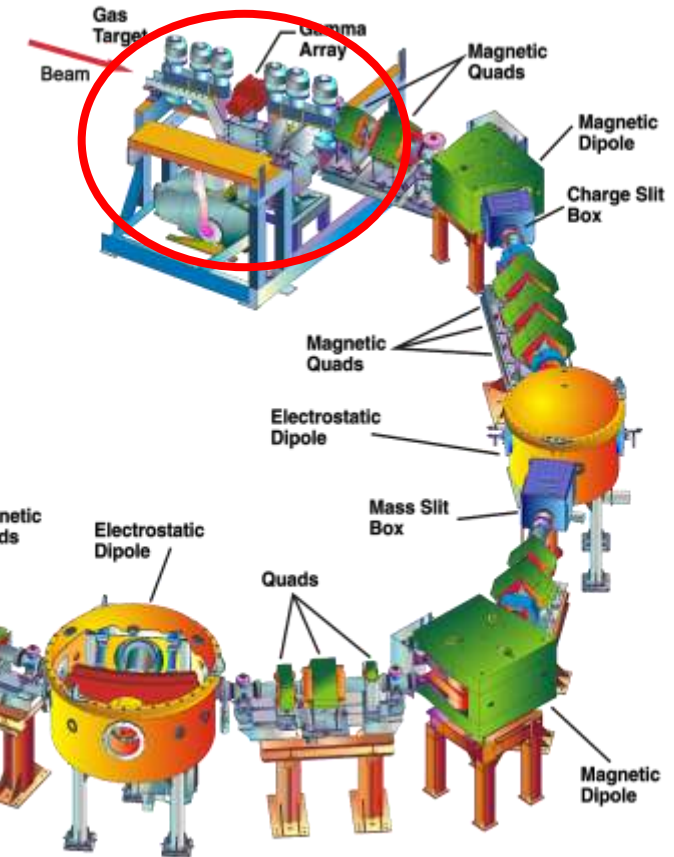
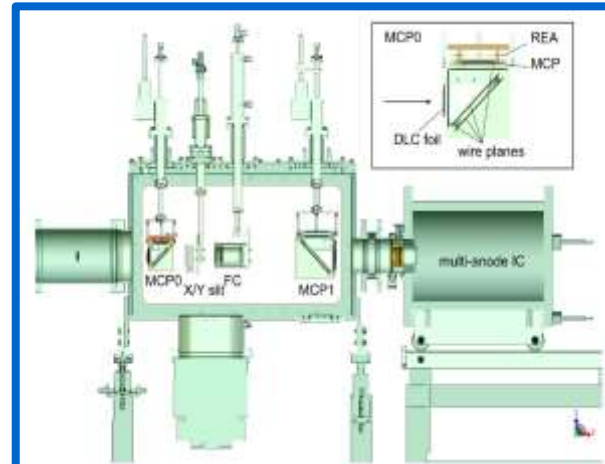


- Hydrogen and helium are the most abundant elements.
- Lowest coulomb barrier.
- Often the only reactions with positive Q-value.
- Proceed more slowly than particle-emitting reactions e.g. (p,α) and (α,p) making them the rate-limiting step in many reaction cycles (CNO).

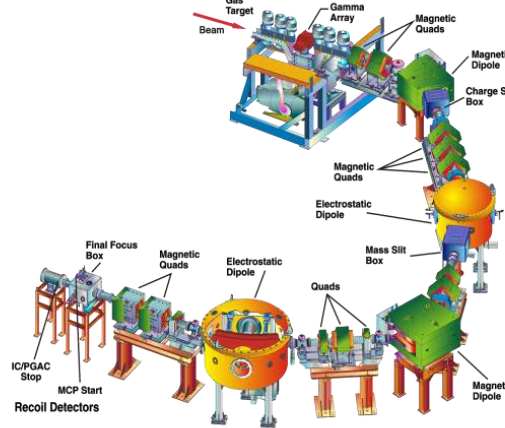
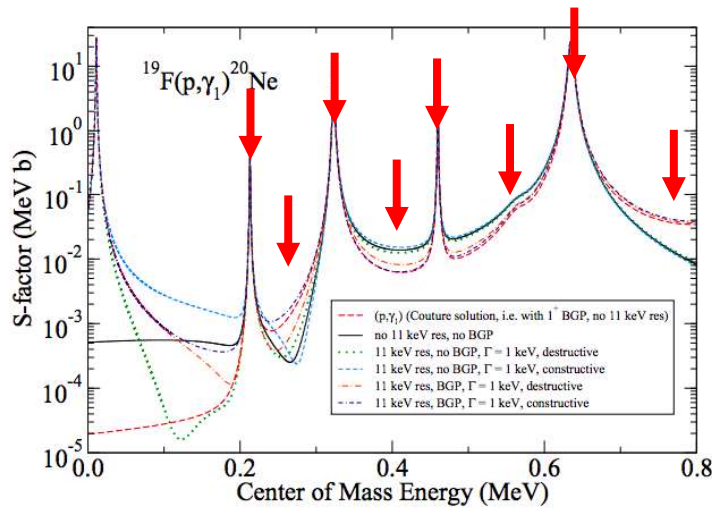
Windowless Gas Target & 4π BGO Array



MCP ToF system and ion chamber / DSSD



M. Williams, *et al.*, Phys. Rev. C **105** 065805 (2022)
M. Williams, *et al.*, Phys. Rev. C **103**, 055805 (2021)
M. Williams, *et al.*, Phys. Rev. C **102**, 035801 (2020)



DRAGON study at TRIUMF approved Jan 2022 (scheduled for September 2023)

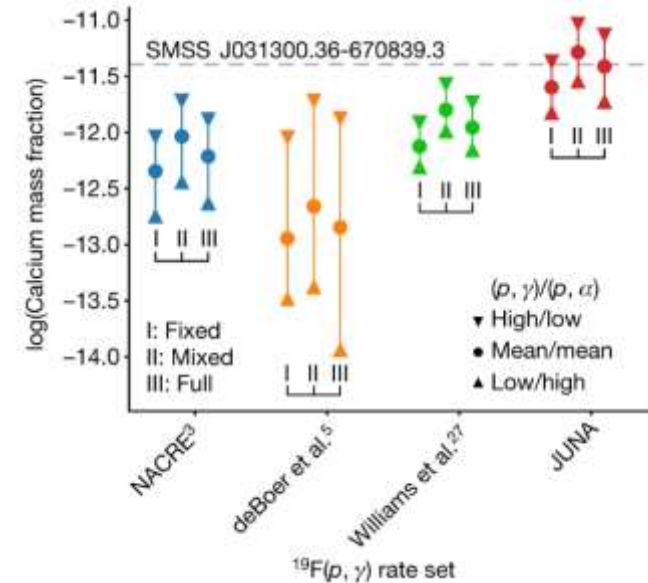
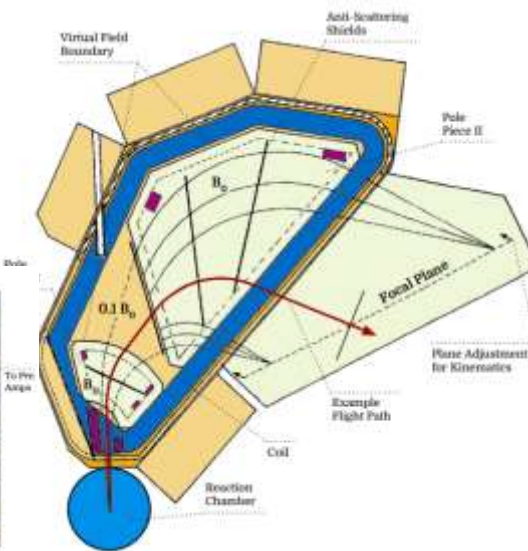
- Constrain interferences.
- Measure multiple decay branches.
- Search for unseen ground-state transitions.

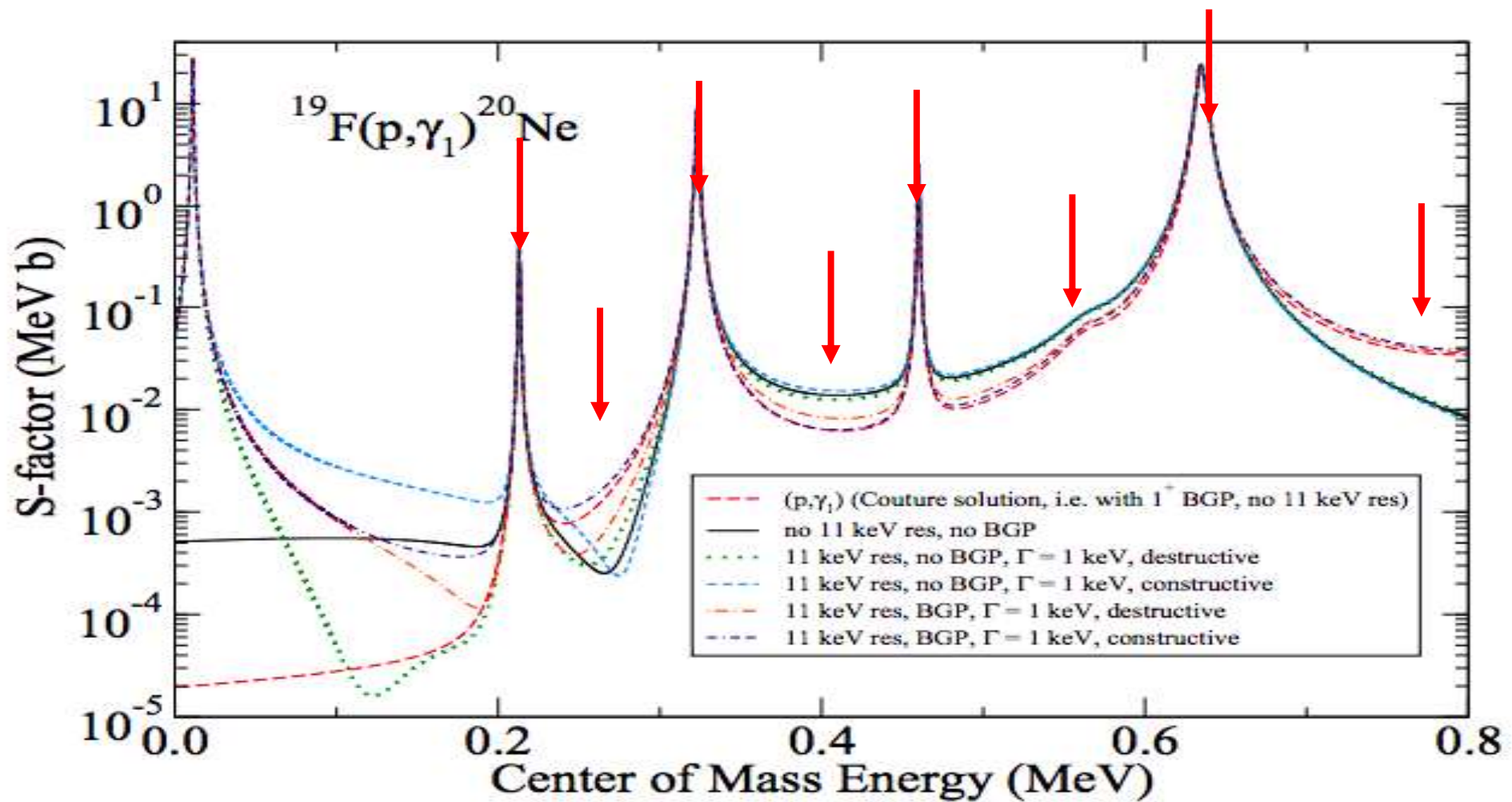
JUNA Study: Zhang *et al.*, Nature **610**, 656-660 (2022)

Found enhancement due to new 215 keV resonance, which seems to match Ca abundance seen in oldest known star.

Study at IJC Lab approved Oct 2021 (tentative for 2024):

Populate states in ^{20}Ne via $^{19}\text{F}(^3\text{He}, d)$.
 Detect break-up alphas and protons in coincidence.
 Widths, BRs, ANCs for key states.

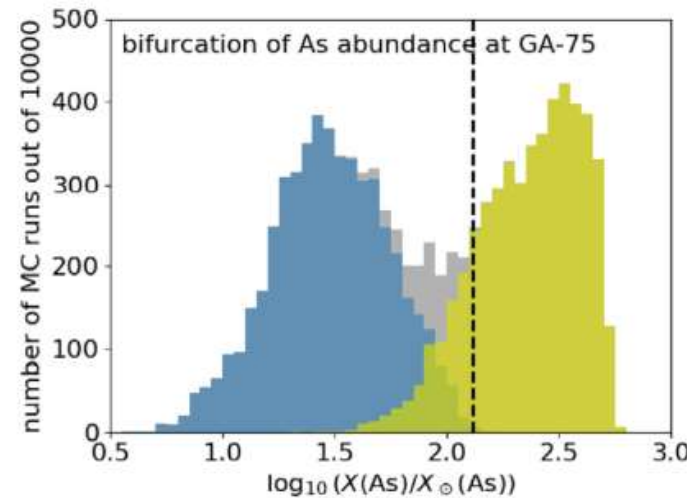
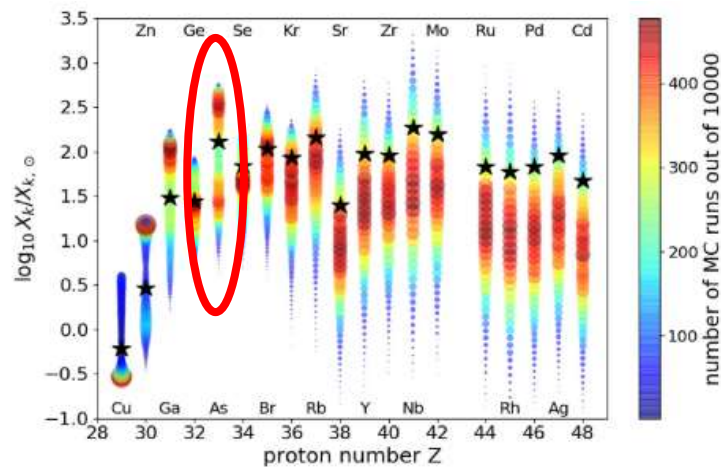
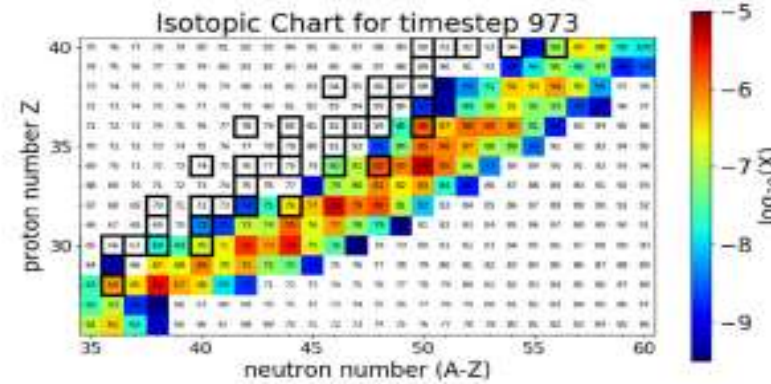
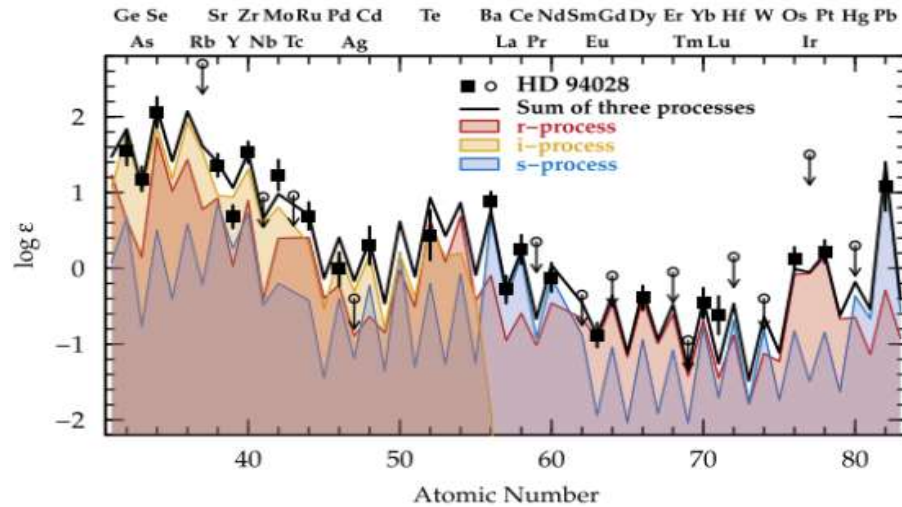




ERF Theme 3: Heavy element synthesis in the early universe

Some metal-poor stars show abundance patterns that do not match with any combination of r- and s-process scenarios

i-process: intermediate neutron capture process



High [As/Ge] ratios seen in metal-poor stars are particularly difficult to explain.

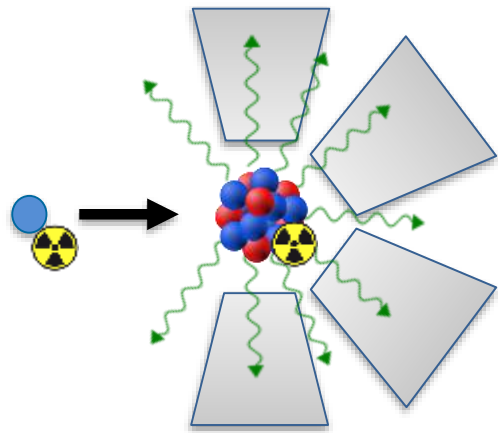
However, nucleosynthesis predictions for the As abundance in an i-process are strongly bifurcated.

The bifurcation is almost entirely due to uncertainties in the $^{75}\text{Ga}(n,\gamma)^{76}\text{Ga}$ rate

Neutron-induced reactions

Neutron captures on radioactive nuclei play a crucial part in heavy element synthesis

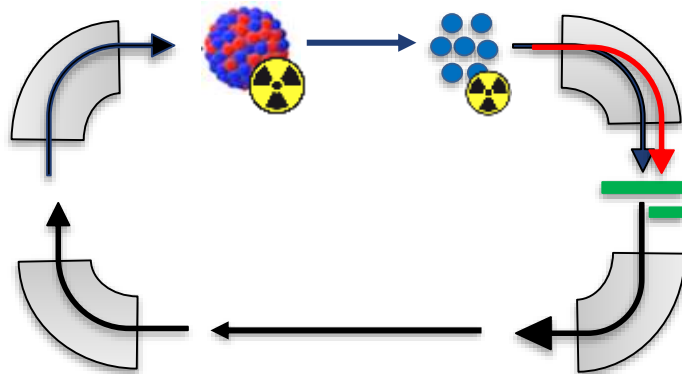
Challenge: How to measure neutron capture on a short-lived nucleus?



Forward Kinematics

- Too short-lived means very little (if any) target material can be produced.
- Radioactive decay from target would produce too high background.

Result: Signal/Background too small to measure <mb level cross-sections.

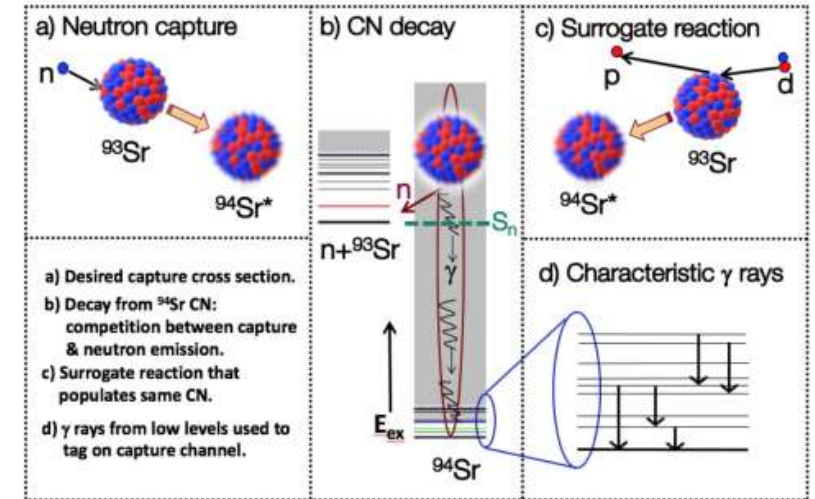


Inverse Kinematics

- Free neutrons are unstable, so need to produce neutrons continuously.
- Would need to boost luminosity by cycling ions in a storage ring at low energy – very challenging!

Result: Not presently feasible.

Surrogate Reaction Method



$$P_{\delta\chi}(E_{ex}) = \underbrace{\sum_{J,\pi} F_{\delta}^{\text{CN}}(E_{ex}, J, \pi)}_{\text{Measured}} \underbrace{G_{\chi}^{\text{CN}}(E_{ex}, J, \pi)}_{\text{Theory}} \underbrace{G_{\chi}^{\text{CN}}(E_{ex}, J, \pi)}_{\text{constrained}}$$

Statistical Model:

$$\sigma_{\alpha\chi}(E_a) = \sum_{J,\pi} \sigma_{\alpha}^{\text{CN}}(E_{ex}, J, \pi) G_{\chi}^{\text{CN}}(E_{ex}, J, \pi)$$

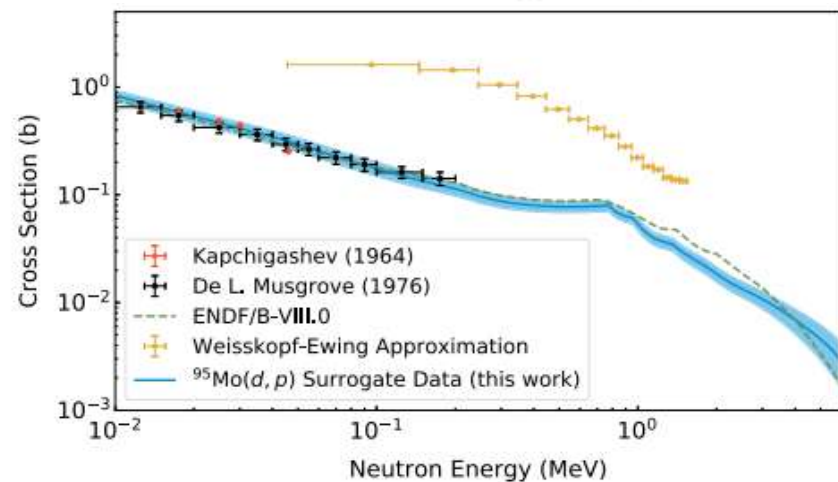
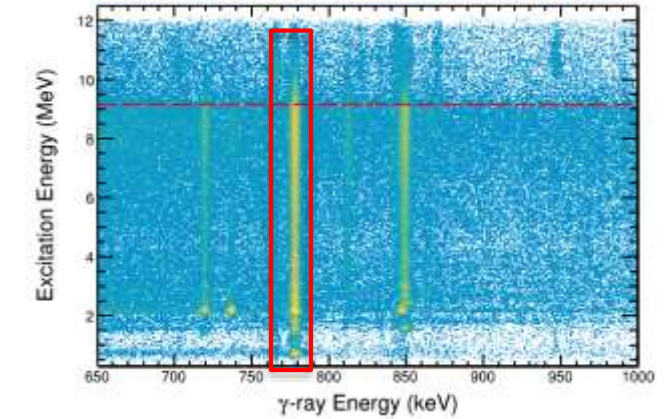
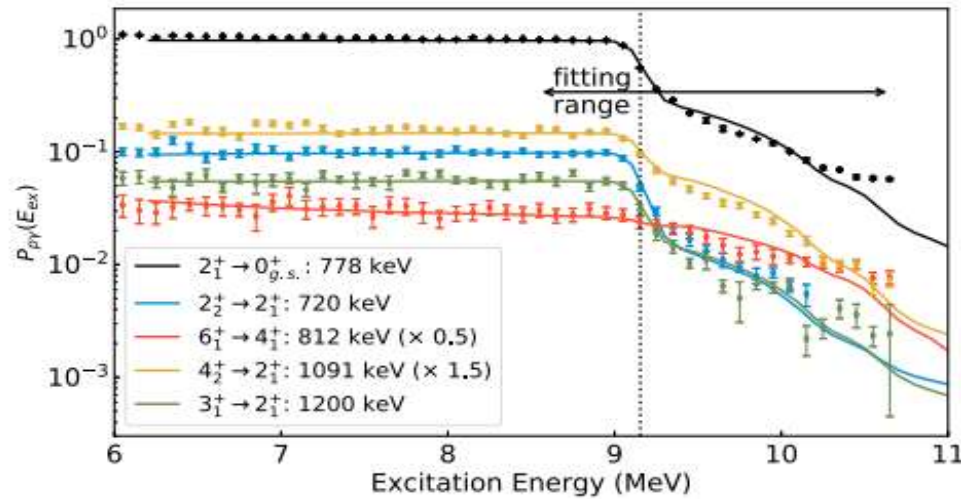
Demonstration of $^{95}\text{Mo}(d,p)$ as a surrogate for $^{95}\text{Mo}(n,\gamma)$

Ratkiewicz *et al.*, Phys. Rev. Lett. **122**, 052502 (2019)

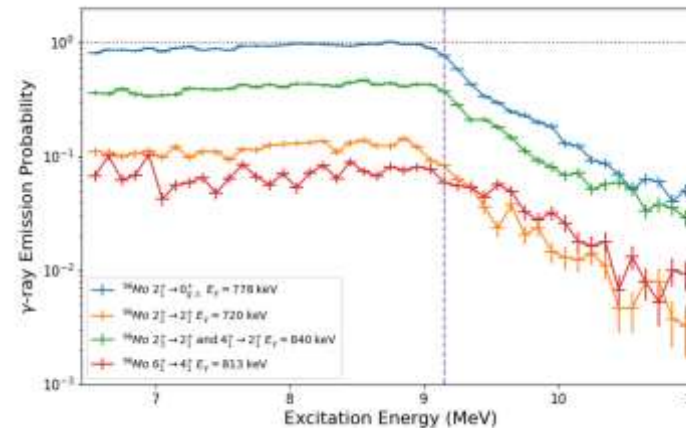
Demonstrating the SRM for inelastic scattering $^{96}\text{Mo}(p,p')$

GODDESS @ Argonne

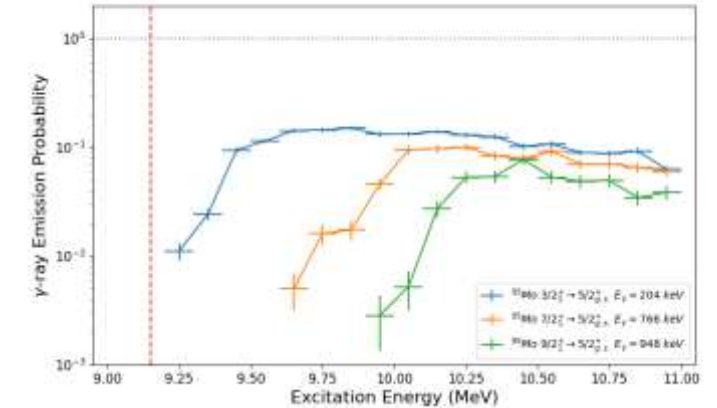
Particle- γ matrix. ^{96}Mo states



^{96}Mo γ -ray emission probabilities

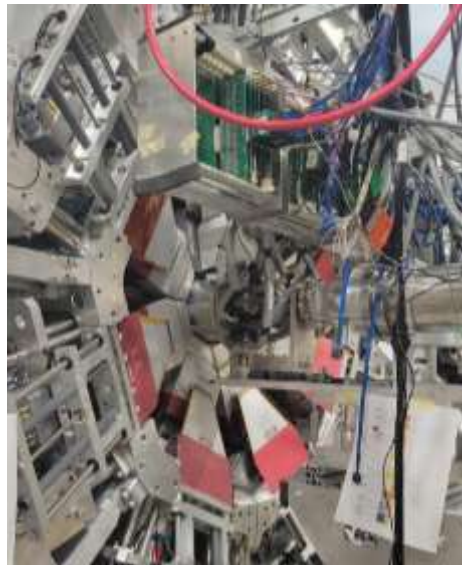


^{95}Mo γ -ray emission probabilities

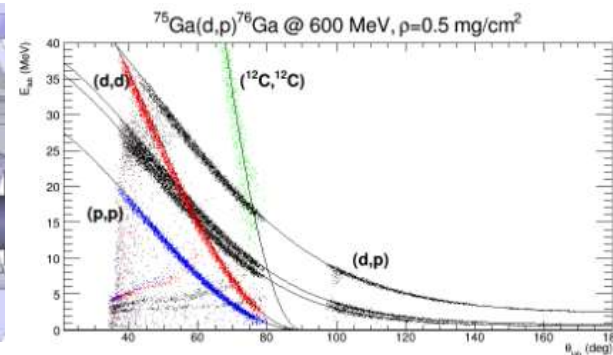
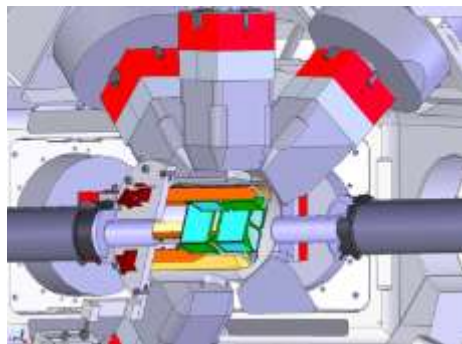
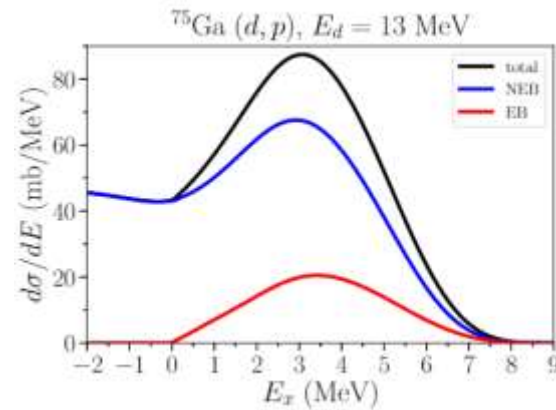


Constraining the $^{75}\text{Ga}(n,\gamma)^{76}\text{Ga}$ reaction with the Surrogate Method

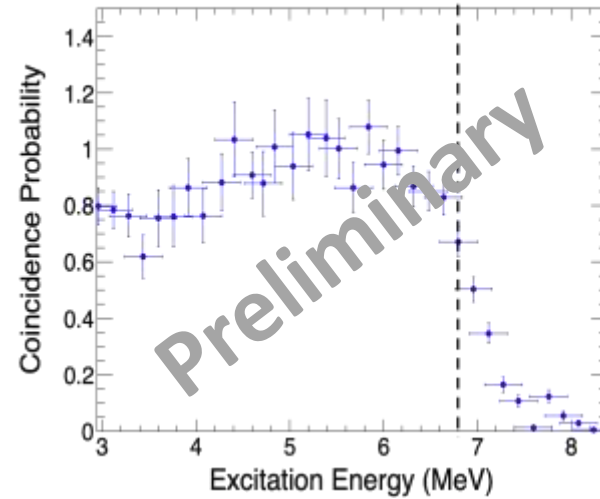
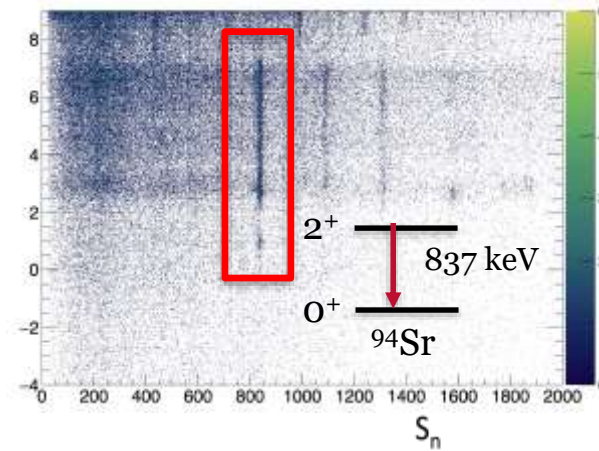
20 shifts approved with high priority at TRIUMF to measure the $^{75}\text{Ga}(d,p\gamma)^{76}\text{Ga}$ surrogate for $^{75}\text{Ga}(n,\gamma)^{76}\text{Ga}$



Experiment will use the TIGRESS HPGe Array and SHARC silicon array.

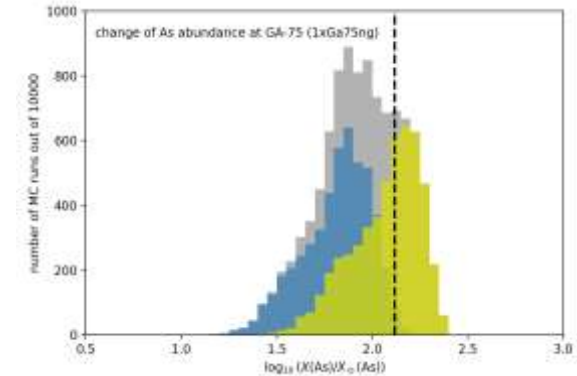
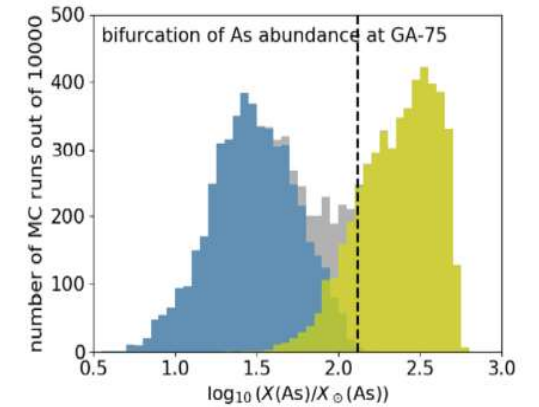


$^{93}\text{Sr}(d,p\gamma)^{94}\text{Sr}$ @ TRIUMF



Analysis by Andrea Richard (LLNL)

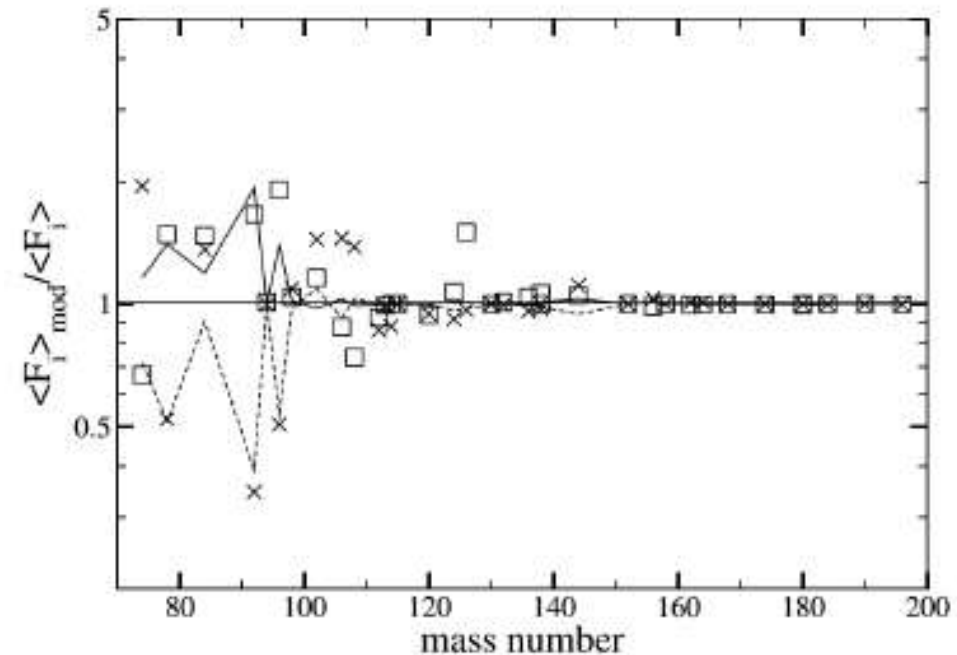
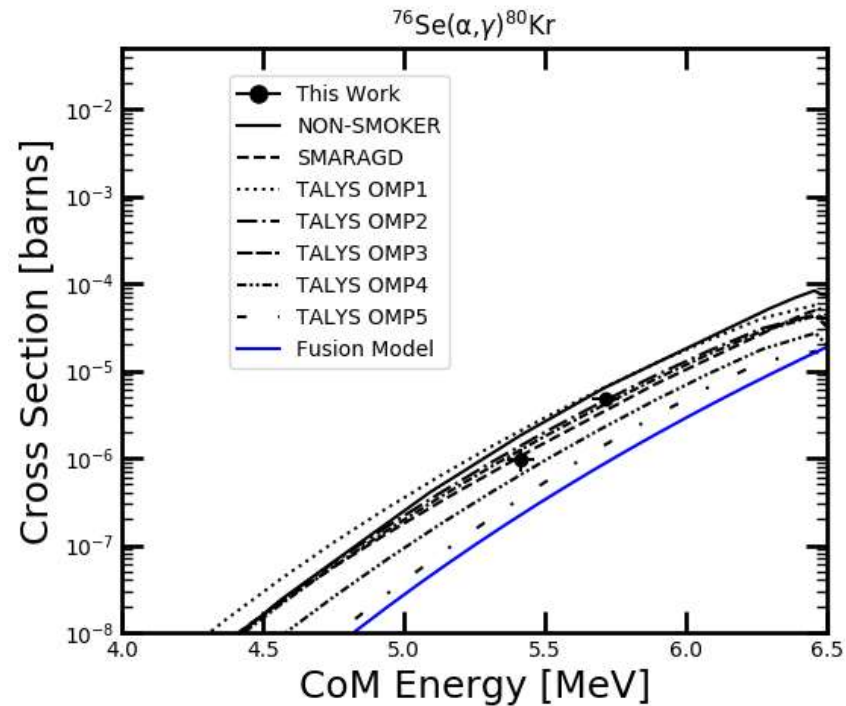
Reduce uncertainty in rate to factor 2 (in-line with observations)



- More data on nuclear reactions in massive stars is key to unlocking the origin of the elements produced in a variety of nucleosynthesis processes
- Reaction studies on radioactive beams present strong challenges that can be overcome by using novel techniques (e.g. new target materials), new equipment (more selective set-ups), and combining experiment with theory (surrogate methods).
- This program has already received high priority allocation >1000 hours of beam time at 3 separate laboratories to measure several key reactions affecting nucleosynthesis in massive stars.

Nuclear uncertainties in the p-process

- Production of p-nuclei involves many reactions on radioactive nuclei, none of which have been measured directly.
- Models rely on cross-sections predicted by Hauser-Feshbach models that can vary depending on the calculation inputs (e.g. Optical model parameters, γ SF, NLD) largely based on studies of stable nuclei.
- For light p-nuclei, production rates are most sensitive to variations in $(\gamma, p) / (p, \gamma)$ cross sections.



Fallis, J. et al. Physics Letters B 807 (2020) 135575.

Rapp, W., et al. The Astrophysical Journal 653.1 (2006): 474.

Rayet, M., et al. Astronomy and Astrophysics 298 (1995): 517.

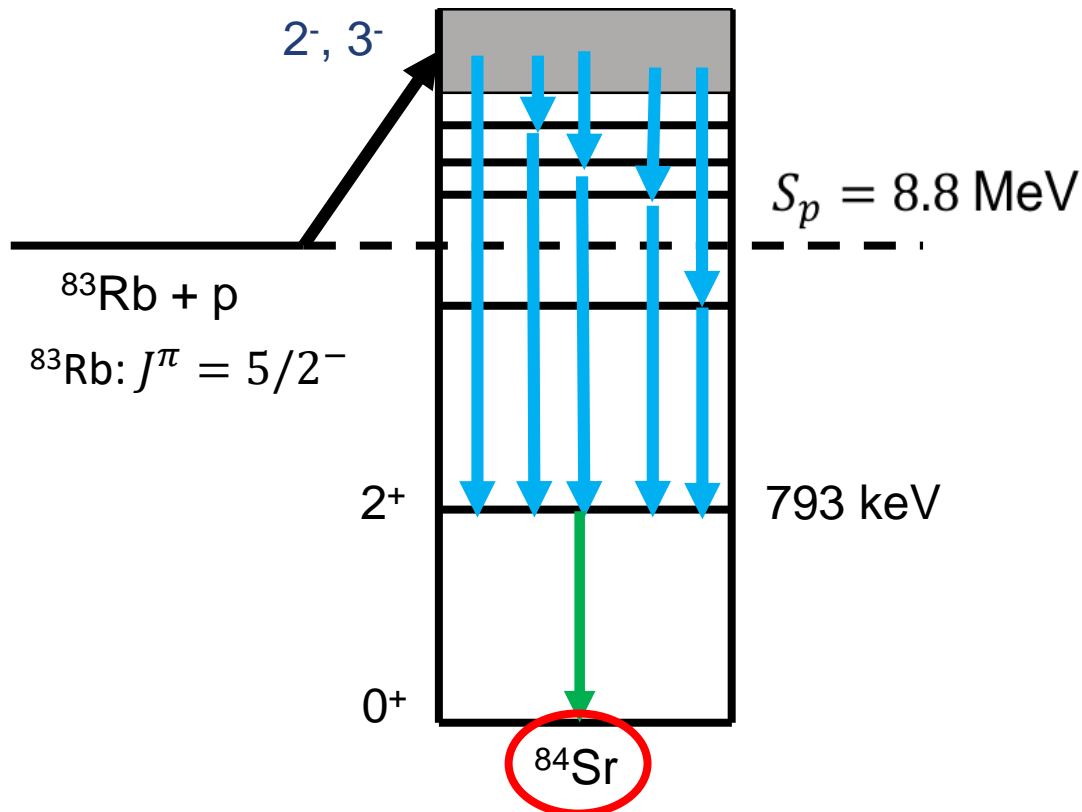
Why are no p-process reactions measured for radioactive nuclei?

- **Low cross-sections:** cross-sections of order few μb (or less) typical for (p, γ) reactions important for light p-nuclei at astrophysical temperatures.
- **Radioactive beams:** Strongly limits available intensity and creates a large γ -ray background.
- **Inverse kinematics:** A+1 recoils are very difficult to separate from more copious unreacted beam, which have similar kinematics and mass.

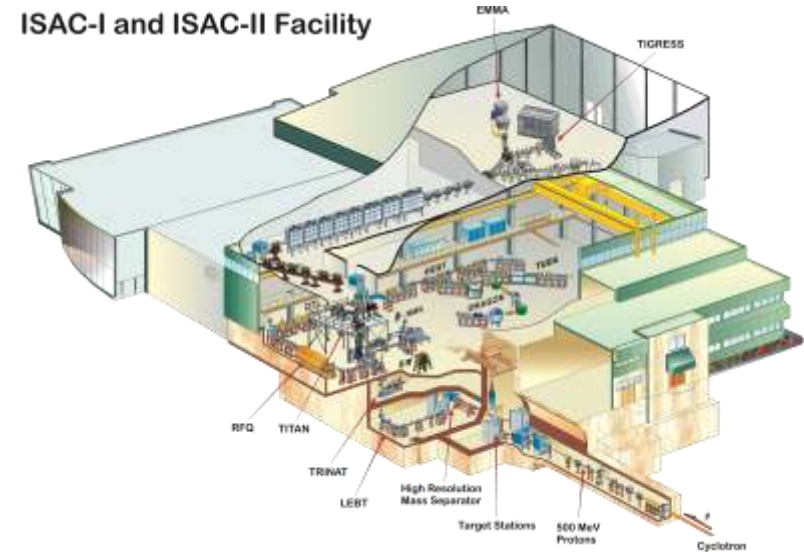
Measurement of $^{83}\text{Rb}(p, \gamma)^{84}\text{Sr}$ at TRIUMF

Can a mass spectrometer and HPGe array be used to measure p-process reactions?

- Targeted $^{83}\text{Rb}(p, \gamma)^{84}\text{Sr}$ reaction (important for ^{84}Sr p-nucleus abundance) using a ^{83}Rb beam produced by 500 MeV protons incident on ZrCx ISAC targets at TRIUMF (Vancouver, Canada) (intensity @ Experiment = 5×10^7 pps)
- Impinged on CH_2 foil targets to populate ^{84}Sr . (thicknesses between 300 and 900 $\mu\text{g}/\text{cm}^2$) at bombarding energies of 2.7 and 2.4 A MeV.



ISAC-I and ISAC-II Facility



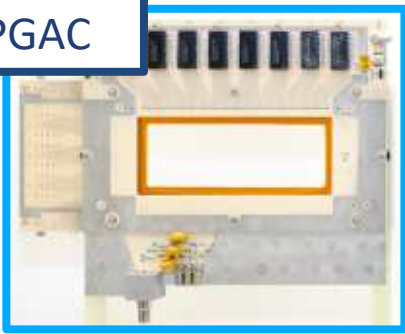
Use the EMMA mass spectrometer to transmit $A=84$ recoil products to the focal plane detectors.

Search for characteristic secondary γ -rays in coincidence with TIGRESS Compton suppressed HPGe array.

12 clovers in use:
x8 at 90° , x4 at 135°

The Electromagnetic Mass Analyser (EMMA)

PGAC



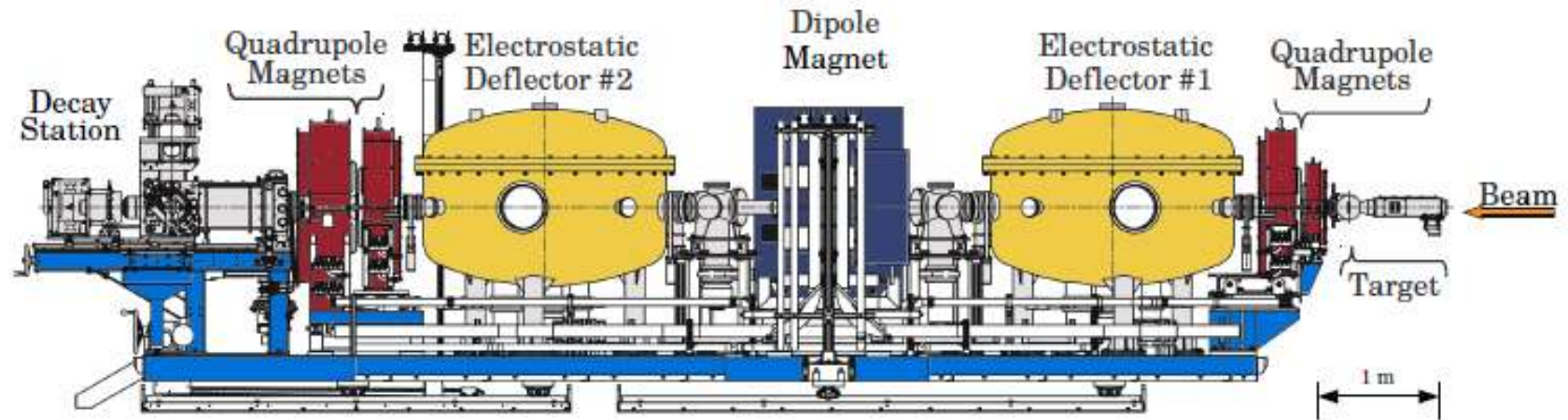
Ion Chamber



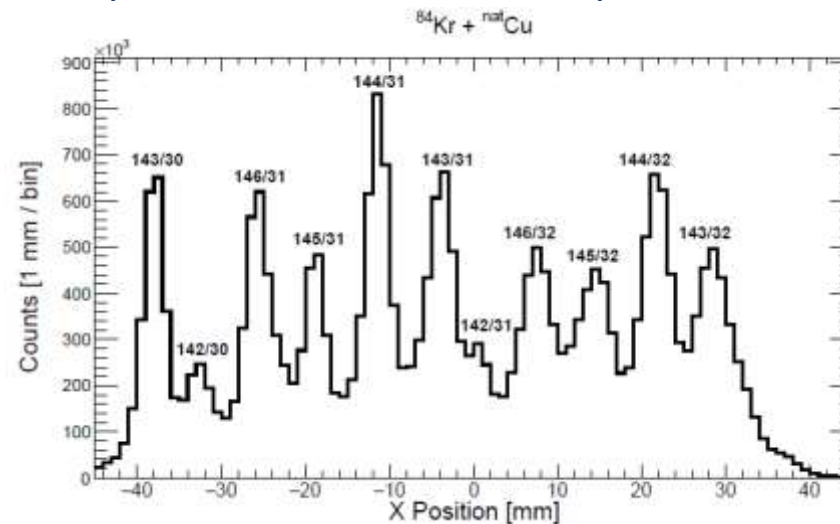
Ion-implanted Silicon



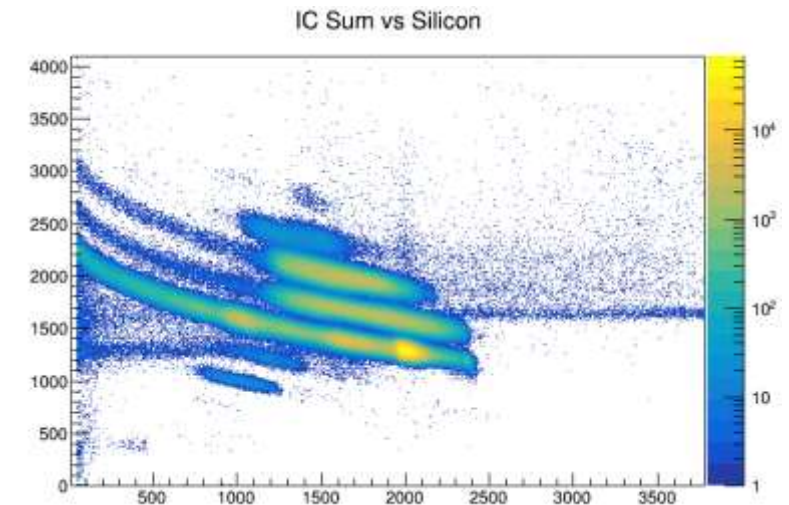
Angular Acceptance: $\pm 3.6^\circ$ | Energy Acceptance: +25% / -17% | m/q acceptance = $\pm 4\%$



PGAC spectrum from Fusion Evap test run:



IC PID plot from ^{17}O experiment:



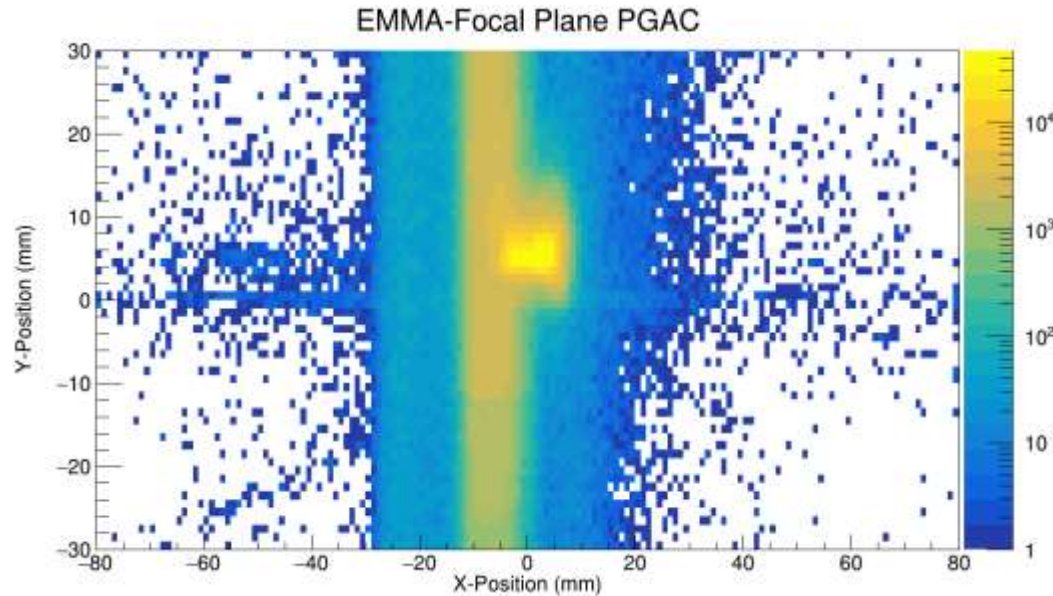
[1] B. Davids, M. Williams, *et al.*, *NIMA* **930**, 191-195 (2019).

The Electromagnetic Mass Analyzer (EMMA)



Stable beam proof-of-principle

- First tested technique using a stable ^{84}Kr beam with an energy of 2.7 A MeV.
- Tuned EMMA to the $q=25^+$ ^{85}Rb recoil charge state with a kinetic energy of 160.5 MeV
- EMMA is not optimized for beam rejection, the $q=25^+$ beam also makes it to the focal plane.



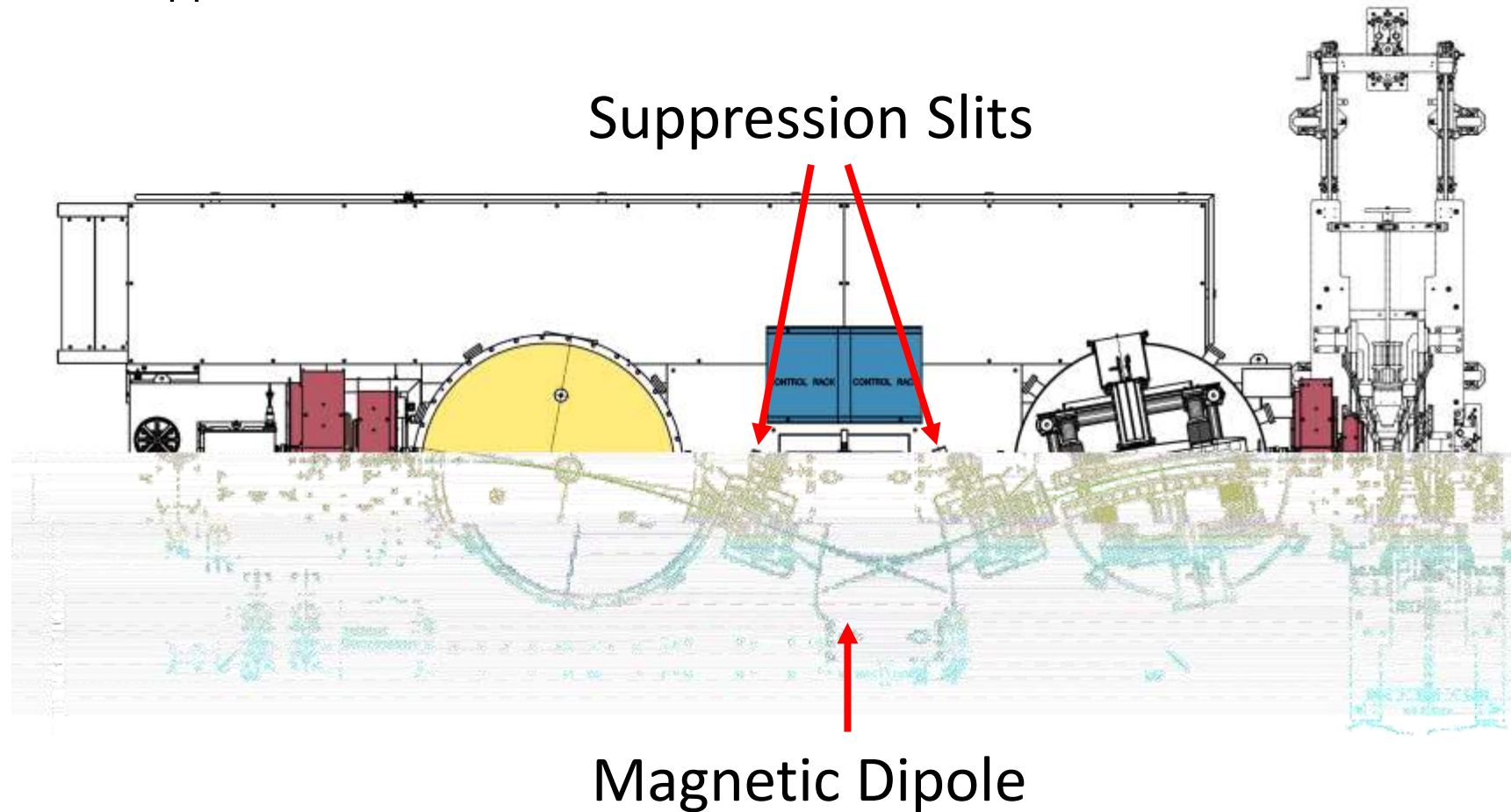
Focal plane slits

Need to use EMMA's slit systems to improve beam suppression.

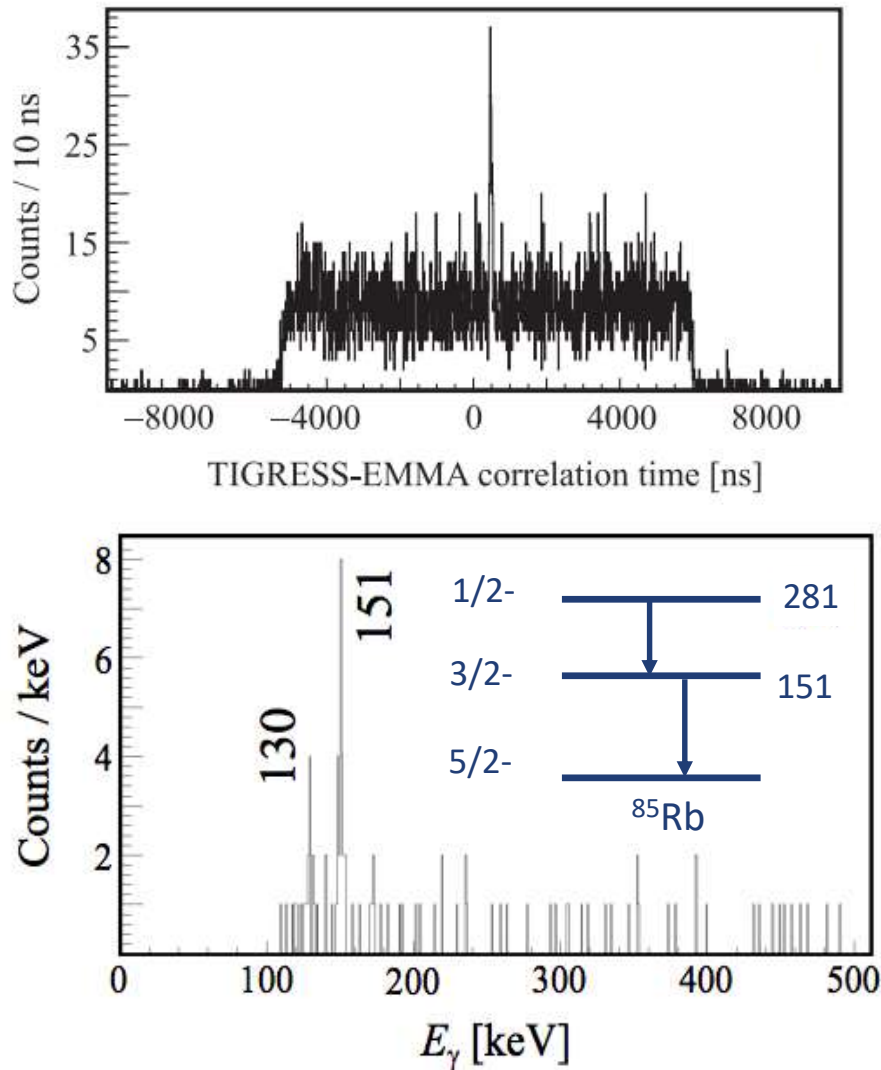
Stable beam test: Increasing Beam Suppression

Further beam suppression was achieved by narrowing the slits either side of the magnetic dipole.

The raw beam suppression factor we achieved was around 5×10^4 with no cuts on the data.

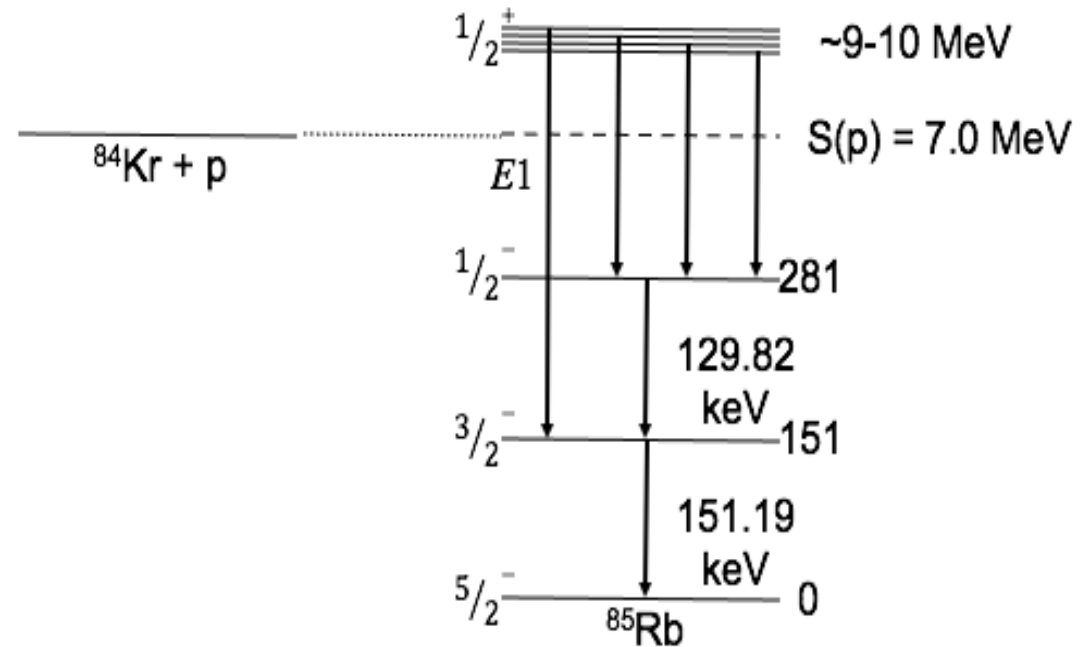


Measurement of $^{84}\text{Kr}(p, \gamma)^{85}\text{Rb}$

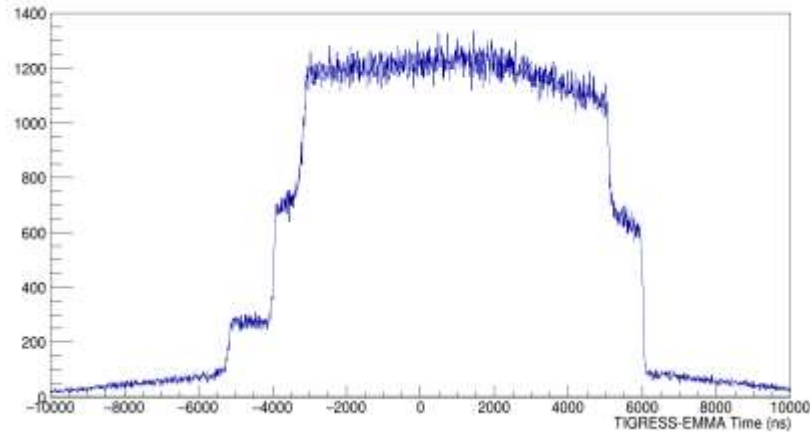


Raw beam suppression was enough to see a clear timing correlation peak between TIGRESS and EMMA events.

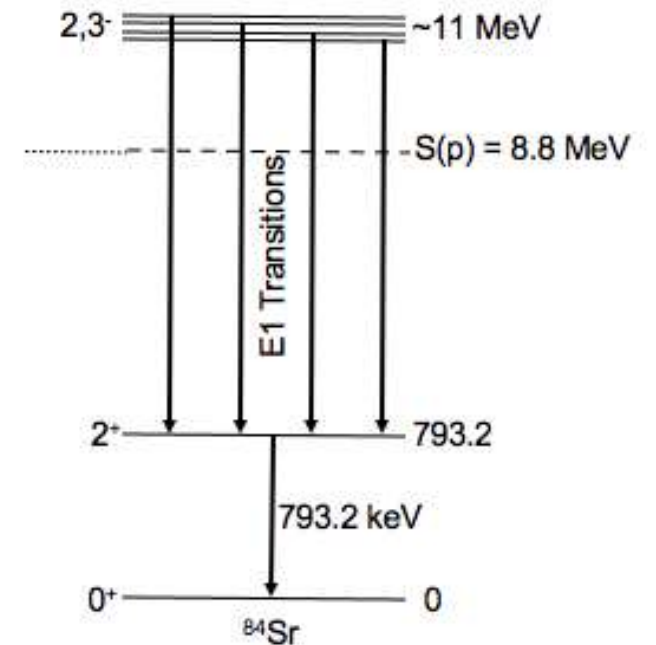
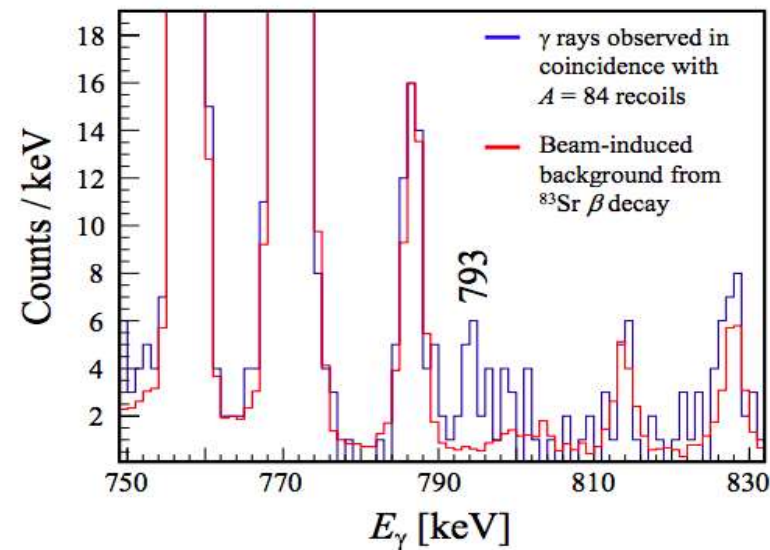
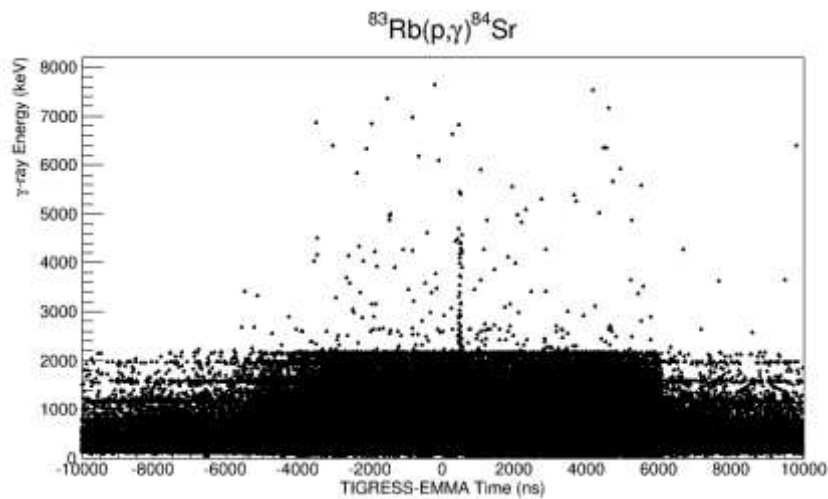
Gating on the timing peak reveals characteristic low-lying γ -rays in the ^{85}Rb final nucleus.



Measurement of $^{83}\text{Rb}(p, \gamma)^{84}\text{Sr}$



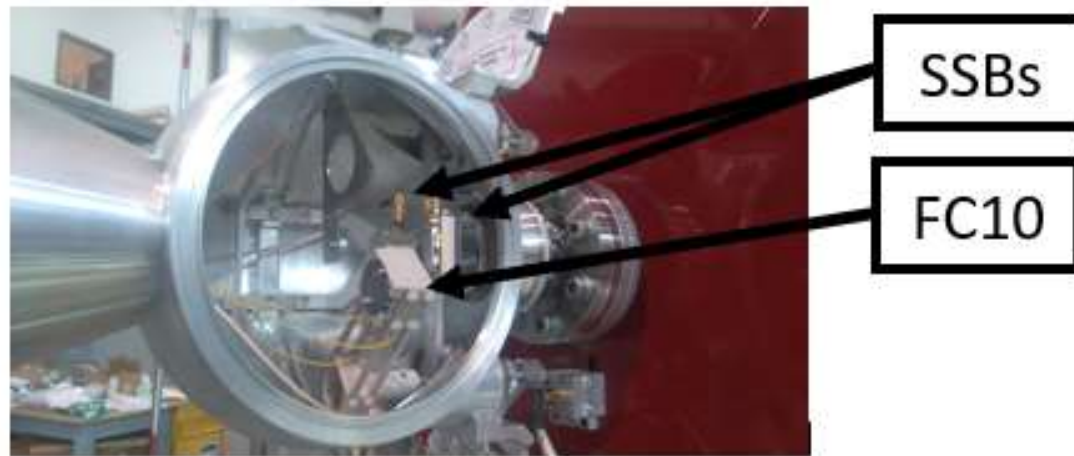
- Large background from ^{83}Sr contamination in the beam, which scatters onto EMMA's entrance aperture \rightarrow obscures the timing peak!
- Plotting γ -ray energy vs the correlation time reveals signal of high energy γ -rays at the expected correlation time.
- Gating around the correlation peak reveals the transition from the first 2^+ to ground state transition in ^{84}Sr . (16 events above background)



G. Lotay, S. Gillespie, M. Williams, et al., Phys. Rev. Lett. **127**, 1:

Beam Normalisation

To extract an absolute cross-section we need to monitor total luminosity over the experiment.



Normalisation factor to relate scattering rate to beam current and target thickness

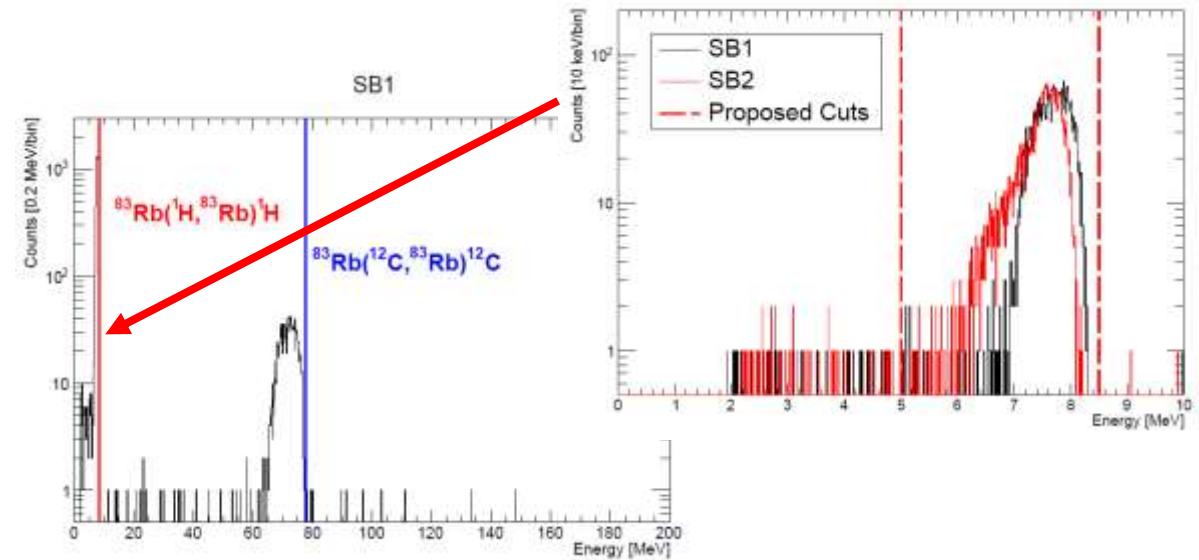
$$R \equiv \frac{fI}{Qe} \frac{\Delta t}{\Delta N_p} n,$$

Beam Intensity

Scattering rate

Target density

Measure scattered protons from CH₂ target



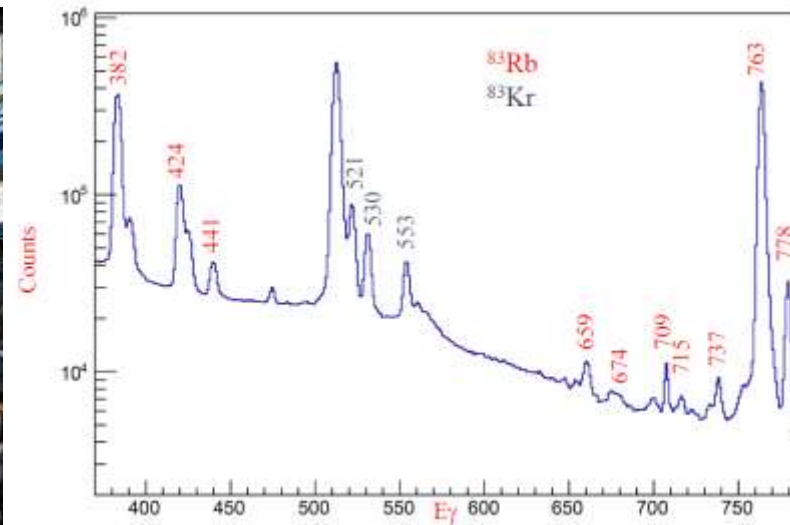
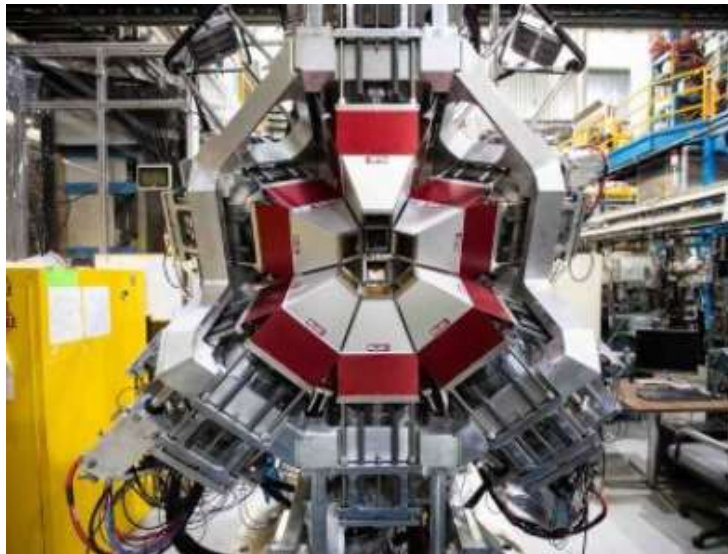
Find time-integrated luminosity by multiplying normalisation by total number of detected protons:

$$\int \mathcal{L}(t) dt = \int \frac{d(N_b n)}{dt} dt = RN_p,$$

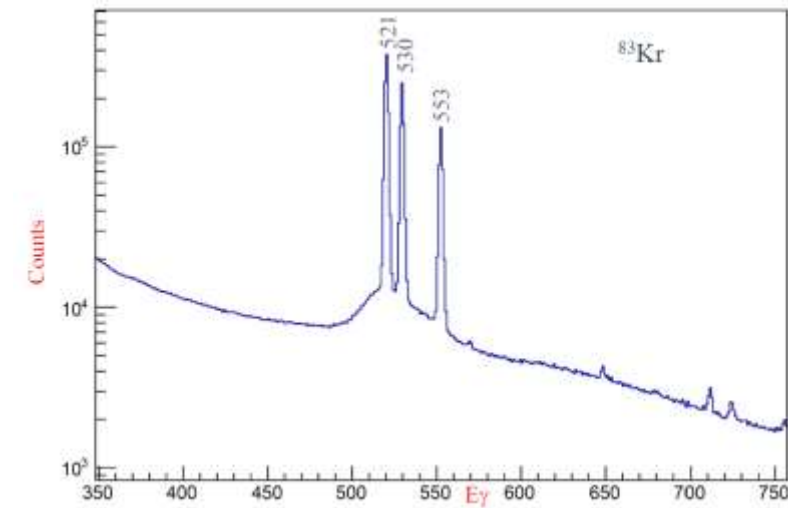
^{83}Sr Beam Contamination

Measured the decay of ^{83}Sr and ^{83}Rb built up on the removable entrance aperture of EMMA.

Aperture placed inside the GRIFFIN decay station, where measurements taken 2 hours and 22 days after the experiment were used to determine the ratio of initial activity.



~2 hrs after experiment



**~22 days after
experiment**

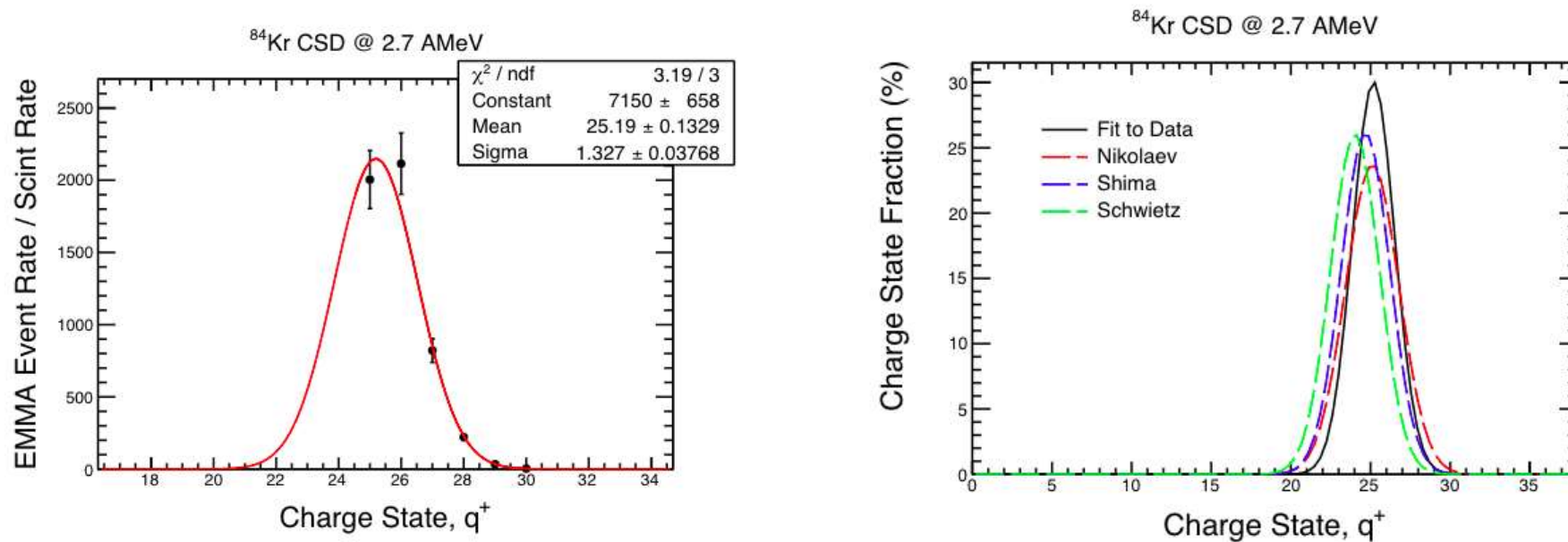
A=83 beam composition is $62 \pm 3\%$ of ^{83}Rb

M. Williams, *et al.*, *Phys. Rev. C* **107**, 035803 (2023).

Recoil Charge State Distributions

Only one recoil charge state is transmitted to the focal plane detectors so need to determine fraction.

Measured the charge state distribution for the (attenuated) Kr stable beam.



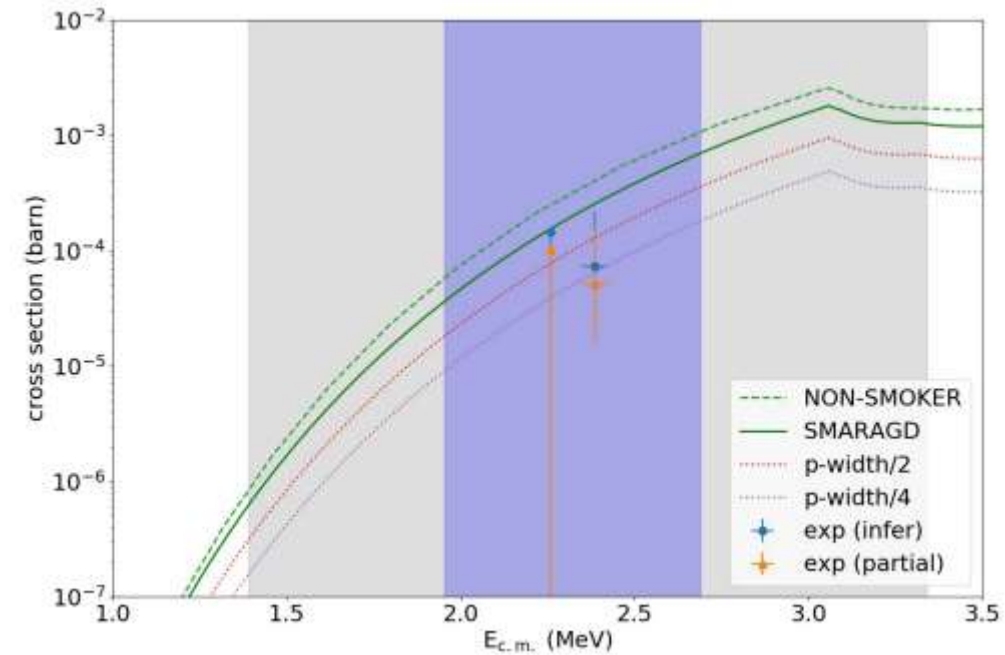
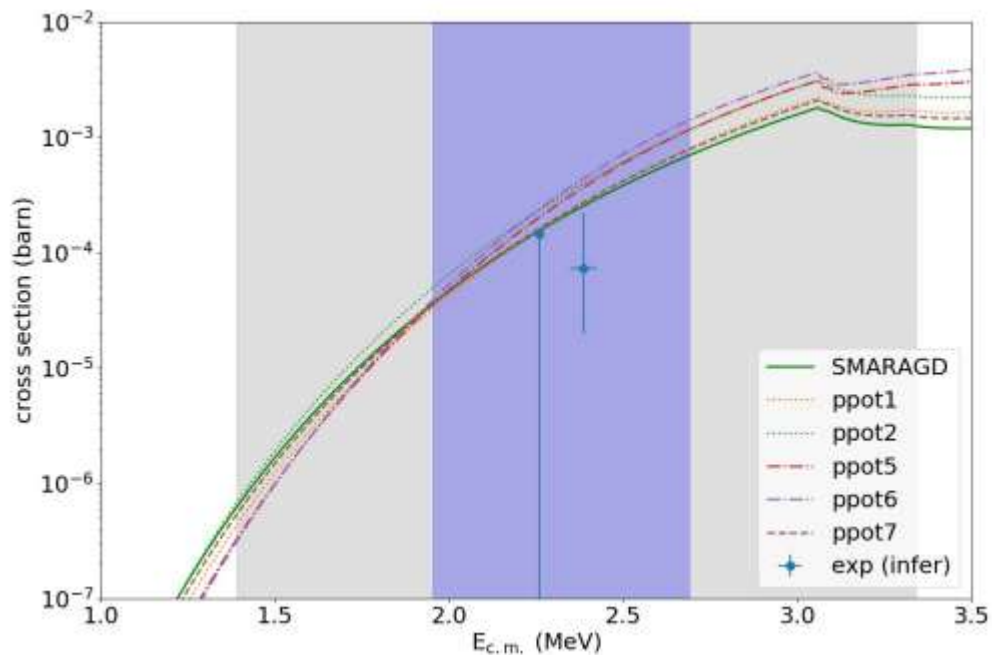
Then used the Z and Energy dependence of semi-empirical model to extrapolate from the stable beam CSD to the recoil CSD.

M. Williams, *et al.*, *Phys. Rev. C* **107**, 035803 (2023).

First measurement of a p-process reaction with a radioactive beam

Partial cross-section is converted to the full reaction cross section using γ -cascade models (included in the SMARAGD code), which predict $71 \pm 10\%$ of (p, γ) reactions result in a $2^+ \rightarrow 0^+(\text{g.s.})$ decay.

Total cross sections are approximately 4x smaller than predicted by Hauser-Feshbach models



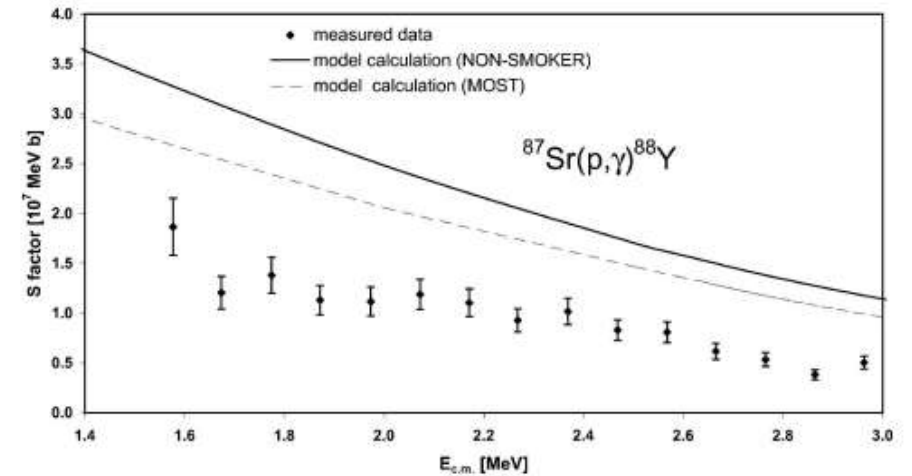
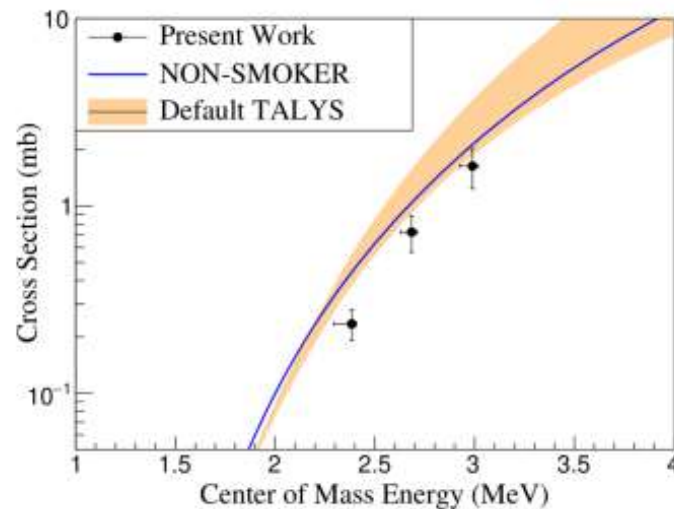
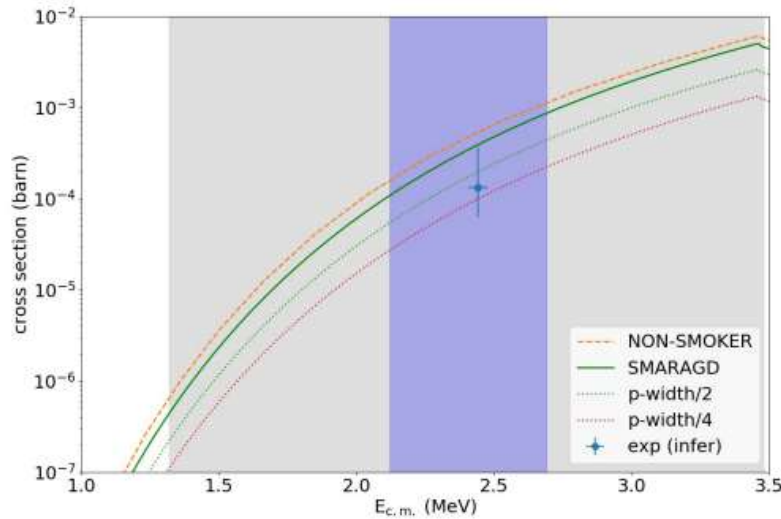
G. Lotay, S. Gillespie, M. Williams, *et al.*, *Phys. Rev. Lett.* **127**, 112701 (2021).

M. Williams, *et al.*, *Phys. Rev. C* **107**, 035803 (2023).

Statistical modeling by T. Rauscher

Evidence of systematic shift in proton-widths important for light p-nuclei

We observe similar over-prediction from statistical models in the $^{84}\text{Kr}(p,\gamma)^{85}\text{Rb}$ reaction.



Similar over-predictions have also been observed in $^{82}\text{Kr}(p,\gamma)^{83}\text{Rb}$, $^{86}\text{Sr}(p,\gamma)^{87}\text{Y}$, $^{87}\text{Sr}(p,\gamma)^{88}\text{Y}$

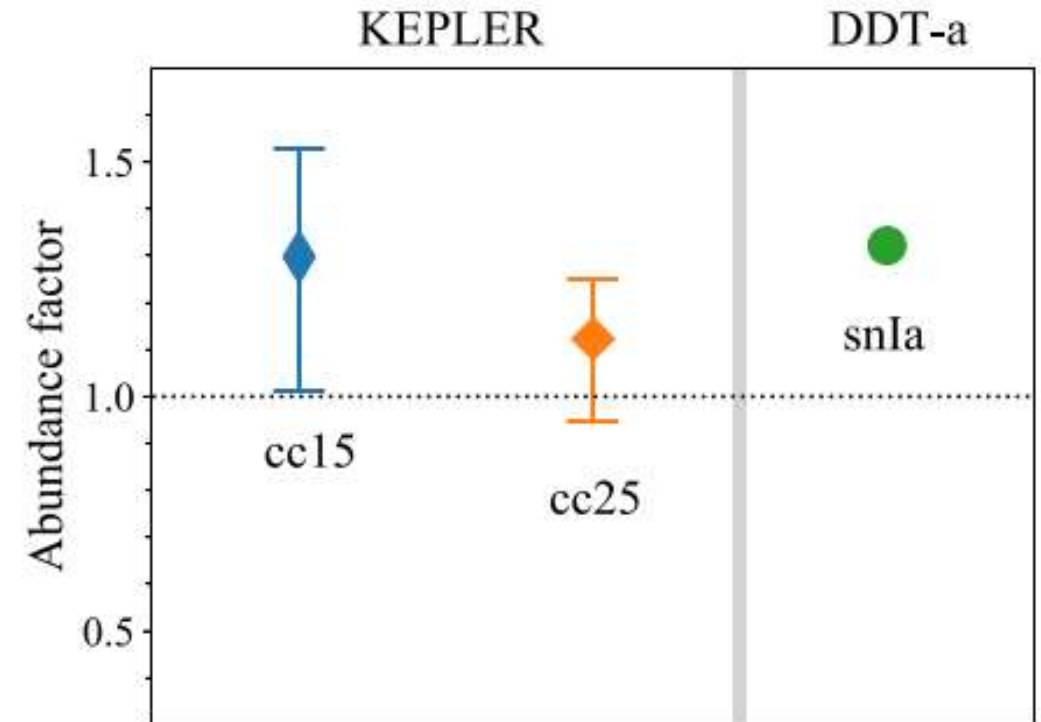
Could there be a systematic over-prediction in (p,γ) reaction cross-sections of importance for the light p-nuclei?

More experimental investigations required!

Astrophysical impact of $^{83}\text{Rb}(p, \gamma)^{84}\text{Sr}$ measurement

Impact investigated for both Type II and Type Ia supernovae explosions

- Lower $^{83}\text{Rb}(p, \gamma)^{84}\text{Sr}$ cross-section leads to less efficient destruction of the ^{84}Sr p-nucleus in supernovae, raising its production factor.
- The total uncertainty in ^{84}Sr production is reduced by a factor of 2 from previous sensitivity study.
- Uncertainties represent the combined effect of all reaction rates variations – not just $^{83}\text{Rb}(p, \gamma)^{84}\text{Sr}$.
- Abundance enhancement not sufficient to explain enhanced ^{84}Sr seen in Allende Meteorite, but could relieve tension – full GCE simulations required!



$15 M_{\odot}$ CCSNe = +30 %

$25 M_{\odot}$ CCSNe = +12 %

Type 1a SNe = +32 %

M. Williams, *et al.*, *Phys. Rev. C* **107**, 035803 (2023).

Astrophysical modeling by N. Nishimura

Reaction	E_γ (keV)	Transition	Integrated luminosity (μb^{-1})	Events	Detection efficiency (%)	$E_{\text{c.m.}}$ (MeV)	Measured σ_{partial} (μb)	Predicted σ_{partial} (μb)
$^{83}\text{Rb}(p, \gamma)^{84}\text{Sr}$	793	$2^+ \rightarrow 0^+$	28(5)	16(6)	$1.1^{+0.1}_{-0.4}$	2.386(23)	52^{+40}_{-22}	181(26)
	793	$2^+ \rightarrow 0^+$	16(2)	<16	$1.1^{+0.1}_{-0.4}$	2.260(7)	<103	110(16)
$^{84}\text{Kr}(p, \gamma)^{85}\text{Rb}$	151	$3/2^- \rightarrow 5/2^-$	12(2)	22(5)	$2.2^{+0.3}_{-0.8}$	2.443(22)	83^{+56}_{-26}	257(40)
	130	$1/2^- \rightarrow 3/2^-$	12(2)	11(4)	$2.1^{+0.3}_{-0.8}$	2.443(22)	44^{+31}_{-17}	106(40)

- Measured partial cross-sections for both the $^{83}\text{Rb}(p, \gamma)^{84}\text{Sr}$ and $^{84}\text{Kr}(p, \gamma)^{85}\text{Rb}$ reactions in what was the first EMMA+TIGRESS experiment.
- This is the first ever measurement of p-process reaction using a radioactive ion beam, obtaining cross-sections within the Gamow window for the γ -process in core collapse supernovae
- Our resulting cross section is approximately a factor of x4 lower than statistical model predictions, demonstrating the necessity of further experimental studies on the p-process.

G. Lotay, S. Gillespie, M. Williams, *et al.*, *Phys. Rev. Lett.* **127**, 112701 (2021).

M. Williams, *et al.*, *Phys. Rev. C* **107**, 035803 (2023).